To the Graduate Council:

I am submitting herewith a thesis written by John F. Brannon, Jr. entitled "Collisional Broadening Studies of Infrared Spectral Lines of Acetylene, Ethylene and Ammonia Using a Tunable Diode Laser Spectrometer." I have examined the final copy of this thesis for form and content and recommend that it be accepted in partial fulfillment of the requirements for the degree of Master of Science, with a major in Physics.

William E. Blass, Major Professor

We have read this thesis
and recommend its acceptance:

Accepted for the Council:

Vice Provost
and Dean of The Graduate School

STATEMENT OF PERMISSION TO USE

In presenting this thesis in partial fulfillment of the requirements for a Master's degree at the University of Tennessee, Knoxville, I agree that the Library shall make it available to borrowers under rules of the Library. Brief quotations from this thesis are allowable without special permission, provided that accurate acknowledgement of the source is made.

Permission for extensive quotation from or reproduction of this thesis may be granted by my major professor, or in his absence, by the Head of Interlibrary Services when, in the opinion of either, the proposed use of the material is for scholarly purposes. Any copying or use of the material in this thesis for financial gain shall not be allowed without my written permission.

Signature John F. Brannon, II

Date 7/8/91

COLLISIONAL BROADENING STUDIES OF INFRARED SPECTRAL LINES OF ACETYLENE, ETHYLENE AND AMMONIA USING A TUNABLE DIODE LASER SPECTROMETER

A Thesis

Presented for the

Master of Science

Degree

The University of Tennessee, Knoxville

John F. Brannon, Jr.

August 1991

ACKNOWLEDGMENTS

I am indebted to a number of individuals who have been a source of inspiration and assistance during my graduate study. I would particularly like to thank my major advisor, Dr. W. E. Blass, for his guidance during my work as well as advice derived from his expertise in the field of infrared spectroscopy. A thank you is extended to Dr. Stephen J. Daunt and Dr. Harry Jacobson for serving as the other members of my thesis committee, and a special thanks goes to Mark Weber for his suggestions and for our many conversations.

Much wisdom and experience was gained from a summer assistantship at the State University of New York at Stony Brook. Dr. Prasad Varanasi, and the Laboratory for Planetary Atmospheres, gave me the opportunity to do part of my thesis work at SUNY and expand my experience in the field.

Paul Lewis and Gerald McElyea, as well as others in the Molecular Spectroscopy Lab, were indispensible in the practical aspects of lab work where I had had little experience, and I deeply appreciate their help.

Finally, a thanks is given to Catherine and my family for their patience during my college work, and the help and understanding that they have given me during this time.

ABSTRACT

The collisional broadening linewidths of acetylene, ethylene and ammonia, broadened by hydrogen and nitrogen, were measured in the 10-14 μm region using a tunable diode laser spectrometer. Helium broadening measurements of ethylene were also made. The spectral lines of the ν_5 band of C_2H_2 were observed at room temperature, while the C_2H_4 and NH_3 measurements were taken over a range of temperatures from 152 K to 295 K. The Lorentz half-widths were found from the observed Voigt profiles, and the collisional broadening coefficients were determined. Line intensities were also retrieved from the C_2H_2 Voigt profiles. Wing corrections were made, following the method of Fridovich, in both the C_2H_2 broadening and intensity retrievals. Finally, the temperature dependence of the ethylene and ammonia broadening coefficients was determined.

TABLE OF CONTENTS

LIST OF TABLES

TABLE PAGE

LIST OF FIGURES

CHAPTER I

INTRODUCTION

Laboratory analysis of molecules that constitute planetary atmospheres is necessary for a better understanding of the molecular processes and interactions that occur in these atmospheres. The need for such information derives from research in the atmospheric sciences, which attempts to model the planetary atmospheres of the solar system. Laboratory measurements and analyses of molecules, where the physical parameters such as temperature and pressure are known, make possible generation of a quantitative model with which data from planetary observations may be compared. For example, high resolution infrared spectral studies in the laboratory are needed to interpret the spectra attained from the recent Voyager missions, as well as spectra from ground based observations of the planets (1). Two projects by NASA, the Mission to Planet Earth, and the Cassini Mission to Saturn and Titan, will produce a greater need for ongoing laboratory efforts in support of such atmospheric work (2-3). The present investigation is a study of the collisional broadening of infrared spectral lines of three molecules that are constituents of planetary atmospheres: the two hydrocarbons acetylene and ethylene, and the molecule ammonia.

Collisional broadening studies of molecules seek to describe the spectral line shapes of a gas when it is mixed with a perturbing gas, such as hydrogen. For example, acetylene gas was mixed with hydrogen to measure the broadening effects of hydrogen upon acetylene. The effects of the perturbing gas upon the spectral lines of the molecule are then analyzed. The perturbing gases used in this broadening work were nitrogen, hydrogen and helium. Nitrogen was chosen as a perturber since it is the dominant gas in the atmospheres of Titan and the Earth. Hydrogen and helium are the two largest constituents, respectively, of the atmospheres of Jupiter and Saturn, so the effects of their interactions on the rotational-vibrational (infrared) spectra of other atmospheric gases are important in the understanding of these atmospheres. These perturbing gases were used with the three molecules acetylene, ethylene, and ammonia to perform the broadening measurements which are the subject of this investigation.

Acetylene

Acetylene, C_2H_2, has been found to be a trace constituent of the atmosphere of the Earth, and the atmospheres of Jupiter, Saturn and Titan (4-11). This hydrocarbon has been found in observations of the cool carbon star IRC + 10216 (12). C_2H_2 is also thought to be in the atmospheres of Uranus and Neptune, and is included in the atmospheric photochemical models of these planets (13- 16).

The presence of acetylene in the atmospheres of the outer planets is explained theoretically by the photodissociation of methane, CH_4. In an H_2 atmosphere, such as Jupiter or Saturn, this decomposition of methane is caused by the absorption of solar radiation which produces the two hydrocarbons ethylene, C_2H_4, and ethane, C_2H_6, plus other products. Acetylene is then produced from the subsequent photolysis of these two hydrocarbons (17). In Titan's atmosphere, which is N_2 dominant, the photodissociation of methane is similar, again with the production of acetylene (18). The abundance of acetylene in our own atmosphere derives from natural and anthropogenic sources, including the use of automobiles. It is predicted that atmospheric C_2H_2 amounts will increase with future increases in automobile emissions (19-20).

Acetylene is a linear molecule with the molecular structure

$$H - C \equiv C - H$$

where the carbon atoms are bonded by two pi and one sigma bond, and each hydrogen is bonded to a carbon by a sigma bond (21). Eight collisionally broadened spectral lines of C_2H_2 were measured in the ν_5 band, in the 14 μm region, at room temperature. The ν_5 normal model is one of the two bending modes of the molecule. The vibrational- rotational energy transitions of the ν_5 band of C_2H_2 are seen in the 14 μm region (22). The collisional broadening coefficients were retrieved from these observed lines, as well as the absolute line intensities. Line positions of the C_2H_2 lines used were found from a compilation by Mark Weber of Kitt Peak FTS data (23). The acetylene work was conducted at the Molecular Spectroscopy Lab at the University of Tennessee, Knoxville (UTK).

Previously published collisional broadening work with the ν_5 band of C_2H_2 includes hydrogen and nitrogen broadening work conducted by Blass and Chin (24,25), and recent

nitrogen and oxygen broadening work by Bouanich et al. (26) and Lambot et al. (27). Using the ($\nu_4 + \nu_5$) combination band at 7.4 μm, nitrogen and air broadened line half-widths at half maximum (HWHM) were determined by Devi et al. (28), while Podolske et al. (29) conducted nitrogen and helium broadening measurements using this band. Finally, self broadened and hydrogen broadened line widths were measured for the ($\nu_1 + \nu_3$) band at 1.525 μm by Varanasi and Bangaru (30). The current nitrogen and hydrogen broadening of the acetylene results are compared with this previous work.

Ethylene

The second molecule used in this work, ethylene, is another trace hydrocarbon that is found in the atmospheres of the Earth, Jupiter, and Titan, as well as IRC + 10216 (10),(31-34). Like acetylene, ethylene is also thought to be in the atmospheres of Uranus and Neptune (13-15). As previously mentioned, ethylene is a product of the photolysis of methane in Jupiter's and Titan's atmospheres. On Earth, ethylene comes from a variety of sources– plants, volcanoes, forest fires, and automobile emissions (31).

The structural representation of the molecule ethylene is

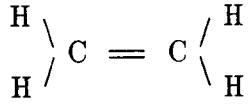

where in this case the carbon are bonded by one sigma and one pi bond and the hydrogen are connected by sigma bonds (35). The ethylene line located at 951.7393 cm^{-1}, found in the ν_7 band, was used for the broadening measurements. The ν_7 band is the out-of-plane bending mode of the molecule (36). Known ammonia lines were used as a calibration to determine the frequency of the line of interest, and work by Lambeau et al. (37) helped determine the assignment of the transition. Nitrogen, hydrogen, and helium were used as perturbers for the collisional broadening measurements.

C_2H_4 data acquisition and analysis were conducted at the State University of New York (SUNY) at Stony Brook. This facility permitted C_2H_4 collisional broadening measurements, as well as absolute line intensity measurements, to be conducted at temperatures comparable to planetary temperatures. Using a nitrogen cooled absorption cell (38), it was possible to take measurements over a range of temperature from 152 K to 295 K. There

are no previously published collisional broadening measurements of C_2H_4 performed at planetary temperatures.

Ammonia

Ammonia, NH_3, is the third molecule to be studied in this investigation. The ammonia molecule, a symmetric top, has a pyramidal structure with the nitrogen atom at the top. Each of the hydrogen atoms are separated by a bond angle of 107.3 degrees (39,40). The ammonia measurements were also conducted at SUNY Stony Brook. NH_3 is of planetary interest because it is a constituent of the atmospheres of the Earth, Jupiter, Saturn, and Uranus (9-11),(41-44). The work with NH_3 consisted of collisional broadening measurements of the aR(0,0) 951.7762 cm^{-1} line, in the ν_2 band, with measurements taken at 206, 251, and 295 K. The Air Force Geophysical Laboratory (AFGL) HITRAN database tape was used to determine the assignment of the transition (45), with the transition notation from Kostiuk et al. (41). Nitrogen and hydrogen were used as the perturbers for the ammonia broadening.

Previous hydrogen broadening of ammonia lines has been conducted at 207 and 300 K with the $(\nu_1 + \nu_2)$ and $(\nu_2 + \nu_3)$ bands by Margolis and Sarangi (46). Hydrogen collisional broadening measurements have also been carried in the 6475 Å band by Keffer et al. (47).

Systems and Analysis Overview

Acquisition of data for these molecules at high resolution in the infrared is possible with the use of a tunable diode laser (TDL) spectrometer system. Herein, high resolution denotes spectral resolution on the order of $10^{-4}cm^{-1}$. There are advantages, and disadvantages, in using a TDL system, but the ability of a TDL spectrometer system to resolve individual line shapes makes it particularly advantageous for collisional broadening studies of spectral lines (1),(48).

In the measurement of spectral lines using a tunable diode laser, a gas is placed in an absorption cell, and the cell is placed in the path of IR emission from a tunable diode laser. (In collisional broadening measurements, a perturbing gas is also introduced into the absorption cell.) Energy of the IR beam is absorbed by the molecules of the gas at wavelengths equivalent to quantized energy level separations which are quantum mechanically allowed rotational-vibrational transitions of the particular molecule. The energy

emission of the diode laser is tuned to particular frequencies to look at these rotational-vibrational energy transitions, hence the name tunable diode laser. All work, at both UTK and SUNY, was conducted with a tunable diode laser spectrometer system, and differences in the systems at the two facilities will be described where appropriate.

Initial laboratory analysis of the machine readable UTK data was carried out using an analysis program written in QuickBasic by Mark Weber. This program was modified to include a second method to determine broadening coefficients. The collisional broadening coefficients were thus determined by two independent methods: direct measurements of the HWHM for the spectral lines along with wing corrections, and the sample/background ratio method. The absolute intensities of the lines were also retrieved in order to test the consistency of the collisional broadening coefficients determined. Final data analysis was conducted on the VAX Cluster at the UTK Computing Center using programs written in FORTRAN. The analysis of the SUNY data consisted of an in-house program, written in QuickBasic, which permitted determination of the collisional broadening coefficients and line intensities. Additional use was made of the SUNY VAX Cluster, the VAX 6000-310 in the Laboratory for Planetary Atmospheres, and the magnetic tape facilities in the CAD Laboratory.

In this report, Chapter II discusses spectral line shapes, and the method by which these lines are analyzed. Chapter III describes the experimental set-ups at UTK and SUNY that were used to conduct the measurements. Measurement methods and the analysis of the spectral lines are treated in chapter IV. Finally, a summary of results is presented in Chapter V, with a comparison with previous work, and recommendations for future work.

CHAPTER II

ANALYSIS TECHNIQUES FOR SPECTRAL LINE SHAPES

Line Shapes

The analysis of a spectral line relies upon the model used to describe the shape, or profile, of that line. In the analysis of collisionally broadened spectral lines, a Voigt profile is usually assumed to be the model for the line shape. The Voigt profile itself is actually a convolution of two profiles, the Doppler profile and the Lorentz profile. To understand the use of a Voigt profile, it is necessary to first describe the Doppler and Lorentz profiles. The definitions for the profiles given are found in Smith et al. (49) and Penner (50), with this discussion following Smith et al. (49).

Let a line profile function be defined by $f(\nu - \nu_0)$ with ν_0 being the frequency at the line center in units of cm^{-1}. A Doppler profile can be described by

$$f(\nu - \nu_0) = P \exp[-(\ln 2)((\nu - \nu_0)/b_D)^2] \tag{2.1}$$

where

$$P = (1/b_D)((\ln 2)/\pi)^{1/2} \tag{2.2}$$

and b_D (cm^{-1}) is the Doppler half-width at half maximum HWHM of the line. b_D may be calculated from

$$b_D = 3.581 \text{ x } 10^{-7} \nu_0 (T/M)^{1/2} \tag{2.3}$$

where T is the temperature in degrees Kelvin, and M is the molecular weight of the absorbing gas in amu's. A Doppler profile describes the broadening of a line due to the thermal random motions of the molecules. This profile can be assumed, for example, when low pressure (e.g. < 1 torr) measurements of acetylene are made to calculate line intensities.

The Lorentz profile is given by

$$f(\nu - \nu_0) = (b_L/\pi)/[(\nu - \nu_0)^2 + b_L^2] \tag{2.4}$$

and b_L (cm^{-1}) is the Lorentz HWHM. The Lorentz profile is used as the model for a line shape when the spectral line is predominately collisionally broadened. When collisional

broadening measurements are conducted, and a gas such as acetylene (at low pressure) is mixed with a perturbing gas, the C_2H_2 spectral lines contain significant Doppler broadening as well as collisional broadening. The Voigt profile, which is the convolution of a Doppler profile and a Lorentz profile, is a reasonable model to describe collisionally broadened spectral lines.

The Voigt profile is defined by

$$f(\nu - \nu_0) = PK(\mathrm{x},\mathrm{y}) = (P\mathrm{y}/\pi)\int_{-\infty}^{\infty} \frac{e^{-t^2}}{\mathrm{y}^2 + (\mathrm{x}-t)^2}dt \tag{2.5}$$

where

$$\mathrm{x} = [(\nu - \nu_0)/\mathrm{b_D}](\ln 2)^{1/2} \tag{2.6}$$

$$\mathrm{y} = (\mathrm{b_L}/\mathrm{b_D})(\ln 2)^{1/2} \tag{2.7}$$

are the dimensionless Voigt parameters and K(x,y) is the Voigt function.

Using the Voigt profile, b_D and ν_0 for each line, and with some basic measurements from the spectral lines themselves, it is possible to retrieve from the collisional broadening measurements the parameters desired. These parameters are the half-width at half maximum and the peak height, or intensity.

Determination of Intensity from Spectral Lines

The intensity of a spectral line is described in the following manner. The transmission of radiation through a gas sample is described by the Beer-Lambert Law

$$\mathrm{I} = \mathrm{I_0}e^{-k(\nu)x} \tag{2.8}$$

An example of this situation would be the transmission of IR radiation from a tunable diode laser through an absorption cell. $\mathrm{I_0}$ is the intensity of the radiation source when there is complete transmission. The parameter x is called the optical density. The optical density is related to the pressure p of the gas sample, and the path length l which the radiation traverses through the gas sample, or

$$x = \mathrm{pl} \tag{2.9}$$

Finally, $\mathrm{k}(\nu)$ is the absorption coefficient and is related to the line profile function by

$$k(\nu) = Sf(\nu - \nu_0) \tag{2.10}$$

where S is the line intensity.

Referring to Equation (2.8) let the transmittance, τ, of the radiation through the gas sample be defined by

$$\tau(\nu) = \mathrm{I}(\nu)/\mathrm{I}_0 = e^{-k(\nu)x} \tag{2.11}$$

The transmittance, which is actually the contour of the line profile, can be seen in Figure 2.1, and may be written

$$\tau(\nu) = y/y_1 \tag{2.12}$$

At the center of the line, $\nu=\nu_0$, and

$$\tau(\nu_0) = y_0/y_1 \tag{2.13}$$

The line intensity can now be found in terms of τ for a particular line profile. Substituting Equation (2.10) into (2.11) gives

$$\tau(\nu) = e^{-Sf(\nu-\nu_0)x} \tag{2.14}$$

For a Doppler profile, at $\nu=\nu_0$, Equation (2.1) becomes

$$f(\nu - \nu_0) = P \tag{2.15}$$

Substituting this into Equation (2.13)

$$\tau(\nu_0) = e^{-SPx} \tag{2.16}$$

or

$$S = (1/Px)\ln(1/\tau(\nu_0)) \tag{2.17}$$

S can be similarly obtained for the Lorentz and Voigt profiles. For the Voigt profile, from Equation (2.5) at $\nu = \nu_0$

$$\tau(\nu_0) = e^{-SPxK(0,\mathrm{y})} \tag{2.18}$$

or

$$S = (1/PxK(0,\mathrm{y}))\ln(1/\tau(\nu_0)) \tag{2.19}$$

For a Doppler profile, S may be found from Equation (2.17) with the measurement for τ following Figure 2.1. For collisional broadening measurements, the line intensity may

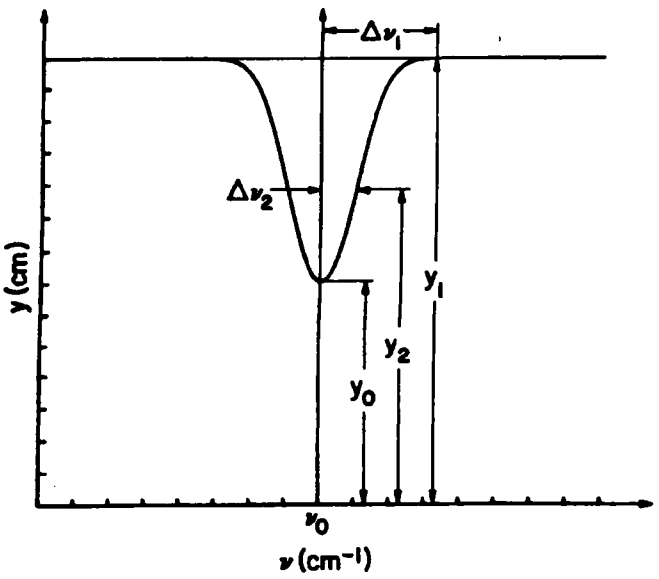

Source: M. A. H. Smith et al., "Molecular Spectroscopy: Modern Research, Volume III," Chapter 3, K. N. Rao, Ed., Academic Press, New York, 1985.

Figure 2.1: Example of a spectral line and the measurements needed to determine the intensity and the HWHM.

be determined from Equation (2.19). In this case the Voigt function, K(0,a), must be calculated. Tabulations have been made for the Voigt function for various values of the variables (51), and FORTRAN programs have been published to calculate K(x,y) for any set of values (52).

Determination of HWHM from Spectral Lines

The second parameter that can be determined from a spectral line is the HWHM. The point where the HWHM is measured is where

$$k(\nu) = (1/2)k(\nu_0) \tag{2.20}$$

Again referring to Figure 2.1, $\tau(\Delta\nu_2)$ at this point, y_2, would be

$$\tau(\Delta\nu_2) = y_2/y_1 \tag{2.21}$$

Substituting Equation (2.20) into (2.21), gives

$$y_2 = y_1\tau(\Delta\nu_2) = y_1 e^{-k(\nu_0)x/2} = y_1[e^{-k(\nu_0)x}]^{1/2} = y_1[\tau(\nu_0)]^{1/2} \tag{2.22}$$

If the transmission is normalized (i.e. y_1=1), y_2 is reduced to

$$y_2 = [\tau(\nu_0)]^{1/2} \tag{2.23}$$

Thus a proper measurement of τ is necessary for a proper determination of the HWHM of the line.

In the case of intensity measurements, where low pressures (<1 torr) of the gas are used, the spectral profile assumed is a convolution of the Doppler broadening plus the component attributed to the instrument function. The Doppler HWHM may be found from the measured HWHM of the profile by

$$b_{obs}^2 = b_D^2 + b_I^2 \tag{2.24}$$

where b_I is the instrument HWHM (53). A Voigt profile is similarly a convolution of two profiles– a Doppler profile and a Lorentz profile. In collisional broadening work it is necessary to retrieve from the measured Voigt HWHM, b_V, the contribution due to collisional broadening, b_L. An empirical equation has been developed by Whiting (54), and modified by Olivero and Longbothum (55), to retrieve b_L from the measured HWHM of the Voigt profile. The modified equation is

$$2b_V = 1.0692b_L - [0.86639b_L^2 + 4b_D]^{1/2} \tag{2.25}$$

which, with some algebra and re-arrangement, becomes

$$b_L/b_V = 7.7255 - 6.7255[1 + 0.3195(b_D/b_V)^2]^{1/2} \tag{2.26}$$

By measuring the HWHM of a broadened line, b_V, and calculating b_D using Equation (2.3), the collisional contribution to that HWHM, b_L may then be retrieved using Equation (2.26).

Wing Corrections to Broadening Measurements

The values determined for the HWHM and the intensity rely on the determination of the transmittance. The value determined for τ, in turn, relies upon the determination of the 0% transmission and 100% transmission lines. In Figure 2.1, 0% transmission would be at y=0 and 100% transmission would be at $y = y_1$. The 100% transmission line, also

called the baseline, is drawn into wings of the spectral line. In collisional broadening measurements, where the line has been broadened, and more of the profile is spread into the wings of the line, it is important to properly position the baseline. Generally, positions for the baseline and 0% transmission are visually marked, whether by hand or computer, and may result in imprecise positioning. Fridovich has presented a method for correcting HWHM measurements for an improper position in the baseline (49),(56). While these corrections may be applied to Doppler, Lorentz, or Voigt profiles, the following discussion, from Smith et al. (49) and Fridovich (56), describes corrections to collisional broadened (Voigt) profiles.

Figure 2.2 shows graphically how wing corrections to the HWHM are determined. The corrections are based on the shape of the profile assumed and the position where the baseline is initially determined. In the case of correcting the HWHM of a Voigt profile, $\tau(\nu_0)$ is determined, and using the contour of a Voigt profile, $\tau(g)$ is calculated, where g (cm^{-1}) is the original baseline position. The value of $\tau(g)$ is used to correct the baseline. ($\tau(g)$ should equal 1 at 100% transmission if the baseline is correctly placed. The difference between 1 and the calculated value of $\tau(g)$ determines how much the baseline needs to be corrected.) The correction in the baseline, which moves the baseline from b to b$'$, leads to a correction in the position of the HWHM. The HWHM position is moved from c to c$'$. However, rather than re-calculate a new HWHM, this method takes the slope of the Voigt profile at the initial position of the HWHM and calculates the increment added to the HWHM produced by moving from c to c$'$.

To determine this correction to the HWHM, some relationships from Figure 2.2 must first be defined. The original transmittance is

$$\tau(\nu_0) = a/\mathrm{b} \tag{2.27}$$

The transmittance at the baseline position may be defined

$$\tau(g) = \mathrm{b}/\mathrm{b}' \tag{2.28}$$

and the new transmittance, caused by the correction, can be written, using Equations (2.27) and (2.28)

$$\tau'(\nu_0) = a/\mathrm{b}' = \tau(\nu_0)\tau(g) \tag{2.29}$$

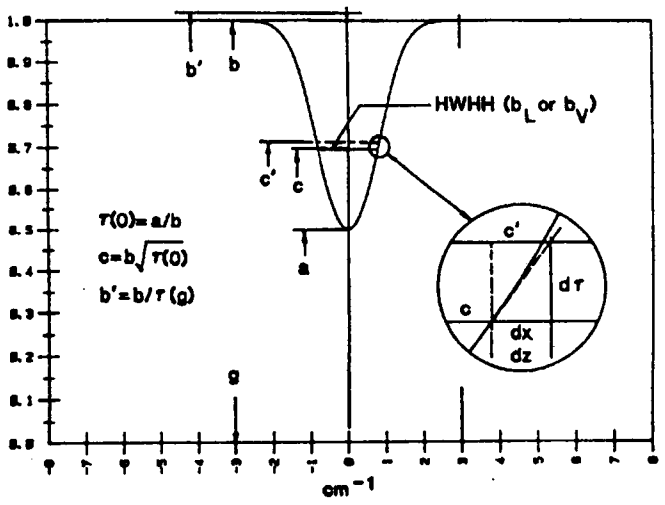

Source: B. Fridovich, *J. Mol. Spectrosc.* **105**, 53-60 (1984).

Figure 2.2: Diagram showing the measurements used to wing correct spectral profiles.

The position of the new HWHM may be determined at (compare with Equation (2.22) for the original HWHM position determination)

$$c' = \mathrm{b}'[\tau'(\nu_0)]^{1/2} = c/[\tau(g)]^{1/2} \tag{2.30}$$

Finally, the change in transmittance may be written

$$\Delta\tau = (c' - c)/\mathrm{b} \tag{2.31}$$

Using Equations (2.29) and (2.30), Equation (2.31) may be written in terms of the original measurements

$$\Delta\tau = [\tau'(\nu_0)]^{1/2}\{[\tau(g)]^{-1/2} - 1\} \tag{2.32}$$

Equation (2.32) is the change in transmittance due to the correction, and will now be used to determine the change, or correction, in the HWHM.

For a Voigt profile, using Equations (2.5) and (2.11), the transmittance may be written

$$\tau(\nu) = e^{-SPxK(\mathrm{x,y})} \tag{2.33}$$

Taking the derivative of Equation (2.33) leads to

$$d\tau(\mathrm{x,y}) = (-SPx)(\tau(\mathrm{x,y}))[(\partial K/\partial \mathrm{x})dx + (\partial K/\partial \mathrm{y})dy] \tag{2.34}$$

From Equations (2.6) and (2.7) dx and dy may be found

$$dx = (d\mathrm{b_V}/\mathrm{b_D})(\ln 2)^{1/2} \tag{2.35}$$

$$dy = (d\mathrm{b}_L/\mathrm{b_D})(\ln 2)^{1/2} \tag{2.36}$$

with $x=x(b_V)$. Now dy can be found in terms of dx. Writing

$$dy = (dy/d\mathrm{b}_L)(d\mathrm{b}_L/d\mathrm{b_V})(d\mathrm{b_V}/dx)dx \tag{2.37}$$

and substituting Equations (2.35) and (2.36) into Equation (2.37) gives

$$dy = (d\mathrm{b}_L/d\mathrm{b_V})dx \tag{2.38}$$

dx and dy can now be substituted into the change in transmittance Equation (2.34)

$$(d\tau(\mathrm{x},\mathrm{y})/dx) = (-SPx)(\tau(\mathrm{x},\mathrm{y}))[(\partial K/\partial \mathrm{x}) + (\partial K/\partial \mathrm{y})(d\mathrm{b}_L/d\mathrm{b_V})] \tag{2.39}$$

The correction $\Delta\nu$ to the HWHM may now be estimated as

$$\Delta\nu = \Delta\tau/(d\tau/d\nu) \tag{2.40}$$

which can be written

$$\Delta\nu = \frac{\Delta\tau}{(d\tau/dx)(dx/d\nu)} \tag{2.41}$$

$(dx/d\nu)$ can be found from Equation (2.6) and substituting into Equation (2.41)

$$\Delta\nu = \frac{\Delta\tau}{(d\tau/dx)((\ln 2)^{1/2}/\mathrm{b}_D)} \tag{2.42}$$

$\Delta\tau$ from Equation (2.32) and $(d\tau/dx)$ from Equation (2.39) can now be substituted into Equation (2.42).

$$\Delta\nu = \frac{-\mathrm{b}_D}{(SPx)(\ln 2)^{1/2}} \frac{[\tau(g)]^{-1/2} - 1}{[(\partial K/\partial \mathrm{x}) + (\partial K/\partial \mathrm{y})(d\mathrm{b}_L/d\mathrm{b_V})]} \tag{2.43}$$

with $\tau(\mathrm{x},\mathrm{y})$ evaluated at the position of the corrected HWHM b_V.

One final approximation is made. Since $[\tau(g)] \approx 1$, the exponential can be expanded in Equation (2.33) to give

$$\tau(g) \simeq 1 - (SPx)K(\mathrm{x_g},\mathrm{y}) \tag{2.44}$$

which gives

$$[\tau(g)]^{-1/2} \simeq [1-(SPx)K(\mathrm{x_g},\mathrm{y})]^{-1/2} \simeq 1+(1/2)(SPx)K(\mathrm{x_g},\mathrm{y}) \tag{2.45}$$

So that the correction to the HWHM may be written in the final form

$$\Delta\nu = \frac{-\mathrm{b}_D}{2(\ln 2)^{1/2}} \frac{K(\mathrm{x_g},\mathrm{y})}{[(\partial K/\partial \mathrm{x})+(\partial K/\partial \mathrm{y})(d\mathrm{b}_L/\mathrm{dbv})]} \tag{2.46}$$

Note that the Voigt function in the numerator of Equation (2.46) is evaluated at the baseline position, x_g, while the partial differential of K with respect to x in the denominator is evaluated at x=b_V. The derivative $(d\mathrm{b}_L/\mathrm{dbv})$ may be found analytically, or by using a delta method, with Equation (2.26). An approximation given by BelBruno (57) for the Voigt function may be used to calculate K(x,y) in the numerator of Equation (2.46), and used with a Delta method to calculate the partial differentials in the denominator. This approximation for the Voigt function is

$$K(\mathrm{x},\mathrm{y}) = \mathrm{y}\sum_{j=1}^{3} \frac{A_j(\mathrm{x}^2+\mathrm{y}^2+B_j)}{(\mathrm{x}^2+\mathrm{y}^2+B_j)^2-4\mathrm{x}^2B_j} \tag{2.47}$$

A_1=0.4613135 B_1=0.1901635

A_2=0.09999216 B_2=1.7844927

A_3=0.00288384 B_3=5.5253437

The accuracy of the approximation is stated to be 0.0002% for x>3.9, y>3 (57).

For a Voigt profile, then, the new HWHM b_V' is

$$\mathrm{b}_V' = \mathrm{b}_V + \Delta\nu \tag{2.48}$$

with the new b_L being calculated from Equation (2.26). The broadening coefficient defined by

$$\gamma_L^0 = \mathrm{b}_L/\mathrm{p} \tag{2.49}$$

is simply b_L divided by the pressure, with pressure in units of atm. γ_L^0 ($\mathrm{cm}^{-1}\mathrm{atm}^{-1}$) is the quantity usually used in reporting HWHM measurements of broadened spectral lines.

Sample/Background Ratio Method

An alternate method, the sample/background ratio method, may also be used in determining the baseline and 0% transmission level positions. Rather than actually replacing the previous wing correction method, this second independent method could be used to give some confidence in the final values determined from the wing corrections for the b_L.

The sample/background ratio method relies on taking a background, or evacuated cell, measurement. Using the sweep integration technique of Jennings (1) with a mechanical shutter (to be discussed in Chapter III), the baseline and 0% transmission level are defined by the signal received. A gas sample may then be added to the cell and the usual measurements obtained. By taking the ratio of a recorded sample measurement with the background measurement, the sample profile is normalized between the 0% and 100% transmission levels. This method, which will be discussed in more detail in Chapter IV, depends on their being little variation in the output of the recorded signal over time.

Temperature Dependence of Spectral Line Measurements

A spectral line measurement depends upon the temperature at which it is measured. In the case of HWHM broadening measurements, this temperature dependence may be written as

$$\gamma_L^0(T)/\gamma_L^0(T_0) = (T_0/T)^n \tag{2.50}$$

where T_0 is a reference temperature, which is usually room temperature (58). A linear fit of $\ln T$ versus $-\ln \gamma_L^0$ may be made to determine n.

For the intensity temperature dependence of a spectral line, the intensity of a line at one temperature T_a is related to the intensity of the same spectral line at another temperature T_b by (23),(59)

$$\frac{S_J(T_b)}{S_J(T_a)} = \frac{N(T_b)}{N(T_a)} \exp\left[\frac{-(E_v + E_r)}{k[(1/T_b) - (1/T_a)]}\right] \frac{Q_v(T_a)Q_r(T_a)}{Q_v(T_b)Q_r(T_b)} \left[\frac{1 - \exp(-\frac{hc\nu_{AB}}{kT_b})}{1 - \exp(-\frac{hc\nu_{AB}}{kT_a})}\right] \tag{2.51}$$

where N is the total population of molecules, $Q=Q_vQ_r$ the total partition function and E_v and E_r are, respectively, the vibrational and rotational energy terms. ν_{AB} is the transition frequency in cm^{-1}, with A being the lower quantum state of the transition, and B being

the higher quantum state. The total band intensity of a particular band may be found by using Equation (2.51) and summing over all intensities belonging to that band.

Some substitutions may be made into Equation (2.51). The rotational partition function may be approximated by

$$\frac{Q_r(T_a)}{Q_r(T_b)} = \left[\frac{T_a}{T_b}\right]^f \tag{2.52}$$

with f=1 for linear molecules and f=3/2 for non-linear molecules.

Also, the number density ratio may be written as

$$\frac{N(T_b)}{N(T_a)} = \left[\frac{T_a}{T_b}\right]^g \tag{2.53}$$

where g=1 for the intensity in units of cm^{-2} atm^{-1} and g=0 for the intensity in units of cm/molecules.

Substituting Equations (2.52) and (2.53) into (2.51) gives

$$\frac{S_J(T_b)}{S_J(T_a)} = \left[\frac{T_a}{T_b}\right]^p \exp\left[\frac{-(E_v + E_r)}{k[(1/T_b) - (1/T_a)]}\right] \frac{Q_v(T_a)}{Q_v(T_b)} \left[\frac{1 - \exp(-\frac{hc\nu_{AB}}{kT_b})}{1 - \exp(-\frac{hc\nu_{AB}}{kT_a})}\right] \tag{2.54}$$

where $p = f + g$. With the units of cm^{-2} atm^{-1} for intensity, p=5/2 for non-linear molecules and p=2 for linear ones.

CHAPTER III

EXPERIMENTAL SET-UP

The acquisition of the spectral lines in this investigation was made possible with two tunable diode laser spectrometer systems: one at UTK and one at SUNY. Previous descriptions may be found in Chin (25) and Blass and Chin (24) for the UTK set-up and Varanasi and Chudamani (38) for the SUNY set-up. Differences in the systems will be noted, with this discussion divided into three sections: optics and alignment, wavenumber calibration, detection and acquisition, and gas handling and vacuum systems.

Optics and Alignment

Figure 3.1 shows the energy path of the diode laser energy through the UTK optical system. The diode laser itself has the following specifications

Operating Conditions	I=1226 mA at ν=721 $cm^{-1}$and T=47 K
Wavenumber Range	650 cm^{-1}(threshold) to 750 cm^{-1}
Power	> 0.01 mW

A diode in the 950 cm^{-1} wavenumber range was used with the SUNY system, with wavenumber defined as inverse wavelength (cm^{-1}). The laser in both systems was cyrogenically cooled using a closed cycle helium refrigerator manufactured by Laser Analytics.

The tuning of a diode laser is made possible by changing the excitation current and temperature of the diode. As mentioned previously, this tuning allows the TDL to emit energy at different frequencies making it possible to look at the different rotational-vibrational energy transitions of molecules. Different diodes, that can each lase over a range of about 100 cm^{-1}, may be used for work in various wavelength ranges. The diodes are lead-salt compounds, and the operating range may be changed by varying the salt composition (1).

Energy emitted from the tunable diode laser in the UTK system is collimated by a 26.7 cm spherical focusing mirror and is reflected onto three flat mirrors placed in succession. The energy then hits a 121.9 cm focal length mirror, passes through the absorption cell, and comes to a focal point at the position of the rotating shutter. The absorption cell

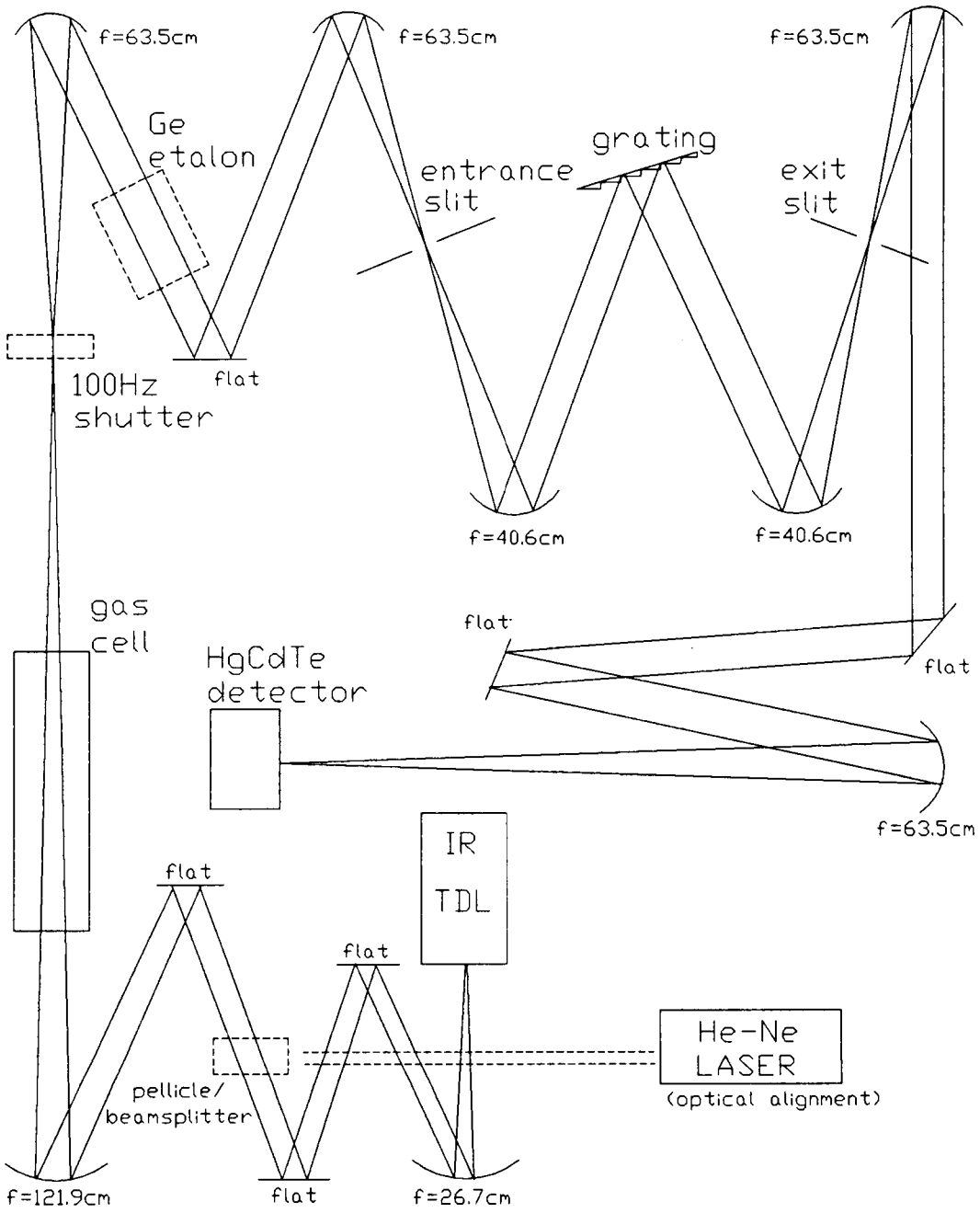

Figure 3.1: Schematic diagram of the IR energy path of the UTK tunable diode laser spectrometer system.

used in the UTK measurements was a 48 cm brass cell with KBr windows. The shutter, rotated with a stepping motor at the frequency of 100 Hz, is used in determining the 0% transmission (100% absorption) level of the spectral signal. The shutter will be discussed in the detection and acquisition section.

The energy beam diverging from the focal point at the shutter is collimated by a 63.5 cm mirror, reflects upon a flat, and is focused by another 63.5 cm mirror on the entrance slit to the mode selection grating monochromator. The grating monochromator, or optical band-pass filter, is needed to isolate a single lasing mode of the TDL. The grating disperses the energy incident upon it, and by rotating the grating, a particular energy frequency range is allowed to continue through the system to the detector. The grating used is 5 cm wide and has 75 rulings per mm with a blaze angle of 26 degrees, 45 minutes.

Passing through the entrance slit of the monochromator, the energy beam is collimated once again before being dispersed by the grating, and is then re-focused by another mirror onto the exit slit to the monochromator. The energy beam emerging from the exit slit is re-collimated one last time, reflects on two flats, and is focused on the detector by a 63.5 cm focusing mirror. This last focusing mirror is placed on a positioning stage to provide for fine focus adjustment of the energy upon the detector. The detector, a HgCdTe element from Santa Barbara Research, is 1 mm wide by 3 mm long, and has a 30° field of view as mounted in the dewar. The detector window is made of Thallium Iodide Bromide (KRS-5). The detector is liquid nitrogen cooled, and the nitrogen is refilled approximately every one and a half days during operation.

The SUNY optical set-up is shown in Figure 3.2. An off-axis parabolic mirror is used to collimate and focus the energy directly after it is emitted from the TDL. A tuning fork chopper, at 400 Hz, is mounted at the entrance slit of the monochromator and is used in the determination of the 0% transmission level of the spectral line. The energy passes through the entrance slit and enters the monochromator. The grating in this system is rotated by a barrel drum.

The diverging energy beam emerging from the exit slit of the monochromator is collimated using another off-axis parabolic mirror. The beam then passes through a mechanical chopper (shutter) and through the absorption cell. The beam is focused by one

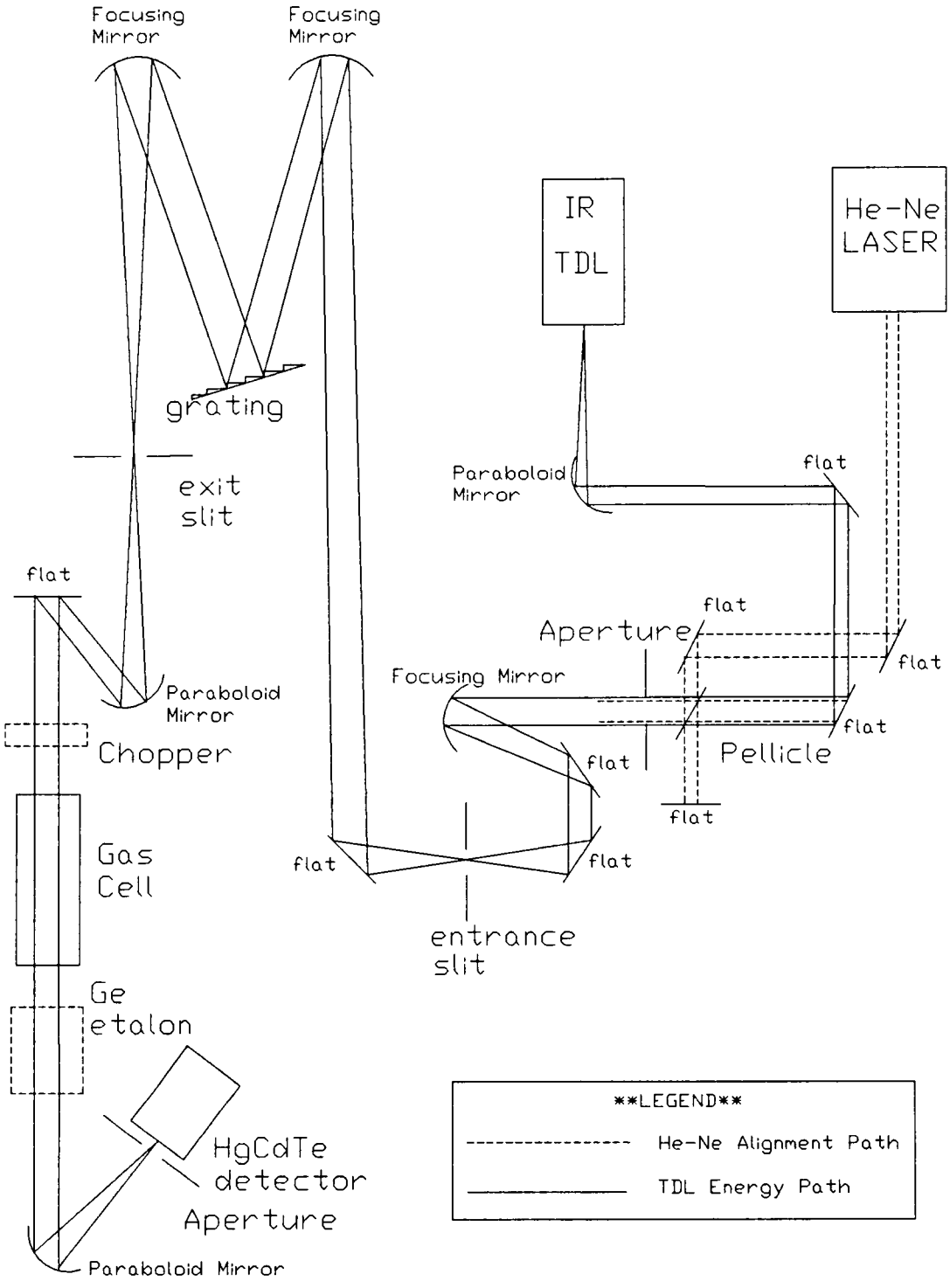

Figure 3.2: Schematic diagram of the IR energy path of the SUNY tunable diode laser spectrometer system.

last off-axis parabolic mirror onto the HgCdTe detector, also from Santa Barbara Research.

The positions of a He-Ne laser, pellicle and beamsplitter used in alignment of the UTK optical system are shown in Figure 3.1. (These are not in the system during regular operation.) The alignment set-up is shown in detail in Figure 3.3. By placing a slit at the position of the detector, replacing the grating with a mirror, and using two extra flats, the optics can be aligned, forward and backward through the system, with the use of one He-Ne laser.

In the design of the alignment system, the detector was placed on a set of moveable rails that permitted it to be easily moved out of its position and a slit, mounted beside the detector, could be placed in the optical path. A mirror replaces the grating so that a stronger He-Ne laser signal may be sent through the system. Following Figure 3.3, the He-Ne signal leaves the laser and proceeds forward to the pellicle and beamsplitter. Herein forward denotes the signal going through the system in the same direction as the TDL energy path, with backward being the opposite. Forward is shown in Figure 3.3 by solid arrows and the backward direction is shown by dashed arrows.

When the He-Ne beam reaches the pellicle some of the energy proceeds forward through the system. The rest of the energy passes through the pellicle and is incident upon the beamsplitter. Using two extra flat mirrors, the energy passing through the beamsplitter is directed to the alignment slit and in the backward direction through the system. The energy not passing through the beamsplitter is redirected back toward the TDL itself to align the three mirrors directly before the TDL. Alignment of the entire system is achieved when the light moving, backward and forward, through the system is coincident. (i.e. the forward and backward reflections of the He-Ne laser signal on the mirrors should all lie on top of each other.)

When the alignment is completed, it should be possible to replace the detector in the energy path, turn on the TDL, and receive a signal at the signal averager from the detector. Fine adjustment, in order to receive the strongest possible signal, may be made by adjusting the 63.5 cm focal length mirror directly before the detector, or the 26.7 cm mirror directly in front of the TDL. The absorption cell and the entrance and exit slits are

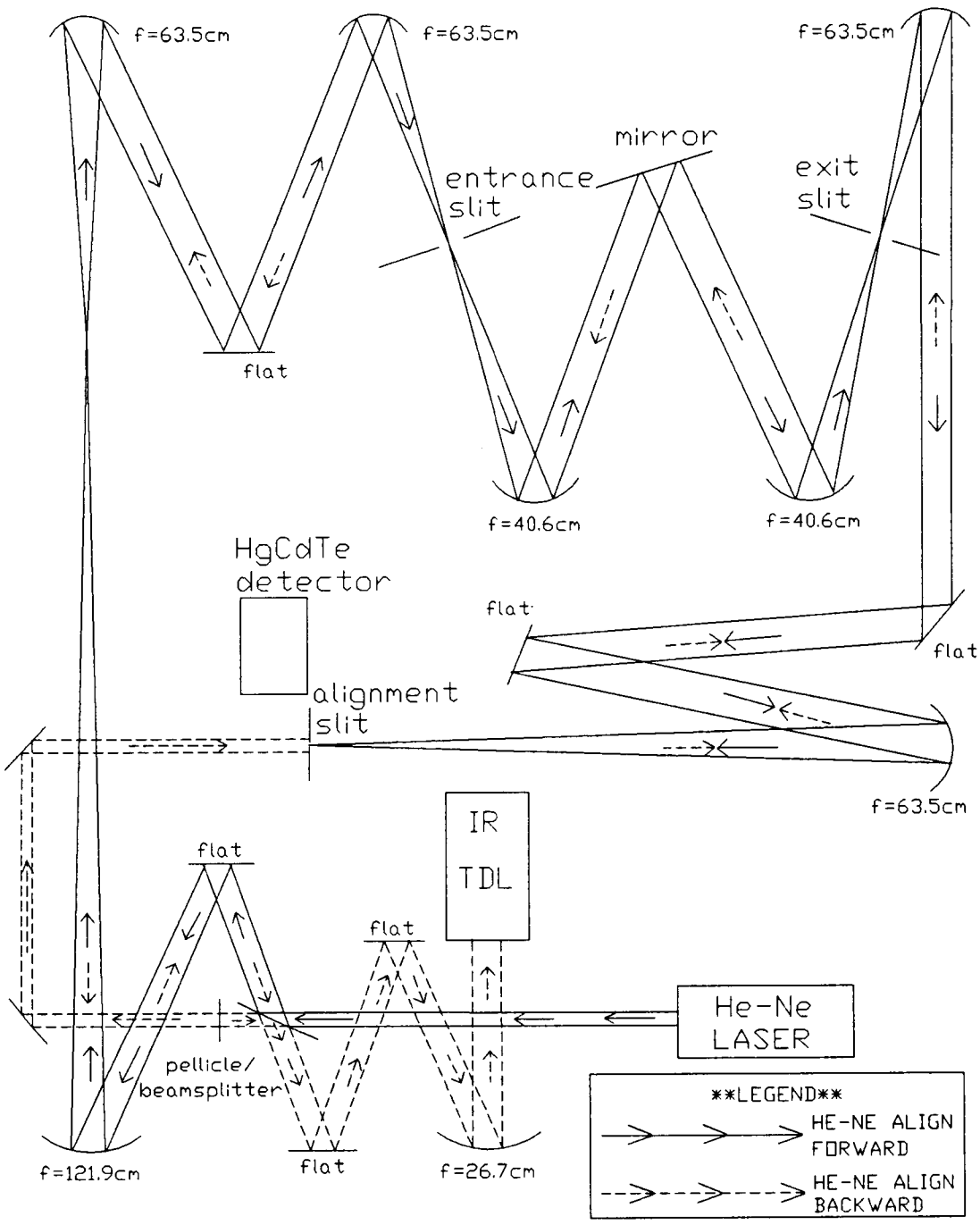

Figure 3.3: Schematic diagram of the optical alignment set-up of the UTK tunable diode laser spectrometer system.

also usually taken out of the optical set-up if more than fine adjustment is being made, and these can now be replaced. The slits are closed completely, and are then opened to approximately 2.0 mm by turning the micrometer adjustment on the slits . It should be noted that non-parallel window surfaces of the absorption cell may move the image at the detector, so that by rotating the absorption cell parallel with the central axis, a stronger or weaker signal may be observed.

The alignment of the SUNY system, shown in the optical set-up of Figure 3.2, is similar to the UTK work, and also uses a pellicle and two extra flat mirrors. These are positioned so that the He-Ne laser beam may be sent forward through the system as well as back toward the TDL. A mirror is also used in the alignment system, and is placed in front of the grating so that a stronger signal may be sent through the optics.

After the optics are aligned, the pellicle and extra mirrors are removed. Fine adjustment of the TDL signal is then made by using two apertures, one between the TDL and the monochromator entrance slit positions, and one directly before the detector. By narrowing the first aperture opening, the position of the first off-axis parabolic mirror may be adjusted, by an x-y-z mount, to send maximum energy through aperture and hence the system. Fine tuning is also possible by adjusting the last mirror before the detector.

Frequency Calibration

Before measurements may be taken with the UTK spectrometer system, the grating has to be correctly positioned in the beam path. (For the SUNY system, a wavenumber verses position calibration of the grating is provided by the commercial supplier.) The grating is rotated by a set of gears that are driven by a stepping motor (Figure 3.4). The stepping motor is PC (XT) driven by a model SC-149 smart stepping controller card. The A-Bus motherboard, used with the controller card, has the capacity to control four separate stepping cards and motors. The motor used with the grating is a Superior Electric synchronous stepping motor, model M061-FCO8, with the following specifications: 1.4 Volts, 3.8 Amps and 200 steps/revolution. A program written in QuickBasic is used to drive the stepping motor. Rather than move the stepping motor in units of steps, a calibration of wavelength versus step number is made with the use of a He-Ne laser.

The He-Ne laser which is used in the alignment of the optics is used to calibrate the

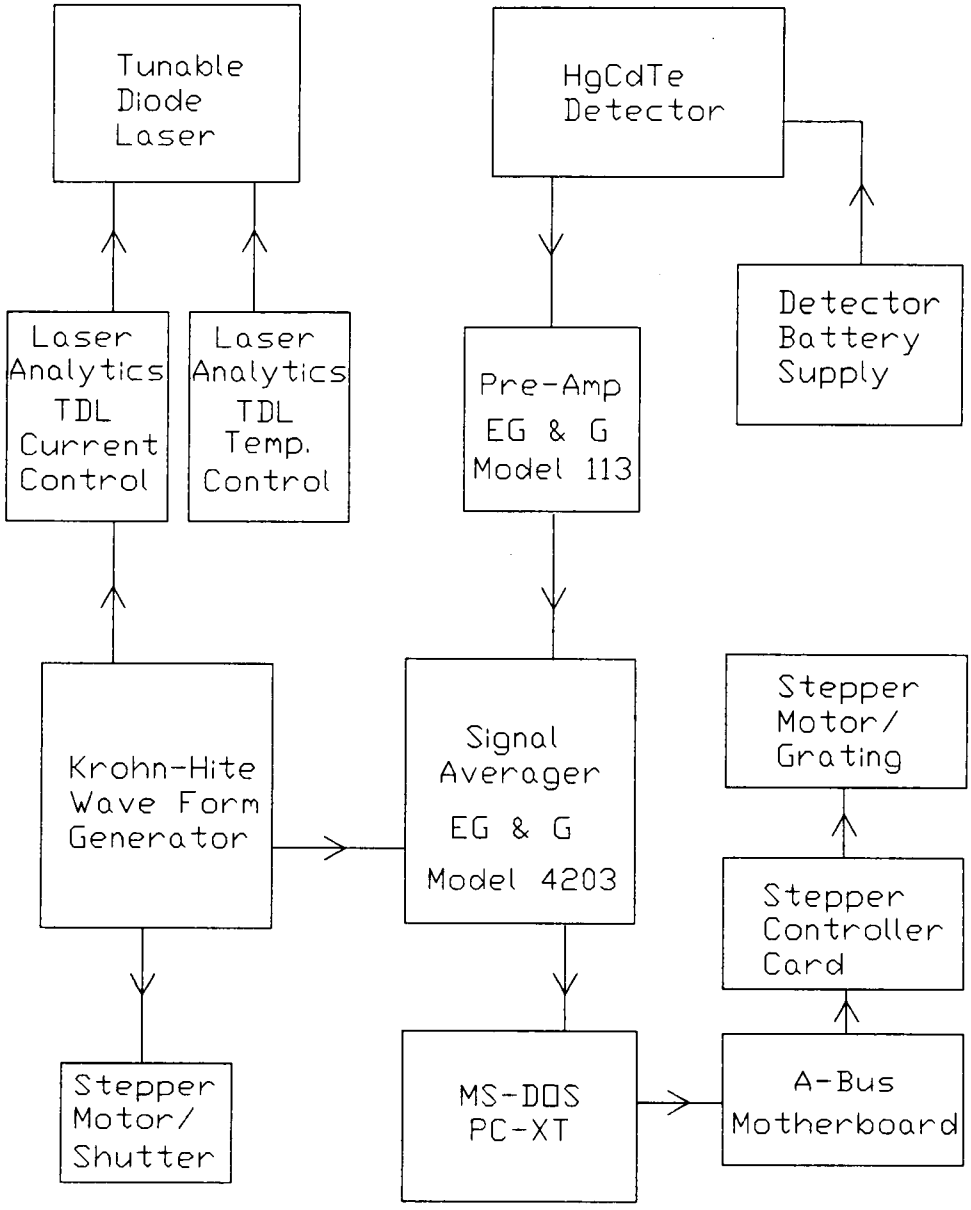

Figure 3.4: Schematic diagram of the UTK TDL detection and data acquisition system.

grating position. With the exit slit of the monochromator closed, the grating is moved to where the central image (zeroeth order) is reflected to the exit slit of the monochromator. This order should be the brightest order dispersed from the grating. A white light source may be used as an aid in finding the central order. Shining the white light source through the entrance slit, the grating is moved to central image, which is where the white light image is incident upon the exit slit. This position is defined as the zeroeth step number. The wavenumber versus step number calibration is then made using the orders of the He-Ne laser dispersed by the grating.

With the central image at step number zero, the grating is moved to where the first order is incident upon the exit slit. The step number of this position is recorded. The grating is then moved to where the second order is incident upon the exit slit. The step number positions are recorded to approximately thirty orders of the dispersed light of the He-Ne laser. The wavenumber $\tilde{\nu}$ (again inverse wavelength in units of cm^{-1}) at the nth order number is

$$\tilde{\nu} = \frac{1}{\lambda n}\left(\frac{10^8 \mathring{A}}{cm}\right) \tag{3.1}$$

with the wavelength of emission from the He-Ne laser, λ=6328$\mathring{A}$. The order number and its corresponding wavenumber are then input into a calibration submenu of the PC program that uses a cubic spline to make an interpolation with the data and produce a $\tilde{\nu}$ versus step number calibration. It is then possible to move the grating by wavenumber rather than step number. This is useful since the spectral line positions of molecules are known in terms of the units cm^{-1}.

The wavenumber calibration of the grating aids in the determination of the position of a particular spectral line. Calibration of the linewidths themselves may be carried out using the fringes of an etalon. A germanium etalon was used in both the UTK and SUNY set-ups. The high refractive index of Ge (n=4) results in a small free spectral range. The free spectral range (the spacing of the fringes) may be found from

$$\Delta\nu = \left[\frac{1}{2nl}\left(1 - \frac{\lambda}{n}\frac{\partial n}{\partial \lambda}\right)\right] \tag{3.2}$$

where l is the cavity length, n is the index of refraction, and λ is the wavelength of the energy (25). After a set of measurements are completed, the germanium etalon is placed

after the first 63.5 cm mirror in the UTK set-up (Figure 3.1) and another measurement is made, recording the etalon fringes. In the SUNY system the etalon is put directly after the absorption cell (Figure 3.2). Both etalons are enclosed in a brass housing which acts as a heat sink. The brass heat sink minimizes the variation of the fringe spacing caused by ambient temperature variations (24). In the analysis of the spectral lines, the etalon recording is superimposed upon the spectral line measurements and the linewidth is calibrated, knowing the spacing of the fringes. This will be discussed in Chapter IV.

Detection and Acquisition Systems

The broadening data was acquired at both UTK and SUNY using the sweep integration technique of Jennings (1). In the UTK system, sweep integration is performed by modulating the TDL current, at 100 Hz, with a sawtooth waveform from the Krohn-Hite waveform generator, model 5400B (Figure 3.4). The rotary motion of the mechanical shutter and the scanning period of the signal averager are synchronized by the trigger output of the waveform generator. When the waveform generator produces a negative going ramp, it also produces a trigger pulse. This pulse triggers the signal averager to scan at the beginning of a current-tuned phase of the laser. Simultaneously the shutter is modulated by the waveform generator at 100 Hz. The shutter, rotated with a stepping motor, 'opens' and 'closes' so that during 80% of the signal averager recording time the energy beam is allowed to go onward through the system. For the other 20% of the time, the shutter is 'closed' and does not allow the beam to continue any farther. During this time no energy is incident upon the detector, and this may be seen at the signal averager as the 100% absorption (0% transmission) level (25). The shutter stepping motor is a model M061-FC08 with the same specifications as the stepping motor used to drive the grating.

In a single scan, the signal from the detector is amplified by a Princeton Applied Research model 113 broadband preamplifier. The output signal is fed directly to the signal averager, where successive sweeps, or recordings, are averaged together. The number of averaged sweeps is determined by the signal averager. Exponential averaging, 2^6, is used while tuning the diode laser system in order to quickly see changes, while normal averaging is conducted during actual measurements. Typical measurements used $\sim$ 4000 scans. The signal averager is a model 4203 from Princeton Applied Research with a model 4001 scope.

While the SUNY system also used the sweep integration technique, there are several differences in the two systems (Figure 3.5). The shutter is used to trigger the scanning cycle rather than the wave generator (38). The frequency of the chopper is set at 400 Hz in this system, and the shutter blocks the energy beam for half the cycle to provide for the 0% transmission level. The signal from the liquid nitrogen cooled HgCdTe detector is amplified by a low-noise a.c.-coupled preamplifier and recorded on a PC (AT). The computer is equipped with a high speed data acquisition board, which is a 12 bit analog to digital converter from RC-Electronics. When the chopper is operating at 400 Hz, the signal averager can collect up to 2048 data points per sweep.

Receiving the best possible signal from a TDL requires adjustments of several parameters in the system. With gas in the absorption cell, the current and temperature controls are initially adjusted until the TDL lases at a rotational-vibrational transition of the molecule of interest. The TDL signal is fine tuned with the use of the current and temperature controls, fine adjustment of the optics, and movement of the grating. The UTK and SUNY systems both use a current controller from Laser Analytics, model LCM, and a temperature controller, also from Laser Analytics, model CTS. The UTK TDL system is tuned for maximum signal and mode purity by using the averaged output at the signal averager. With the SUNY system, an oscilliscope is used in conjunction with a tuning fork chopper at a frequency of 400 Hz to assure a single clean mode. The gas pressure is increased in the absorption cell until the line is saturated, which means at the line center the energy from the TDL is completely absorbed (i.e. 0% transmission at the line center). The tuning fork chopper is mounted on the entrance slit of the monochromator, and when the spectral line is saturated, the peak absorption level should coincide with the zero of the tuning fork's square wave when the mode of the laser emission is pure.

Gas Handling and Vacuum Systems

Of particular relevance to planetary atmospheric studies is the ability at Stony Brook to conduct studies of molecules at temperatures relevant to atmospheric conditions. This is made possible with the use of a nitrogen cooled absorption cell (38). A diagram of the cold cell system is shown in Figure 3.6. The cell is a 9.29" stainless steel tube with ZnSe windows and spring-loaded thermoplastic O-rings. The cell is cooled by means of a commercially

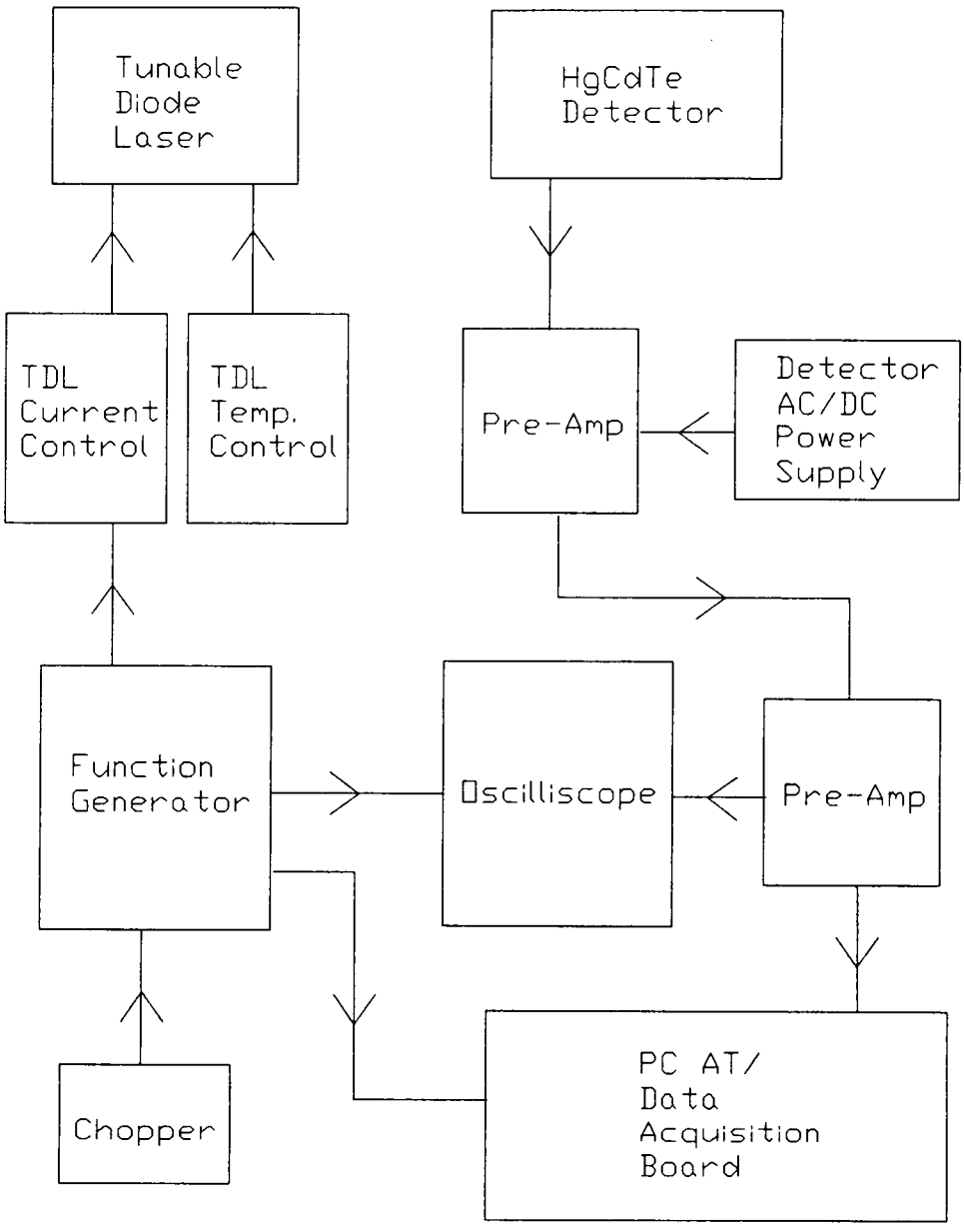

Figure 3.5: Schematic diagram of the SUNY detection and data acquisition system.

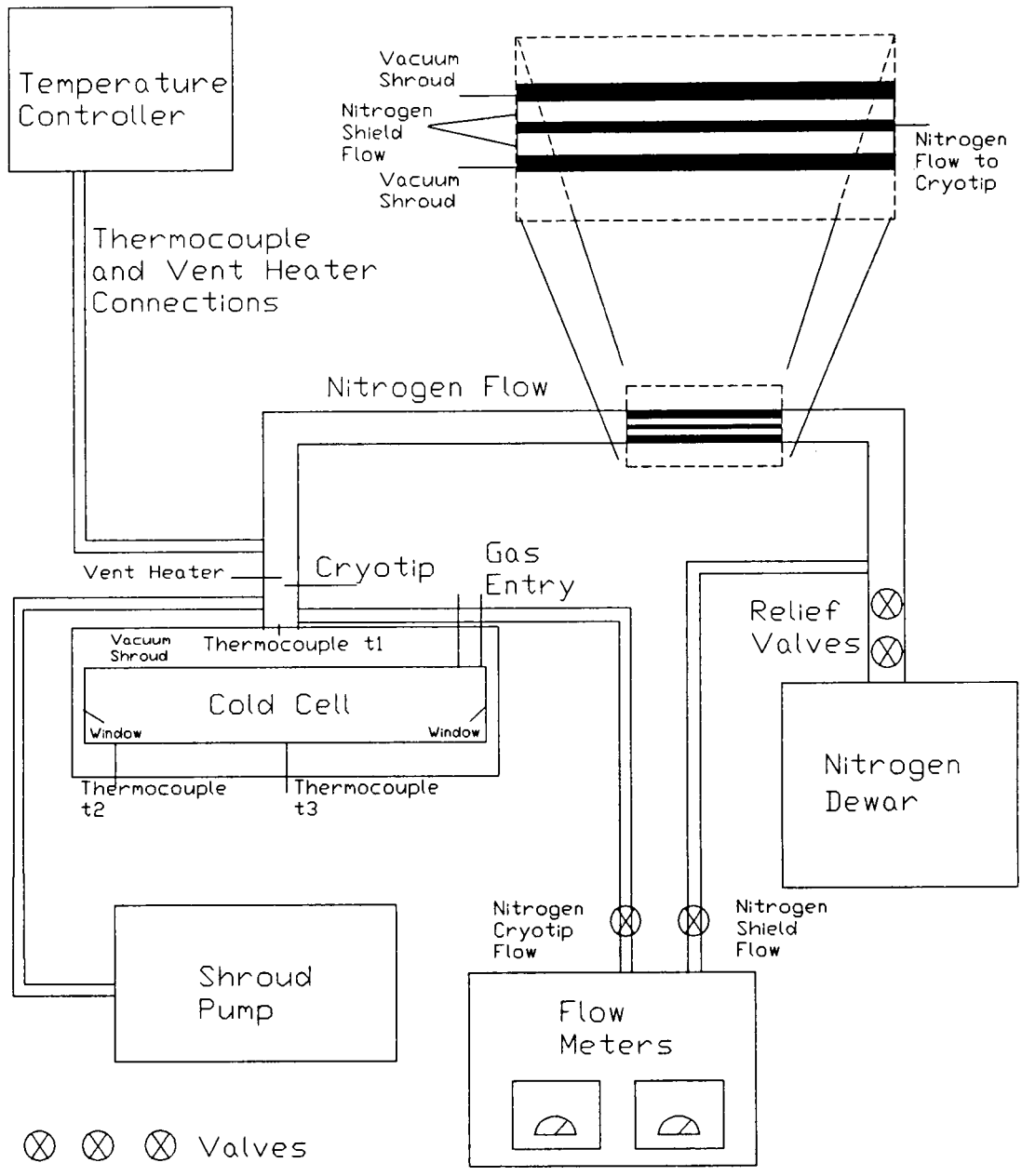

Figure 3.6: Schematic diagram of the SUNY low temperature absorption cell.

available cryogenic refrigerator that uses a liquid nitrogen transfer system. The temperature of the refrigerator's cryotip is thermostatically controlled with a temperature indicator-controller. A carefully monitored flow of liquid nitrogen to the cryotip cools it to within a couple of degrees Kelvin of the desired temperature, whereupon, a small nichrome wire heater wrapped around the cryotip, and actuated by the temperature controller, fixes the temperature firmly within a fraction of a degree. The absorption cell, the cryotip and the transfer system have vacuum shrouds around them to act as heat shields. A return nitrogen shield flow in the nitrogen transfer line also protects the steady flow of the nitrogen to the cryotip (see inset of Figure 3.6). The vacuum shroud around the cell also prevents condensation of moisture upon the cell. The temperature of the absorption cell is monitored using iron (7%)-doped gold and chromel thermocouples placed at three different locations. The first thermocouple (t1) is mounted on the cryotip itself. The other two thermocouple, (t2) and (t3), are placed at the bottom center and bottom end of the cell. The readings of these thermocouples (t2) and (t3) do not differ by more than 0.5 K, which is within the accuracy of the temperature indicator-controller. With the use of this coolable absorption cell, measurements may be made at a range of temperatures relevant to atmospheric conditions, rather than data taken only at room temperature. During normal operation, the dewar supplying the liquid nitrogen was refilled approximately every four to five days.

The rest of the SUNY gas handling system includes stainless steel gas lines and Swagelock stainless steel valves and fittings. Gas pressures were measured with an MKS Bartaron pressure indicator and three pressure heads: one reading up to 100 torr, one up to 1000 torr, and one head reading pressures up to 10,000 torr.

The gas manifold for the UTK absorption cell is shown in Figure 3.7. The gas manifold itself is constructed of stainless steel piping, and valves and fittings from Swagelock. Several openings are available to connect several gases at once, or to pump down extra absorption cells. The gas manifold is pumped by a diffusion pump with a backing pump. A roughing pump is also available to pump out large amounts of gas. An MKS Baratron pressure gauge was used with 1 and 1000 torr capacitance manometers.

The UTK vacuum system for the detector and laser are shown in Figure 3.8. (The

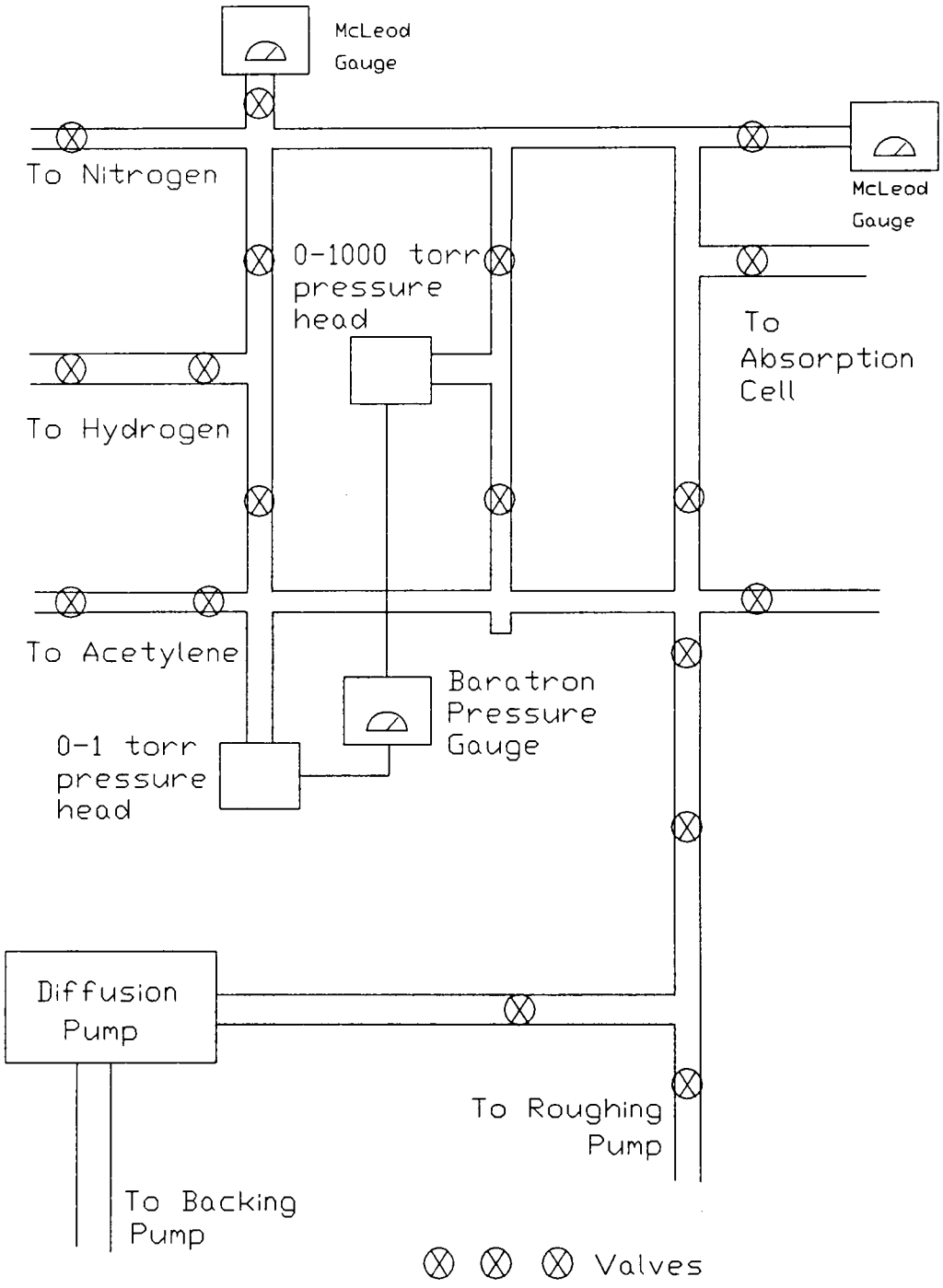

Figure 3.7: Schematic diagram of the UTK TDL gas manifold and absorption cell vacuum system.

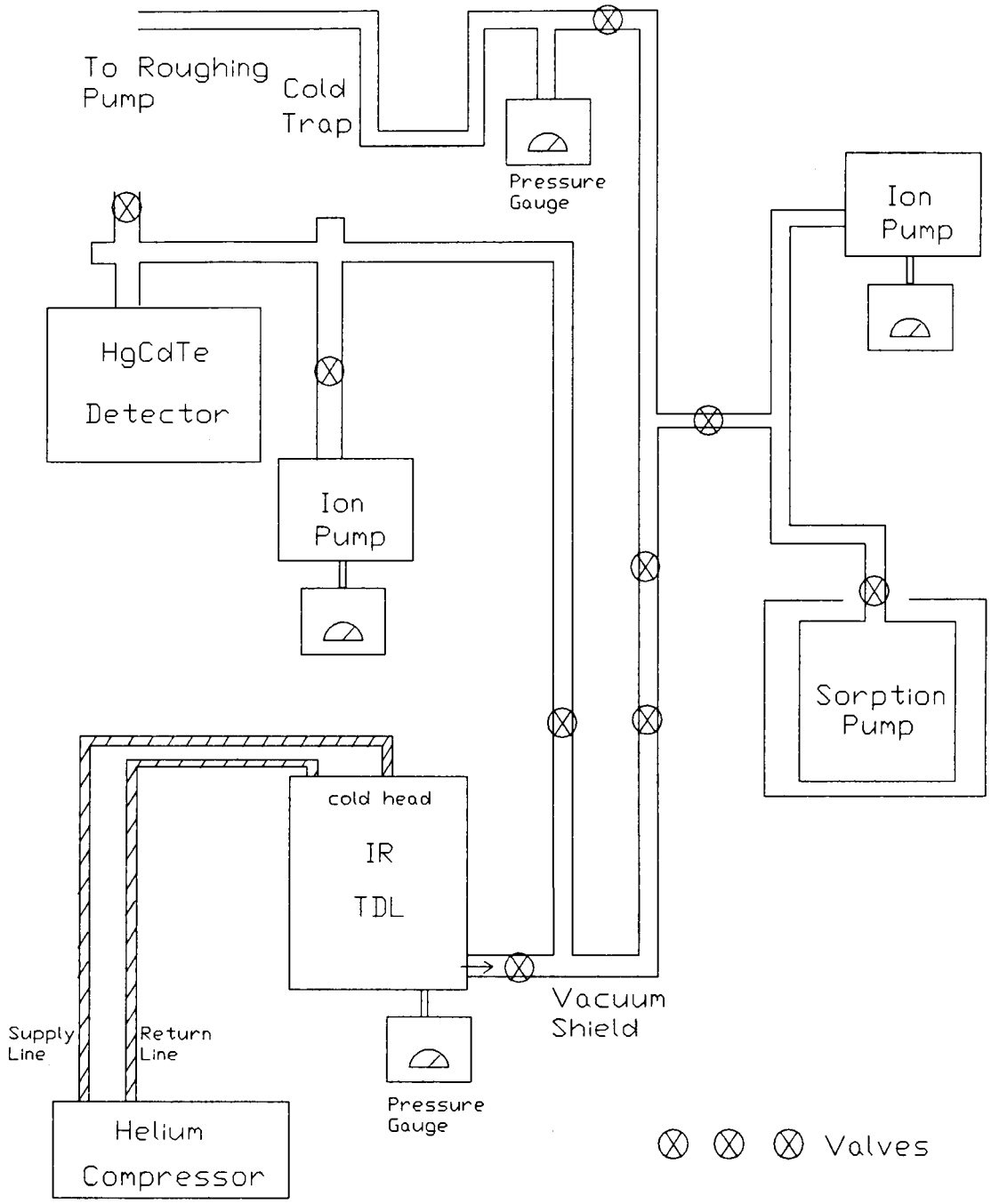

Figure 3.8: Schematic diagram of the UTK TDL laser manifold and detector vacuum system.

SUNY system used an ion pump with the diode laser, and the detector was systematically pumped out with a vacuum system in adjoining facilities.) The UTK system has an ion pump for the HgCdTe detector, with a Perkin Elmer 10 mA power supply. The laser is pumped with another ion pump using a 150 mA power supply. A roughing pump and a sorption pump are initially used to create a vacuum in the system. The roughing pump is separated from the rest of the system by a cold trap in the event of oil back-flow. The vacuum systems for the detector and the laser are connected by a single valve which allows both ion pumps to be used in the event one side loses its vacuum.

CHAPTER IV

COLLISIONAL BROADENING - PROCEDURE AND ANALYSIS

Measurement Procedure

Power up of the TDL system is necessary before measurements can be made. For the UTK system this consists of power up for: TDL temperature and current controls, temperature controller heater, waveform generator, preamp, PC, signal averager, shutter, and the power supply for the grating stepping motor. The TDL temperature needs to come to equilibrium at the set point desired. It is necessary to cool down the detector and periodically check the battery supply for the detector. These steps are necessary for the SUNY set-up except that the detector has an AC power supply and an oscilliscope is used to view the signal rather than a signal averager.

Gas can then be introduced into the absorption cell to tune the system. In the case of the acetylene work at UTK, the grating is initially left at the central image, and the temperature and current controls are adjusted until spectral lines are found. Some fine tuning of the optics can now be done at this point. Line positions for the ν_5 band of acetylene have been well determined and a spectral atlas was used in identifying the lines (60). When an identification is tentatively made, the grating can be rotated, by means of the QuickBasic PC program driving the stepping motor, to the frequency where the line is identified. After a correct identification of the line is made, fine tuning is carried out to receive the best signal possible. Eight lines of the ν_5 band of acetylene were identified and used in the broadening measurements: Q(3), Q(15), Q(16), Q(19), Q(24), Q(26), R(6) and R(8).

For room temperature measurements the SUNY tuning follows a similar procedure. A spectral atlas and a complete listing of line positions were not available at the time of the ethylene work, however, so ammonia lines were used as a calibration of the ethylene line position. Ethylene was introduced into the cold cell. (If the cold cell is used at room temperatures, the nitrogen flow is not in operation, and the vacuum shroud is at atmospheric pressure.) A smaller cell containing ammonia is also placed in the path of TDL energy beam. It is thus possible to distinguish between the lines simply by removing

the ammonia cell from the energy path. The ammonia line positions were previously identified from the AFGL Hitran database tape (45). The ammonia line used in the broadening measurements is in the ν_2 band of ammonia at 951.7762 cm^{-1}. Using the NH_3 line positions, and an etalon trace, it was possible to identify the frequency position of the ethylene line, which was determined to be 951.7393 cm^{-1}. This was compared to a line position listing by Lambeau et al. (37), and the band and transition of the line were found. The line was determined to be the $5_{0,5} \leftarrow 5_{1,5}$ transition in the ν_7 band of ethylene.

After the spectral line of interest is identified, measurements can be made. The temperature and current control settings are recorded for future reference, and the ambient temperature is recorded. At UTK the frequency of the line, from the spectral atlas is recorded, as well as the stated frequency of the grating position from the PC program. This helps determine the reliability of the grating frequency calibration over time (i.e. does the frequency calibration hold after repeated movement of the grating). When it was well calibrated, the grating frequency would agree with the atlas frequency for the line to within 0.5 cm^{-1}. The absorption cell is evacuated and the 'zero' pressure reading of the Baratron pressure gauge is recorded. With the signal tuned as well as possible, a background (evacuated cell) recording is made. This background recording will be used in the sample/background analysis of the spectral line. An etalon trace measurement is then made at this point, or directly after the broadening measurements have been completed. 4000 scans, taken in average mode with the signal averager, were usually averaged for the background measurement and subsequent pressure measurements. The etalon measurement usually consisted of 5000 scans to achieve a better signal to noise ratio. The data in these measurements were recorded with channel A on the signal averager using 1024 channels (data points). The frequency range of the signal averager recording can be changed by adjusting the amplitude on the waveform generator. A lower amplitude produces a more narrow range of frequency as observed at the signal averager.

The SUNY background and etalon measurements taken at room temperature followed the same procedure. 200 scans were made per measurement with the SUNY PC data acquisition board with 2048 data points. The drum setting, used to determine the frequency position of the grating, is recorded as well. For temperatures less than room temperature,

the nitrogen cooled absorption cell is used. Before the cell may be used, the dewar is filled with liquid nitrogen, and the relief valves are partially closed so that pressure may build up in the dewar. With sufficient pressure the gravity flow of the nitrogen to the cryotip can begin. Before the flow is started, the temperature indicator-controller and the wire heater wrapped around the cryotip are powered up. A temperature set point is input into the temperature controller. The shield flow in the nitrogen transfer line is begun as well as the cryotip flow itself. As the shield flow becomes constant the cryotip flow is seen to stabilize. The cell is cooled down to the temperature at the desired set point. The temperature is maintained by the action of the cryotip cooling and the wire heater wrapped around the cryotip. It takes some time for the cell to come to equilibrium throughout the cell (i.e. for the temperature readings of the two thermocouples on the cell to be within 0.5 K of each other). Two to four hours is generally needed for the cell to come to equilibrium when the cell is initially cooled or if the temperature set point is changed. After equilibrium is reached measurements can proceed as for room temperature measurements. It should be noted that the cooling of the cell can alter the position of the absorption cell windows, and hence the energy beam from the TDL going through the cell to the detector. Some tuning may be necessary to again receive a good signal at the detector. The equilibrium temperatures of the thermocouples, t1, t2, and t3, are recorded, and the background and etalon measurements are then conducted as described before.

After each measurement is complete, the data can then be stored on PC. For the UTK system, this consists of a data dump directly from the signal averager to the PC. A submenu in the QuickBasic program that drives the grating is used to dump the data. The data is saved with the SUNY set-up inside the data acquisition program. Back-up copies of the data measurements are made on floppy disk with both systems.

After the background and etalon measurements are taken, pressure broadening measurements are carried out. For the UTK measurements, the gases were supplied by Matheson with the stated purities of nitrogen and acetylene being 99.99% and for hydrogen 99.999%. The valve connecting the gas manifold to the pumping system is closed (Figure 3.7) and C_2H_2 is introduced into the cell. The 1 torr pressure head is used at this time. Gas is added to the cell until the line is saturated and this recording is made. (This will

be used later in the analysis of the line.) The pressure of C_2H_2 is reduced to less than one torr, the pressure is recorded, and the pressure gauge is switched to the 1000 torr pressure head. The 'zero' pressure of the 1000 torr head is recorded, and the perturbing gas is then introduced into the cell. Care is taken that the pressure of the perturbing gas entering the gas manifold and cell is higher than the pressure already existing in the manifold and cell so a backflow doesn't occur. The amounts of gas used vary according to the strength of the spectral line at hand. The acetylene pressures used varied from 7.5 to 93.2 mtorr. The perturbing gas pressures varied from 7.45 torr to 96.3 torr. After the perturbing gas is added to the cell, the pressure is recorded, a recording is made, and the data is dumped to the PC as before. The pressure in the manifold and cell is then reduced by pumping out part of the mixture, and a lower pressure recording is made. The pressure is reduced two to three times so that broadening measurements are recorded at three to four different pressures. More than one recording at each pressure may be conducted to determine a standard deviation at each pressure. This was carried out with the pressure broadening of the R(6) and R(8) lines.

A couple of simple tests were employed to determine if there were any leaks in the cell or manifold, which would affect a proper determination of the pressure. The first one was to simply record the pressure of the gas mixture in the cell, and then record it at a future time to see if any changes had occurred. This was tried several times, in one case up to fifty minutes, and the pressure appeared to remain steady. Also, after the set of measurements upon Q(26) had been completed, the final gas mixture in the cell was left overnight, and the same mixture was re-recorded the next morning. The pressure recorded was the same as the previous evening and another measurement was taken.

The SUNY broadening measurements followed the same procedure with the following exceptions. A C_2H_4-H_2 mixture was prepared in the laboratory, with commercially available gas samples, in a lecture bottle with the mixing ratio (by volume) 0.0528 (C_2H_4:H_2). Real gas corrections were incorporated, with a program written in BASIC, using van der Waals equation of state . The other perturbing gases were mixed in the absorption cell at the time of the measurement. The pressure range used in the measurements were 22.83 torr to 120.7 torr. For low temperature measurements, the mixture in the cell has to come

to temperature equilibrium with the cell (since you are introducing room temperature gas into a colder cell) so it is necessary to wait several minutes before the measurement can be made. Once the gas is at equilibrium, the measurements can be made as before. A saturation measurement was not recorded with each line but was checked, with the tuning fork chopper, to assure the saturation level was coincident with the 0% transmission level. An additional background measurement is made at the end of a set of absorption recordings to compare with the first background measurement made.

Determination of b_L and γ_L^0

An example of pressure broadened line measurements for a spectral line using the UTK system is shown in Figure 4.1. The line shown is the R(6) line of C_2H_2 broadened by hydrogen at three different pressures: 60.3, 80.3 and 96.3 torr. 88.2 mtorr of acetylene was used in the measurement. An etalon trace is also superimposed upon the pressure recordings. The spectral line is shown in absorptance space. The SUNY measurements were recorded in transmission space (i.e. 0% to 100% transmission, from bottom to top of the profile).

Analysis of the UTK broadening measurements was carried out using an analysis program written in QuickBasic by Mark Weber. (The analysis procedure for the SUNY broadening measurements will be discussed in the last section of this chapter dealing with the temperature dependence of spectral lines.) The UTK program was written so that a spectral profile from a signal averager recording could be read and directly displayed on screen using a PC-AT. By using the analysis program, the HWHM and the intensity can be determined as described in Chapter II.

An example of a spectral profile imported into the analysis program is shown in Figure 4.2. Marker positions are shown for the baseline determination as well as the 0% transmission level. A cursor is used to move about the profile displayed on the screen, and the marker positions are visually placed. The cursor speed can be changed by keyboard input of the digits 1-6, with 6 being the fastest movement. Before a spectral line itself is imported, an etalon trace file is used to calibrate the line width frequency. The etalon trace is imported, and the minima of the fringes are designated by placing a marker to each side of each individual minima. An n degree polynomial, with n input from the keyboard, is then used

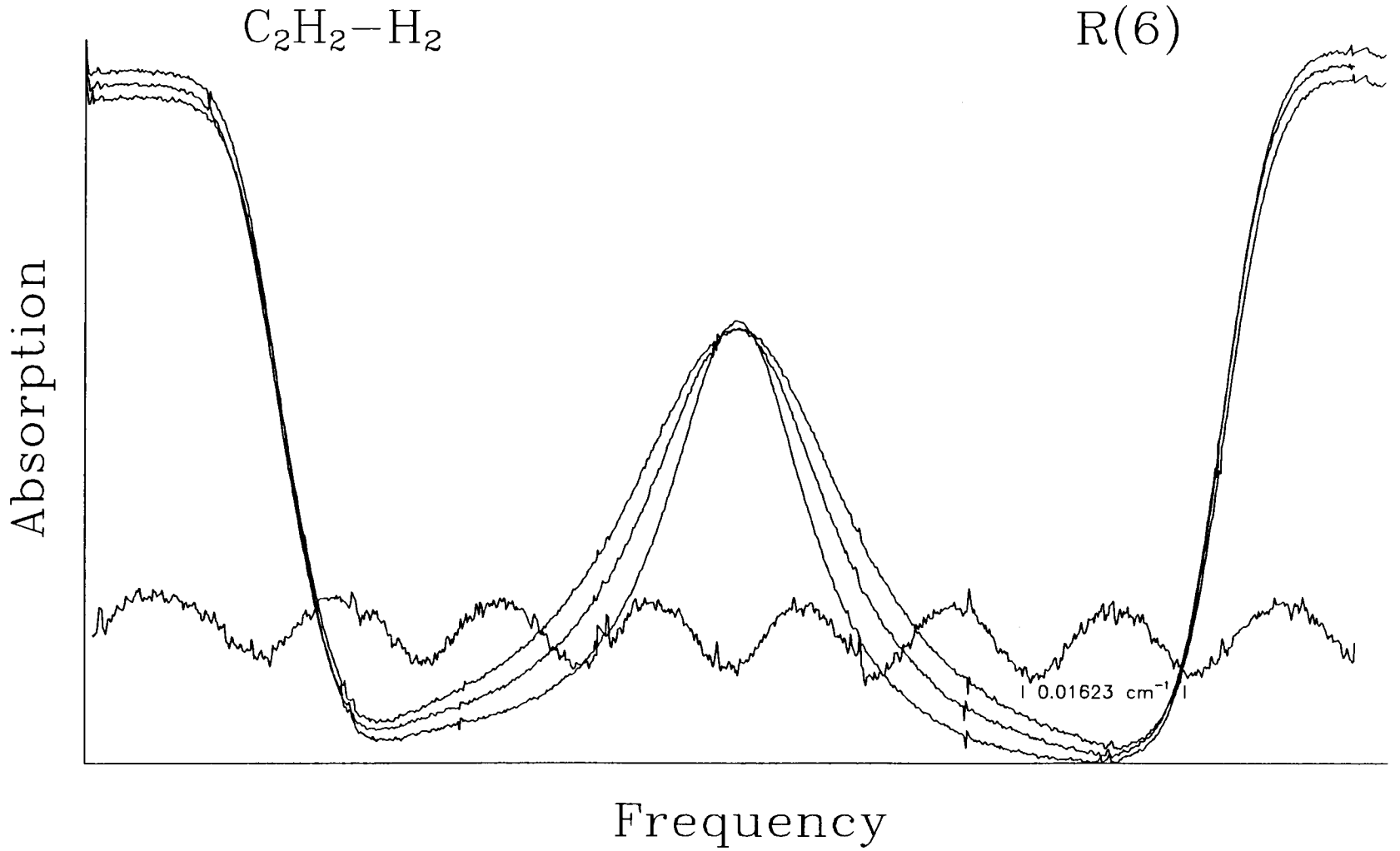

Figure 4.1: Sample line profiles from the UTK spectrometer system. The line shown is the R(6) line of C_2H_2, at 43 mtorr, broadened by H_2 at three different pressure: 60.3, 80.3, and 96.3 torr. An etalon trace is included.

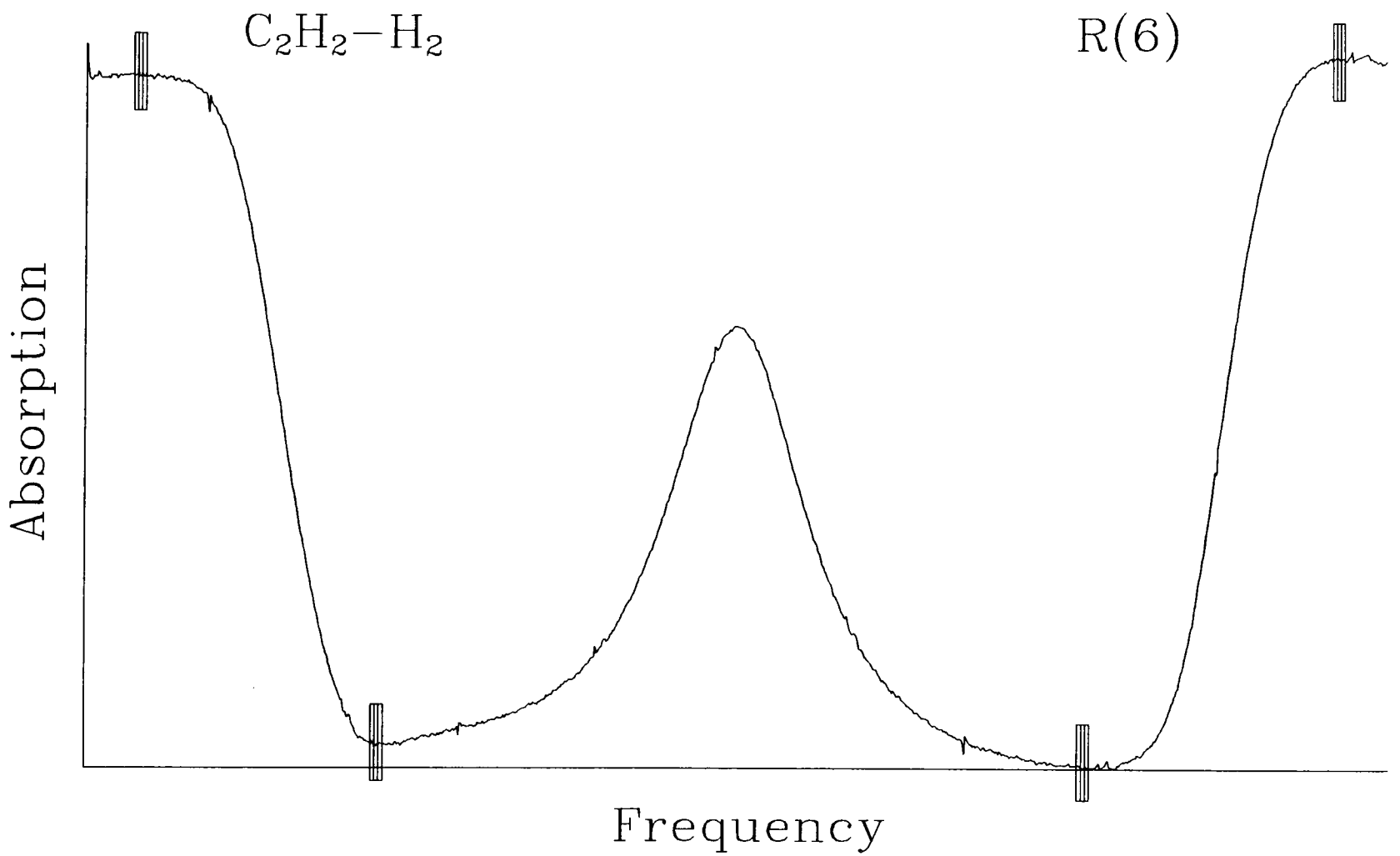

Figure 4.2: Sample line profile from the UTK spectrometer system with the marker positions, from the analysis program, for the baseline and the 0% transmission (100% absorption) level. The line shown is the R(6) line of C_2H_2 broadened by H_2.

to fit the minima between the marker positions, and the distance between minima is determined. This distance is found in units of channel numbers as recorded by the signal averager. It is necessary to convert the channel number scale into frequency. The spacing of the fringes, in cm^{-1}, can be found by using Equation (3.2), and for the UTK etalon used, this value is 0.01623 cm^{-1}. This frequency versus channel number calibration will not be the same for different lines. In other words, the horizontal frequency scale can change, for example, if the amplitude of the waveform generator is changed, or due to the fact fringe spacing varies according to variations in the ambient temperature (1),(24). Also it should be noted that the minima of the etalon fringes, in the UTK analysis, are fit rather than the maxima because we are looking at 0% to 100% energy from top to bottom in the spectral profile. (The maxima are used in the SUNY analysis since the profile is inverted.)

After the spectral line widths are calibrated using the etalon, the UTK analysis program requires the saturation file to next be imported. Marker positions for the baseline and the 0% are placed, as they are in Figure 4.2, on the spectral profile, as well as markers to denote the peak of the saturated line. Ideally, the saturation level should be coincident with the 0% transmission level (i.e. the gas is completely absorbing all energy at the line center). If this is not the case, then the difference, termed the saturation correction, can be accounted for when the profile is normalized between the baseline and 0% transmission levels.

A pressure broadened line is now imported into the program for analysis. The baseline and 0% transmission levels are marked as in Figure 4.2 on the spectral profile. By taking the saturation correction, and the baseline and 0% transmission levels, the analysis program normalizes the profile between zero and one. The transmittance and the HWHM can now be determined following the discussion of Chapter II. τ is determined from Equation (2.13) following Figure 2.1. After τ is found, the HWHM may be found for a normalized profile from Equation (2.23). In the case of the collisional broadening work, this HWHM is the Voigt HWHM b_V. The analysis program displays the final values for τ, the HWHM, and the equivalent width for the line. The analysis program also records the position of the baseline markers and outputs these values to a data file.

After the analysis of a set of collisional broadened spectral lines is complete, the col-

lisional broadened HWHM b_L are calculated from the measured Voigt HWHM b_V, using Equation (2.26). b_D is needed in this calculation and may be found from Eq. (2.3). The molecular weight, needed for the calculation of b_D, is 26 amu for C_2H_2. Finally, the collisional broadening coefficient, γ_L^0, can be found from Eq. (2.49), which is b_L divided by the pressure in atmospheres. This pressure is the gas pressure recorded with the 1000 torr head minus the 'zero' pressure recorded before the perturbing gas was added to the cell. A QuickBasic program, written by Alan Ewing, calculated γ_L^0 from the measured values and provided a standard deviation for the set of γ_L^0 calculated for each line. Table 4.1 gives the values of b_V, b_L, b_D and γ_L^0 for the lines of acetylene broadened by hydrogen. Table 4.2 lists these values for C_2H_2-N_2 broadening work.

The values for γ_L^0 in Tables 4.1 and 4.2 are hereafter called the uncorrected hydrogen and nitrogen broadened measurements. This is to distinguish them from the next step where these original measurements for the HWHM are taken for the broadened lines and were wing corrected following the discussion in Chapter II.

Wing Corrections to γ_L^0

Wing corrections were made to the uncorrected hydrogen and nitrogen broadening measurements in the event that the baseline positions chosen in the analysis were imprecise. A FORTRAN program was written to determine these wing corrections, and the program is included in the Appendix. This program takes the original measurements for the broadened lines, and using Equation (2.46), calculates the correction needed to the HWHM.

A data file was first constructed to be used with the wing correction program. This data file included the pressure, b_D, the original b_V measured from the spectral line, and the original position of the baseline markers, $\tau(g)$, (Figure 2.2). The next step was to determine the partial derivatives in Equation (2.46), which were calculated in the wing correction program using a delta method with Equation (2.47). Equation (2.47) is the approximation to the Voigt function by BelBruno (57). The Voigt function, evaluated for (x_g,y) was also calculated using Equation (2.47). (db_L/db_V), in the denominator of Equation (2.46), was calculated analytically in the program by taking the derivative of Equation (2.26). These values were used with Equation (2.46) and the correction to the HWHM (in this case b_V) was determined. The new value for b_L was re-calculated using Equation (2.26), and the new

Table 4.1: Collisional broadening half-widths b_V, Lorentz half-widths b_L, and broadening coefficients γ_L^0 retrieved from the uncorrected hydrogen broadened data.

ΔJ	J	Temp (K)	b_D (10^{-4} cm^{-1})	Pressure (torr)	b_V [a] (10^{-3} cm^{-1})	b_L [a] (10^{-3} cm^{-1})	γ_L^0 ($cm^{-1}atm^{-1}$)
0	3	299	8.8553	7.45	1.4948	0.9461	0.0965
				14.95	2.2590	1.8905	0.0961
				24.95	3.4002	3.1537	0.0961
				32.45	4.0054	3.7959	0.0889
0	15	298	8.8529	16.95	2.2130	1.8372	0.0824
				21.85	2.7133	2.4056	0.0837
				32.85	3.9814	3.7707	0.0872
				50.90	5.5278	5.3758	0.0803
0	16	297	8.8398	17.45	2.3444	1.9903	0.0867
				27.35	3.3186	3.0670	0.0852
				37.35	4.2660	4.0699	0.0828
				44.80	5.0931	4.9287	0.0836
0	19	298	8.8605	11.30	1.7117	1.2290	0.0806
				21.80	2.7406	2.4354	0.0849
				30.40	3.4653	3.2231	0.0806
				38.80	4.1127	3.9084	0.0766
0	24	298	8.8686	14.75	1.9955	1.5785	0.0813
				27.30	3.0628	2.7887	0.0776
				32.85	3.4549	3.2116	0.0743
				43.30	4.2243	4.0250	0.0706
				56.80	5.2463	5.0856	0.0680
0	26	298	8.8778	14.80	1.9370	1.5069	0.0774
				19.85	2.2137	1.8360	0.0703
				36.15	3.7938	3.5716	0.0751
					3.8822	3.6650	0.0771
				43.80	4.6613	4.4802	0.0777

Table 4.1: (continued).

ΔJ	J	Temp (K)	b_D (10^{-4} cm^{-1})	Pressure (torr)	b_V [a] (10^{-3} cm^{-1})	b_L [a] (10^{-3} cm^{-1})	γ_L^0 ($cm^{-1}atm^{-1}$)
1	6	298	9.0318	39.80	4.7229	4.5379	0.0867
					4.7039	4.5181	0.0863
					4.6987	4.5127	0.0862
				60.30	6.8772	6.7499	0.0851
					6.8324	6.7043	0.0845
					6.8193	6.6910	0.0843
				80.30	8.9332	8.8352	0.0836
					8.9439	8.8460	0.0837
					8.8753	8.7766	0.0831
				96.3	10.536	10.453	0.0825
					10.539	10.456	0.0825
					10.542	10.459	0.0825
1	8	298	9.0887	27.35	3.2711	3.0014	0.0834
					3.2711	3.0014	0.0834
					3.2239	2.9503	0.0820
				42.85	4.7852	4.6003	0.0816
					4.7707	4.5852	0.0813
					4.8190	4.6354	0.0822
				60.85	6.5346	6.3990	0.0799
					6.5585	6.4234	0.0802
					6.5178	6.3818	0.0797
				77.35	8.1136	8.0043	0.0786
					8.1645	8.0559	0.0792
					8.1021	7.9927	0.0785

[a]The precision of quoted b_V and b_L values is no better than $\pm 0.01 \times 10^{-3}$ cm^{-1}. The values are quoted to five significant figures for computational purposes only.

Table 4.2: Collisional broadening half-widths b_V, Lorentz half-widths b_L, and broadening coefficients γ_L^0 retrieved from the uncorrected nitrogen broadened data.

ΔJ	J	Temp (K)	b_D (10^{-4} cm^{-1})	Pressure (torr)	b_V [a] (10^{-3} cm^{-1})	b_L [a] (10^{-3} cm^{-1})	γ_L^0 ($cm^{-1}atm^{-1}$)
1	6	295	8.9938	41.60	4.6762	4.4909	0.0820
					4.6699	4.4843	0.0819
					4.6613	4.4754	0.0818
				61.60	6.6289	6.4980	0.0802
					6.6375	6.5068	0.0803
					6.6133	6.4821	0.0800
				78.60	8.1772	8.0710	0.0780
					8.2163	8.1106	0.0784
					8.2256	8.1200	0.0785
1	8	295	9.0504	33.80	3.6554	3.4158	0.0768
					3.6362	3.3954	0.0763
					3.6649	3.4259	0.0770
				49.30	5.0284	4.8538	0.0748
					5.0924	4.9200	0.0758
					5.0470	4.8731	0.0751
				63.80	6.2033	6.0617	0.0722
					6.1861	6.0441	0.0719
					6.1795	6.0373	0.0719
				79.80	7.5110	7.3940	0.0704
					7.5117	7.4008	0.0705
					7.5654	7.4492	0.0709

[a]The precision of quoted b_V and b_L values is no better than $\pm 0.01 \times 10^{-3}$ cm^{-1}. The values are quoted to five significant figures for computational purposes only.

γ_L^0 was found (Equation 2.49). Although Fridovich (56) mentions that iterations aren't necessary, an iterative loop was included in this program to determine if the wing corrections were being made properly.

The iterative loop was constructed in the following manner. A FORTRAN program adapted from the algorithm by Armstrong (52) was used to calculate the Voigt function. This program was included in the wing correction program as a subroutine. The values calculated for the Voigt function from the subroutine were checked against the tables for the Voigt function in Posener (51). If the correction to the HWHM (b_V) was greater than a chosen value, for example 10^{-6}, then the program called the Voigt function subroutine. With the wing corrected b_L and with b_D, the Voigt function (Equation 2.5) was determined at a point where the Voigt profile was very small, for example 10^{-8}. In other words, a Voigt profile for the broadened line was assumed, and using the values of b_L and b_D for the wing corrected line, the baseline marker position $\tau(g)$ was found very far into the wings of the profile (where the Voigt function approached 0.) This new baseline marker position, along with the wing corrected b_V are returned to the main program and used as a set of values to which wing corrections could be applied. If the wing corrections were being made correctly, there should be little or no correction to this set of values. This indeed was the case, and the second calculation for the correction to b_V was less, usually on the order of 10^{-5} cm^{-1} for a Voigt function calculated at less than 10^{-8}. By calculating the baseline position for smaller values of the Voigt function, the wing correction became less, which would essentially be like defining the baseline closer to the ideal position of 100% transmission. By choosing a higher value for the Voigt function (making the baseline position closer to the line center) the converse was true and larger wing corrections would be calculated. The iterative loop was used only as a means to determine if the program was working as planned, and the first calculation for the wing correction is reported. Table 4.3 lists the values for b_V, b_L, b_D and γ_L^0 for the wing corrected lines of acetylene broadened by hydrogen. Table 4.4 lists these values for wing corrected C_2H_2-N_2 broadening work.

Sample/Background Ratio Versus Wing Corrections

The sample/background ratio was also used to determine the baseline and 0% transmission levels. This method, which was used in the collisional broadening work at SUNY

Table 4.3: Collisional broadening half-widths b_V, Lorentz half-widths b_L, and broadening coefficients γ_L^0 retrieved from the wing corrected hydrogen broadened data.

ΔJ	J	Temp (K)	b_D (10^{-4} cm^{-1})	Pressure (torr)	b_V [a] (10^{-3} cm^{-1})	b_L [a] (10^{-3} cm^{-1})	γ_L^0 (cm^{-1}atm^{-1})
0	3	299	8.8553	7.45	1.5084	0.9644	0.0984
				14.95	2.3184	1.9591	0.0996
				24.95	3.6044	3.3717	0.1027
				32.45	4.2331	3.3717	0.0945
0	15	298	8.8529	16.95	2.2287	1.8555	0.0832
				21.85	2.7379	2.4329	0.0846
				32.85	4.0591	3.8524	0.0891
				50.90	5.7518	5.6057	0.0837
0	16	297	8.8398	17.45	2.3615	2.0099	0.0875
				27.35	3.3794	3.1323	0.0870
				37.35	4.4061	4.2162	0.0858
				44.80	5.2735	5.1147	0.0868
0	19	298	8.8605	11.30	1.7187	1.2379	0.0833
				21.80	2.7888	2.4888	0.0868
				30.40	3.5580	3.3221	0.0831
				38.80	4.2396	4.0413	0.0792
0	24	298	8.8686	14.75	2.0135	1.6001	0.0824
				27.30	3.1930	2.9300	0.0816
				32.85	3.5960	3.3621	0.0778
				43.30	4.5073	4.3204	0.0758
				56.80	5.8747	5.7312	0.0767
0	26	298	8.8778	14.80	1.9621	1.5373	0.0789
				19.85	2.2705	1.9021	0.0728
				36.15	3.9807	3.7689	0.0792
					4.0035	3.7929	0.0797
				43.80	4.9081	4.7361	0.0822

Table 4.3: (continued).

ΔJ	J	Temp (K)	b_D (10^{-4} cm^{-1})	Pressure (torr)	b_V [a] (10^{-3} cm^{-1})	b_L [a] (10^{-3} cm^{-1})	γ_L^0 ($cm^{-1}atm^{-1}$)
1	6	298	9.0318	39.80	4.8021	4.6201	0.0882
					4.7898	4.6074	0.0880
					4.7777	4.5948	0.0877
				60.30	7.0912	6.9678	0.0878
					7.0593	6.9353	0.0874
					7.0410	6.9167	0.0872
				80.30	9.3793	9.2860	0.0879
					9.4152	9.3222	0.0882
					9.3600	9.2664	0.0877
				96.30	11.251	11.173	0.0882
					11.249	11.171	0.0882
					11.253	11.175	0.0882
1	8	298	9.0887	27.35	3.3204	3.0686	0.0849
					3.3250	3.0735	0.0850
					3.2956	3.0419	0.0841
				42.85	4.9051	4.7342	0.0838
					4.9411	4.7714	0.0844
					4.9743	4.8057	0.0851
				60.85	6.8401	6.7173	0.0838
					6.8219	6.9988	0.0836
					6.8547	6.7322	0.0840
				77.35	8.5881	8.4903	0.0834
					8.6760	8.5791	0.0842
					8.5675	7.4695	0.0832

[a]The precision of quoted b_V and b_L values is no better than $\pm 0.01 \times 10^{-3}$ cm^{-1}. The values are quoted to five significant figures for computational purposes only.

Table 4.4: Collisional broadening half-widths b_V, Lorentz half-widths b_L, and broadening coefficients γ_L^0 retrieved from the wing corrected nitrogen broadened data.

ΔJ	J	Temp (K)	b_D (10^{-4} cm^{-1})	Pressure (torr)	b_V [a] (10^{-3} cm^{-1})	b_L [a] (10^{-3} cm^{-1})	γ_L^0 (cm^{-1}atm^{-1})
1	6	295	8.9938	41.60	4.8108	4.6306	0.0846
					4.8225	4.6428	0.0848
					4.7987	4.6181	0.0844
				61.60	6.9713	6.8468	0.0845
					6.9831	6.8588	0.0846
					6.9427	6.8177	0.0841
				78.60	8.7335	8.6341	0.0835
					8.6939	8.5941	0.0831
					8.6857	8.5858	0.0830
1	8	295	9.0504	33.80	3.7461	3.5245	0.0793
					3.7229	3.4999	0.0787
					3.7639	3.5434	0.0797
				49.30	5.2790	5.1215	0.0790
					5.3588	5.2036	0.0802
					5.2827	5.1253	0.0790
				63.80	6.6628	6.5379	0.0779
					6.6206	6.4949	0.0774
					6.6311	6.5055	0.0775
				79.80	8.2344	8.1332	0.0775
					8.2682	8.1674	0.0778
					8.2867	8.1862	0.0780

[a]The precision of quoted b_V and b_L values is no better than $\pm 0.01 \times 10^{-3}$ cm^{-1}. The values are quoted to five significant figures for computational purposes only.

(38), was incorporated in the UTK analysis to provide some confidence in the values of the wing corrected broadening coefficients. By using two independent methods, it could be seen if the calculated values were dependent upon the method used to evaluate them.

The spectral analysis program was edited to include the sample/background ratio method. The collisional broadened lines are analyzed in the following manner. The etalon is used for the frequency calibration as before and a saturation line may be used to find the saturation correction. The background (evacuated cell) measurement is then imported into the analysis program. It is assumed that the 100% and 0% transmission levels of the background measurement are the true baseline and 0% transmission. Let $y^b(i)$ be the value of the ith channel number for the background recording as recorded by the signal averager. The zero transmission level of the background recording is marked using a polynomial fit. Let $y_z^b(i)$ be the value of the ith channel number at the level of the fitted line to the zero transmission level. A pressure broadened line is next imported into the analysis program, and its zero transmission level is marked, with $y^s(i)$ being the ith channel value and $y_z^s(i)$ the value at the fitted zero transmission level. The ratio of the sample and background values is taken to normalize the spectrum between the 0% and 100% transmission levels. $y^r(i)$, the ratio of the sample and background measurements, is calculated by using the relationship

$$y^r(i) = \frac{y_z^s(i) - y^s(i)}{y_z^b(i) - y^b(i)} \tag{4.1}$$

The raw data values for the sample and background Measurements y(i) and y(i) are subtracted from the value determined at their respective zero transmission levels to 'zero' the data to that level. With both measurements zeroed to the same level (in other words the two zero transmission levels are now coincident) the ratio of the two measurements is taken to normalize the spectral profile. The transmittance can now be found for the normalized profile as before (Equation (2.23)) and the HWHM level, and the HWHM, for the profile can be determined.

For comparison with the wing corrected broadening coefficients, Table 4.5 lists the values for b_V, b_L, b_D and γ_L^0 for the lines of C_2H_2-H_2 broadening determined by the sample/background ratio method. (Background measurements were not recorded for Q(3) and Q(26), so no sample/background broadening coefficients are reported.) Table 4.6

Table 4.5: Collisional broadening half-widths b_V, Lorentz half-widths b_L, and broadening coefficients γ_L^0 retrieved from the hydrogen broadened data using the sample/background ratio method.

ΔJ	J	Temp (K)	b_D (10^{-4} cm^{-1})	Pressure (torr)	b_V [a] (10^{-3} cm^{-1})	b_L [a] (10^{-3} cm^{-1})	γ_L^0 (cm^{-1}atm^{-1})
0	15	298	8.8529	16.95	2.2548	1.8858	0.0846
				21.85	2.7919	2.4927	0.0867
				32.85	4.1487	3.9465	0.0913
				50.90	5.8687	5.7255	0.0855
0	16	297	8.8398	17.45	2.4222	2.0792	0.0906
				27.35	3.4667	3.2258	0.0896
				37.35	4.5576	4.3739	0.0890
				44.80	5.4490	5.2952	0.0898
0	19	298	8.8605	11.30	1.7062	1.2220	0.0822
				21.80	2.8217	2.5251	0.0880
				30.40	3.4934	3.2532	0.0813
				38.80	4.1937	3.9933	0.0782
0	24	298	8.8686	14.75	2.0300	1.6199	0.0835
				27.30	3.3096	3.0557	0.0851
				32.85	3.7104	3.4837	0.0806
				43.30	4.9816	4.8124	0.0845
				56.80	6.9517	6.8303	0.0914

Table 4.5: (continued).

ΔJ	J	Temp (K)	b_D (10^{-4} cm^{-1})	Pressure (torr)	b_V [a] (10^{-3} cm^{-1})	b_L [a] (10^{-3} cm^{-1})	γ_L^0 ($cm^{-1}atm^{-1}$)
1	6	298	9.0318	39.80	4.8765	4.6973	0.0897
					4.8584	4.6785	0.0893
					4.8403	4.6597	0.0890
				60.30	7.2259	7.1048	0.0895
					7.1927	7.0710	0.0891
					7.2179	7.0966	0.0894
				80.30	9.6123	9.5212	0.0901
					9.7176	9.6275	0.0911
					9.6490	9.5582	0.0905
				96.3	11.798	11.724	0.0925
					11.690	11.615	0.0917
					11.690	11.615	0.0917
1	8	298	9.0887	27.35	3.2711	3.0014	0.0834
					3.2711	3.0014	0.0834
					3.2239	2.9503	0.0820
				42.85	4.7852	4.6003	0.0816
					4.7707	4.5852	0.0813
					4.8190	4.6354	0.0822
				60.85	6.5346	6.3990	0.0799
					6.5585	6.4234	0.0802
					6.5178	6.3818	0.0797
				77.35	8.1136	8.0043	0.0786
					8.1645	8.0559	0.0792
					8.1021	7.9927	0.0785

[a]The precision of quoted b_V and b_L values is no better than $\pm 0.01 \times 10^{-3}$ cm^{-1}. The values are quoted to five significant figures for computational purposes only.

Table 4.6: Collisional broadening half-widths b_V, Lorentz half-widths b_L, and broadening coefficients γ_L^0 retrieved from the nitrogen broadened data using the sample/background ratio method.

ΔJ	J	Temp (K)	b_D (10^{-4} cm^{-1})	Pressure (torr)	b_V [a] (10^{-3} cm^{-1})	b_L [a] (10^{-3} cm^{-1})	γ_L^0 ($cm^{-1}atm^{-1}$)
1	6	295	8.9938	41.60	4.8383	4.6592	0.0851
					4.8235	4.6438	0.0848
					4.7883	4.6073	0.0842
				61.60	7.1323	7.0106	0.0865
					7.1830	7.0622	0.0871
					7.0943	6.9720	0.0860
				78.60	9.0692	8.9734	0.0868
					9.1740	9.0793	0.0878
					9.1452	9.0502	0.0875
1	8	295	9.0504	33.80	3.8502	3.6345	0.0817
					3.8032	3.5849	0.0806
					3.8203	3.6030	0.0810
				49.30	5.5047	5.3535	0.0825
					5.4624	5.3101	0.0819
					5.4645	5.3122	0.0819
				63.80	7.0855	6.9680	0.0830
					7.0845	6.9670	0.0830
					7.0354	6.9170	0.0824
				79.80	9.0315	8.9393	0.0851
					8.9392	8.8460	0.0842
					9.0378	8.9456	0.0852

[a]The precision of quoted b_V and b_L values is no better than $\pm 0.01 \times 10^{-3}$ cm^{-1}. The values are quoted to five significant figures for computational purposes only.

lists these values for wing corrected C_2H_2-N_2 broadening work. By inspection, the sample/background broadening coefficients in Tables 4.5 and 4.6 do compare with the wing corrected values in Table 4.3 and 4.4. In order to determine which method used in calculating the broadening coefficients was the more accurate, a fitting program written by Mark Weber was used to fit pressure versus b_L following Equation (2.49). This is a linear equation, so that a straight line should fit the pressure versus b_L plot, with the slope of the line being the broadening coefficient γ_L^0. The pressure versus b_L fit should also pass through the origin. Three fits to the equation were calculated using: the uncorrected b_L values, the wing corrected b_L values, and the b_L determined from the sample/background ratio method. The fitting program output the slope and y-intercept for the line, as well as the correlation coefficient. In almost all cases the best fit to the line was found using the wing corrected b_L. The sample/background ratio method usually gave a lower value for the correlation coefficient (with 1.0 being a perfect fit to a straight line) and the y-intercept was higher than that found in the wing corrected plots. The most probable reason that the sample/background ratio gave less desirable results is that drift in the signal averager recordings occurred while the measurements were being made. Upon superposition of several sets of measurements this was found to be the case.

The values for b_L and γ_L^0 determined from the wing corrected calculations were thus taken as the best determination of the collisional broadening HWHM for the spectral lines. In the final step of analysis, the wing corrected pressure versus b_L fits were forced through origin, which gave a better fit to the line than a free zero fitting gave. Figures 4.3-4.12 show the plots of pressure versus b_L for the wing corrected values, forced through zero. Residuals were calculated for the difference between the measured γ_L^0 and the γ_L^0 calculated from the pressure versus b_L linear fit. These are plotted, with their respective spectral lines, at the bottom of Figures 4.3-4.12.

Determination of Line Intensities

The absolute line intensities were also calculated from the acetylene broadening data using Equation (2.19) for the line intensity of a Voigt profile. These calculations were made to provide some confidence in the half widths at half maximum that were determined from the broadening data. The absolute intensities retrieved were compared to the values

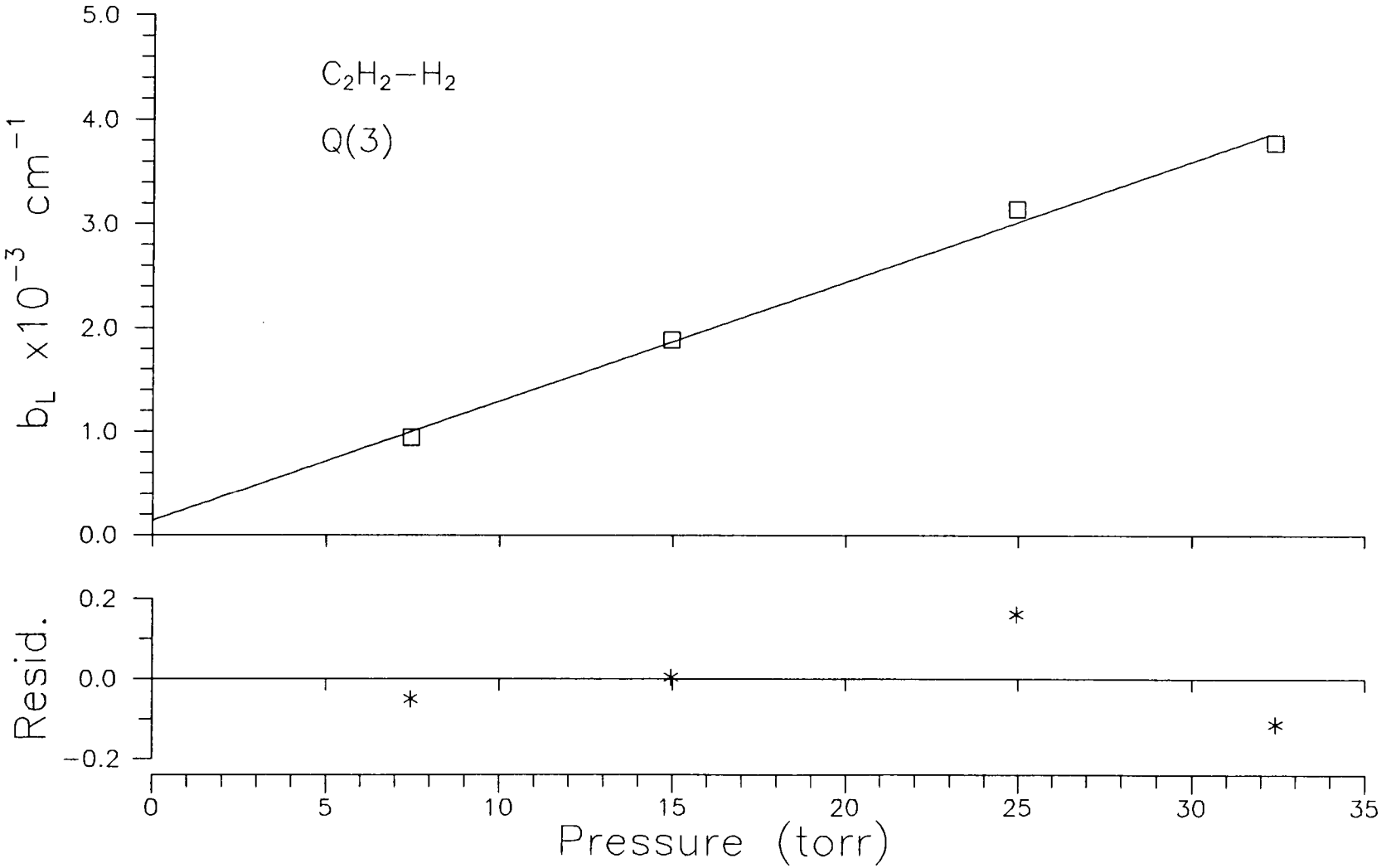

Figure 4.3: Plot of pressure versus wing corrected b_L for the Q(3) line of C_2H_2 broadened by H_2. Residuals found from the linear fitting of pressure versus b_L forced through zero.

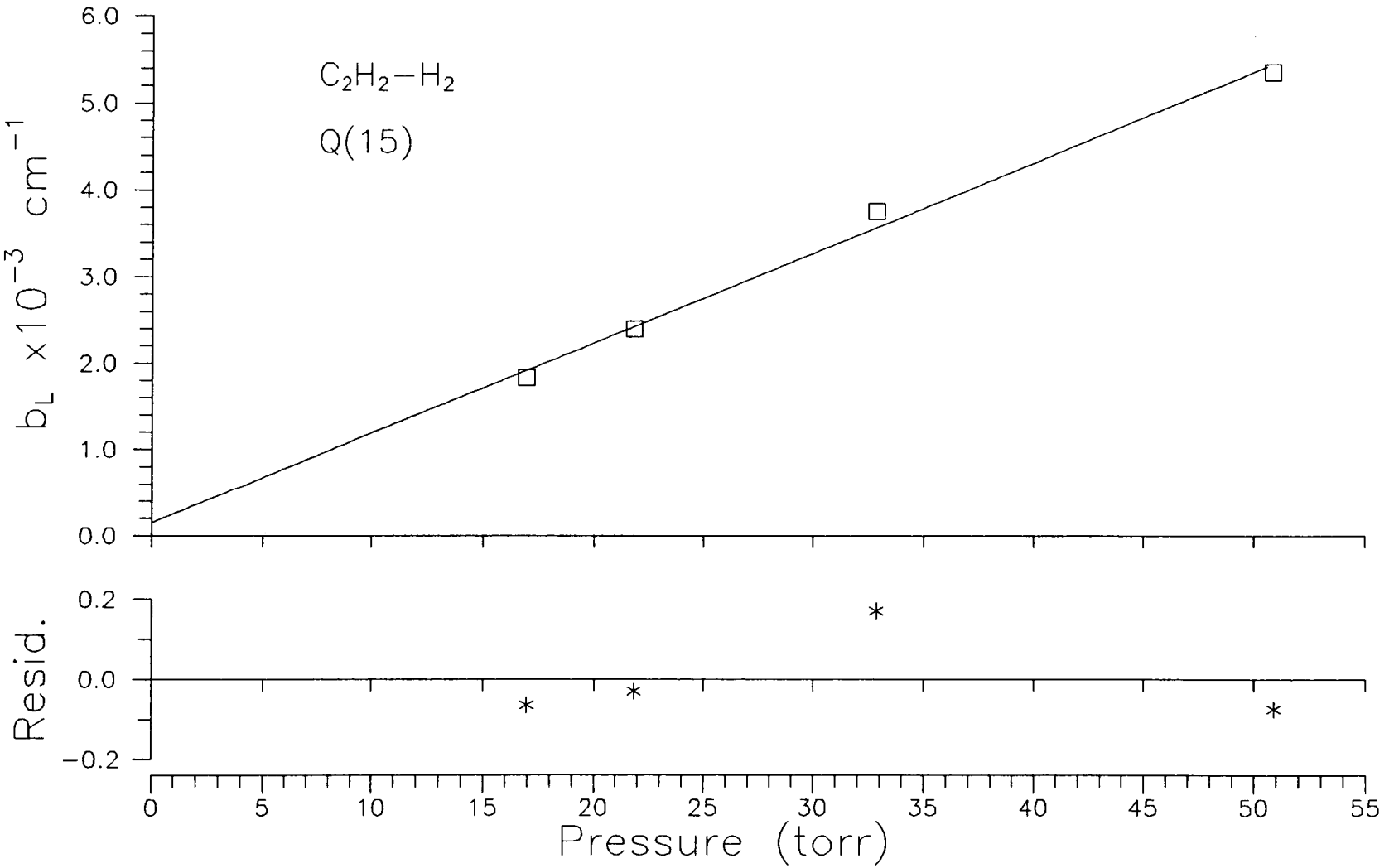

Figure 4.4: Plot of pressure versus wing corrected b_L for the Q(15) line of C_2H_2 broadened by H_2. Residuals found from the linear fitting of pressure versus b_L forced through zero.

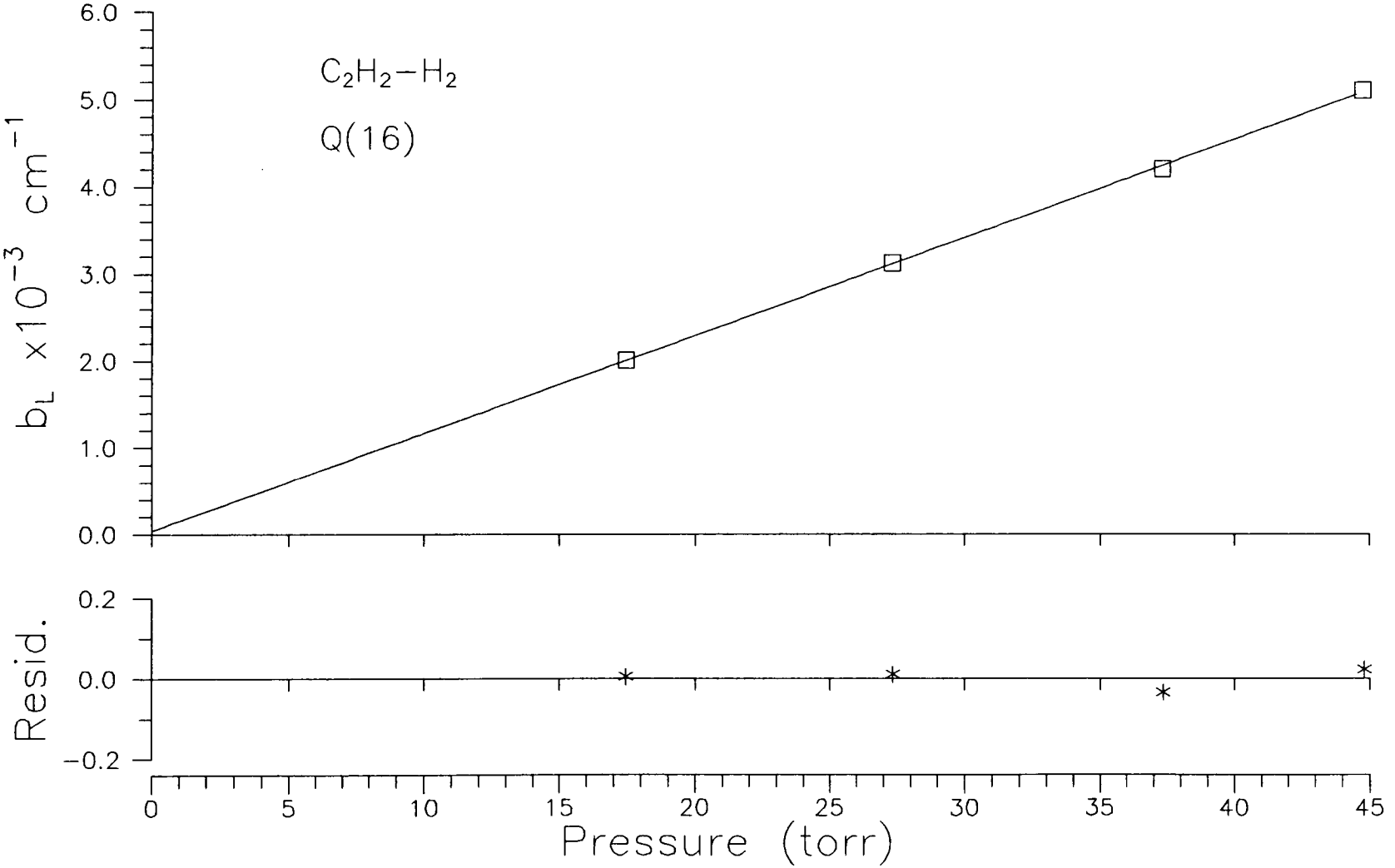

Figure 4.5: Plot of pressure versus wing corrected b_L for the Q(16) line of C_2H_2 broadened by H_2. Residuals found from the linear fitting of pressure versus b_L forced through zero.

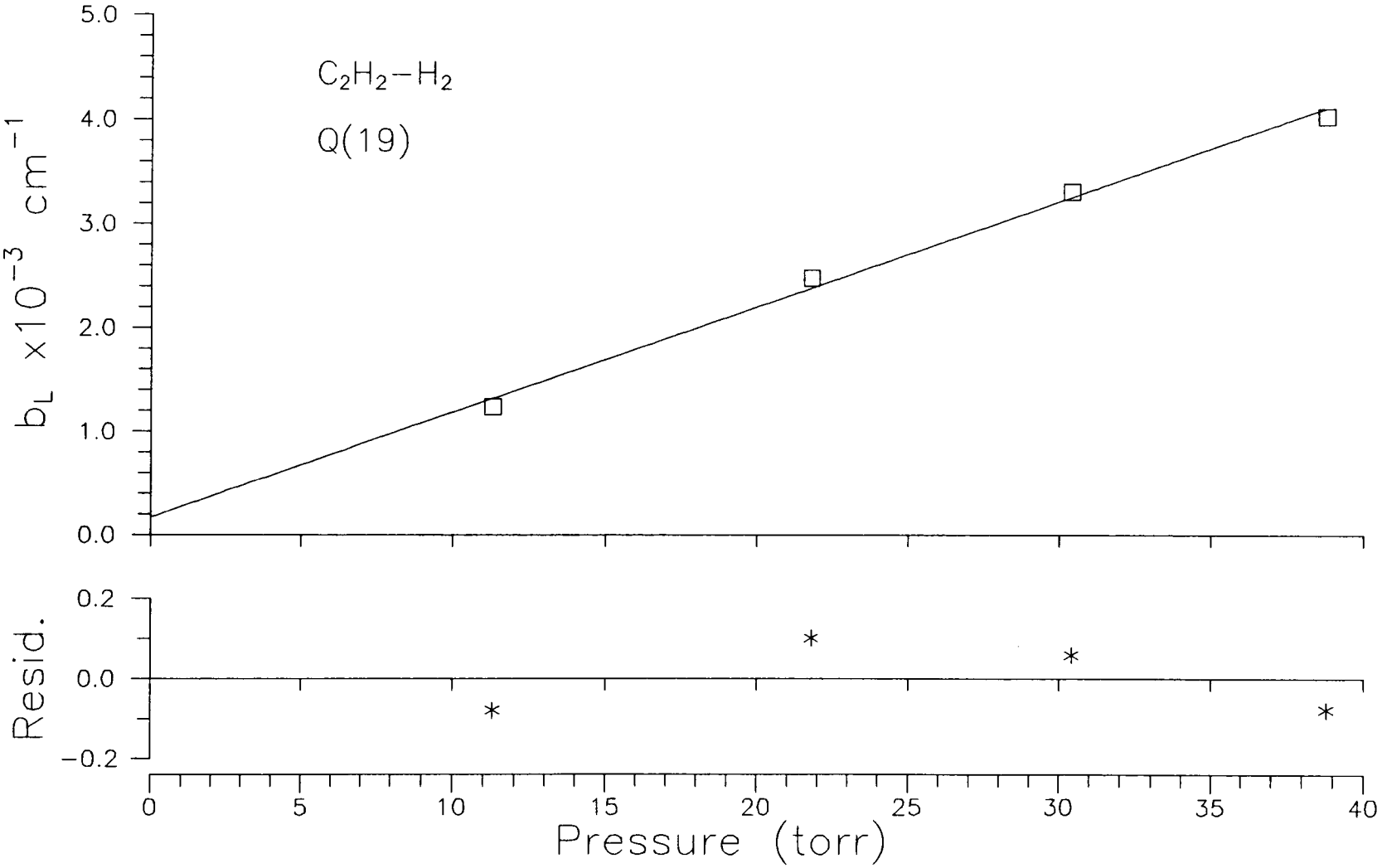

Figure 4.6: Plot of pressure versus wing corrected b_L for the Q(19) line of C_2H_2 broadened by H_2. Residuals found from the linear fitting of pressure versus b_L forced through zero.

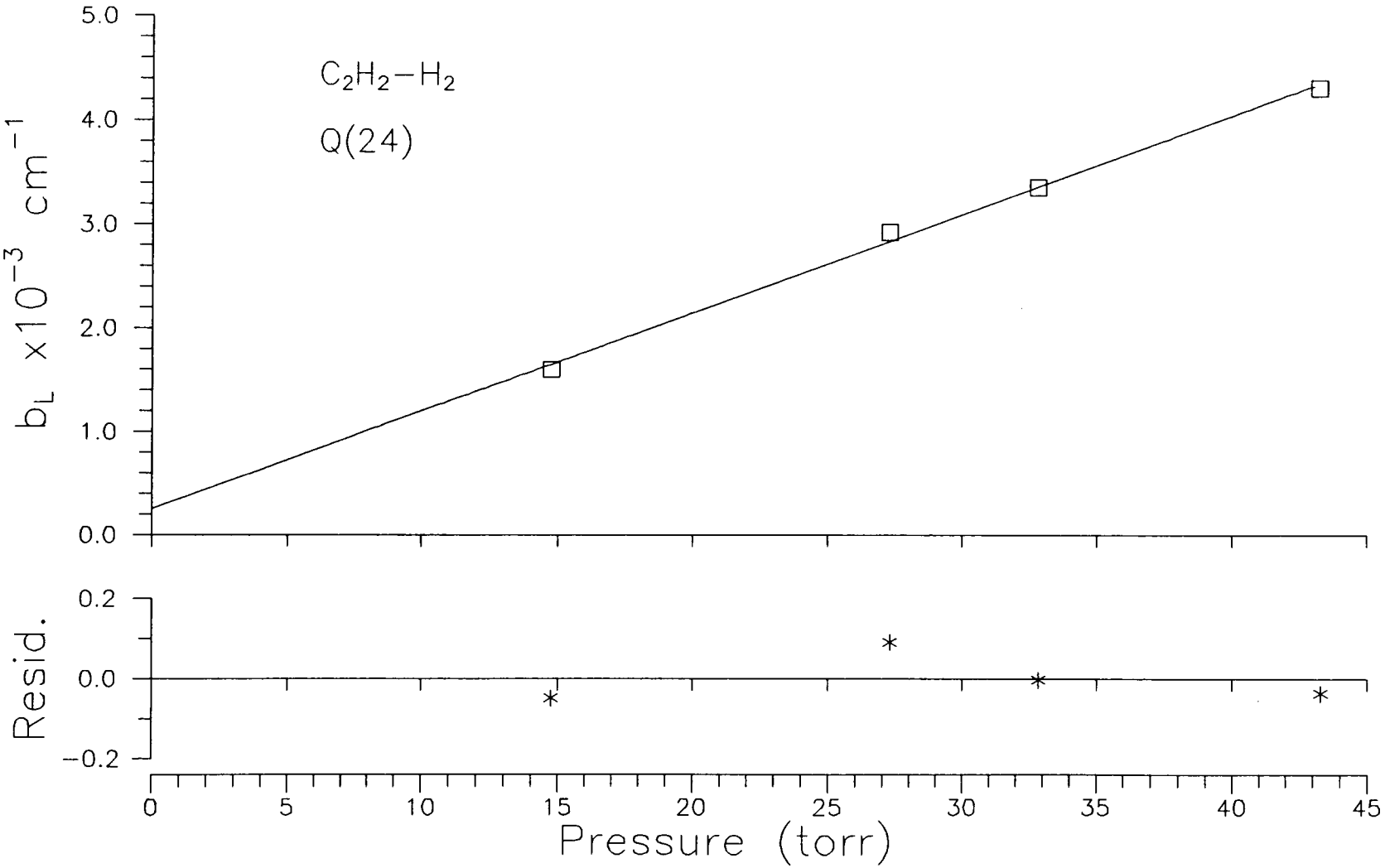

Figure 4.7: Plot of pressure versus wing corrected b_L for the Q(24) line of C_2H_2 broadened by H_2. Residuals found from the linear fitting of pressure versus b_L forced through zero.

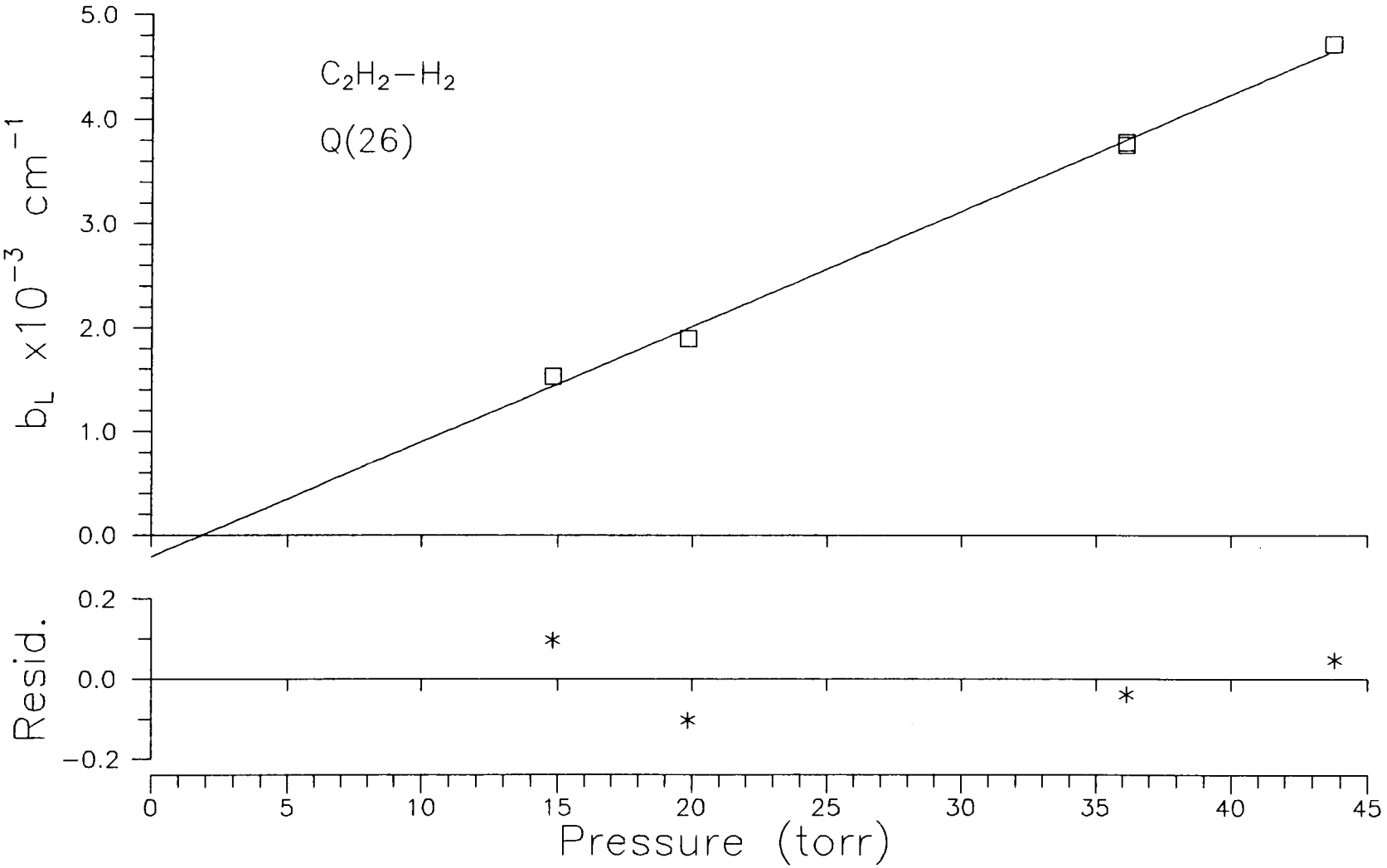

Figure 4.8: Plot of pressure versus wing corrected b_L for the Q(26) line of C_2H_2 broadened by H_2. Residuals found from the linear fitting of pressure versus b_L forced through zero.

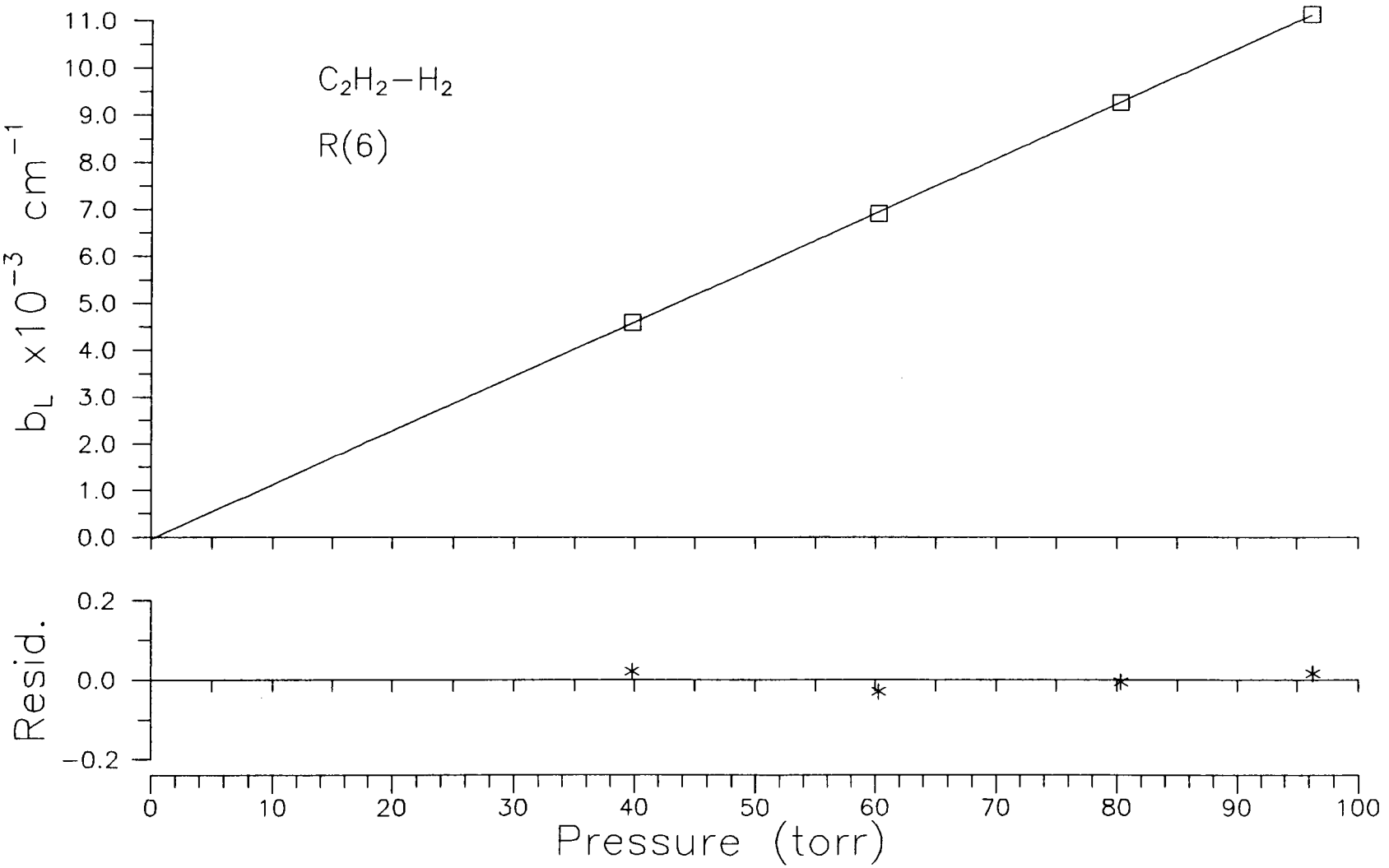

Figure 4.9: Plot of pressure versus wing corrected b_L for the R(6) line of C_2H_2 broadened by H_2. Residuals found from the linear fitting of pressure versus b_L forced through zero.

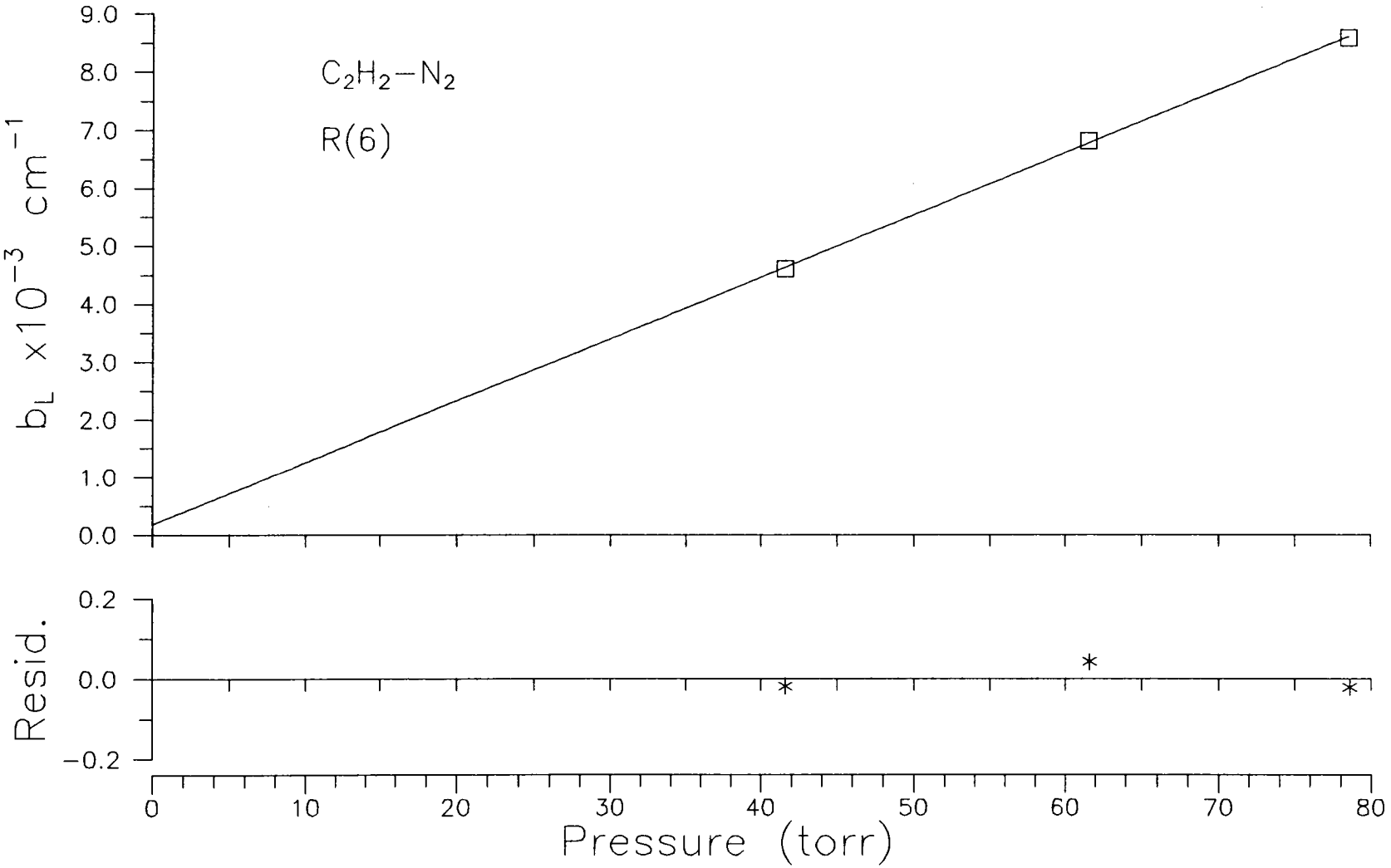

Figure 4.10: Plot of pressure versus wing corrected b_L for the R(6) line of C_2H_2 broadened by N_2. Residuals found from the linear fitting of pressure versus b_L forced through zero.

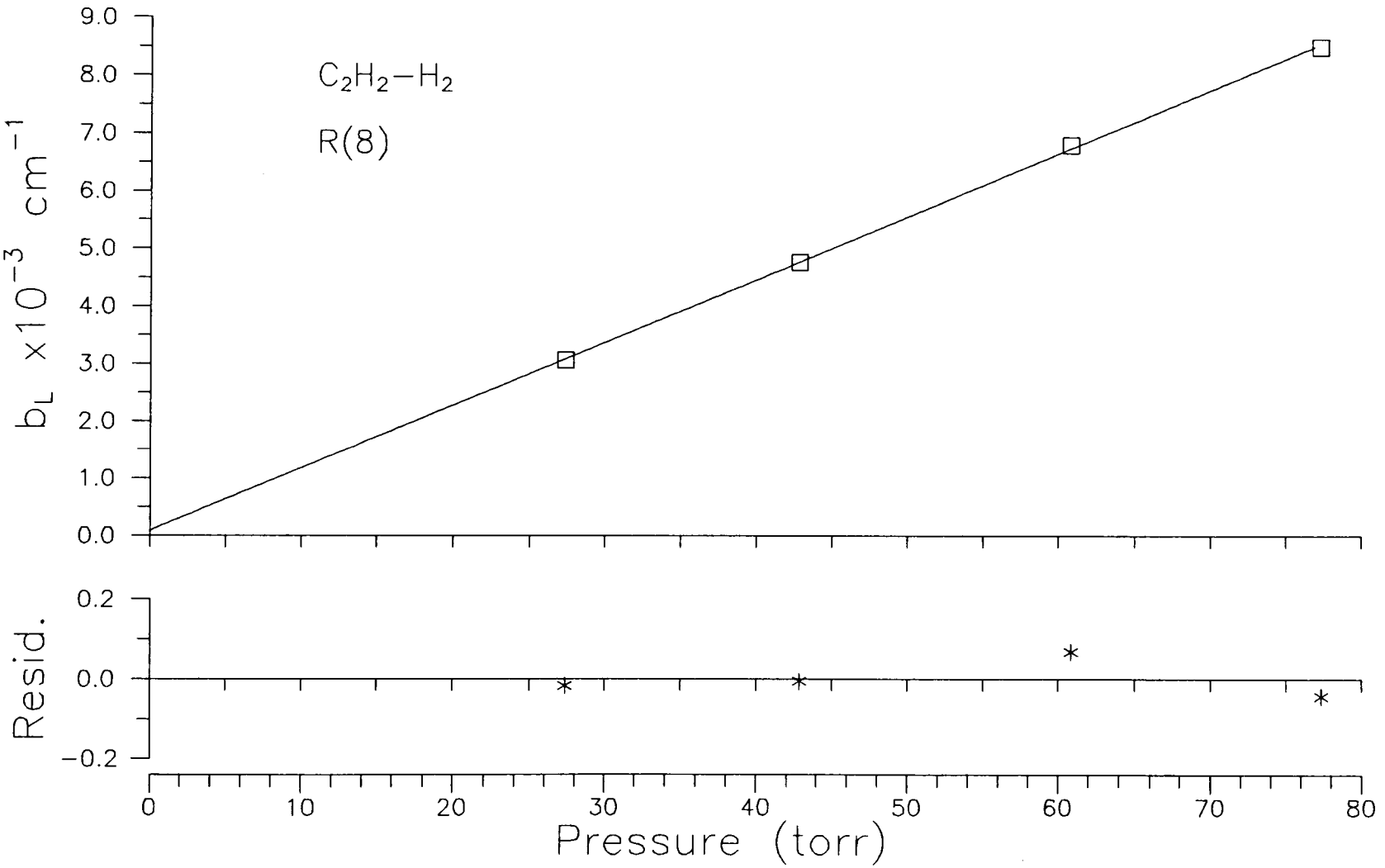

Figure 4.11: Plot of pressure versus wing corrected b_L for the R(8) line of C_2H_2 broadened by H_2. Residuals found from the linear fitting of pressure versus b_L forced through zero.

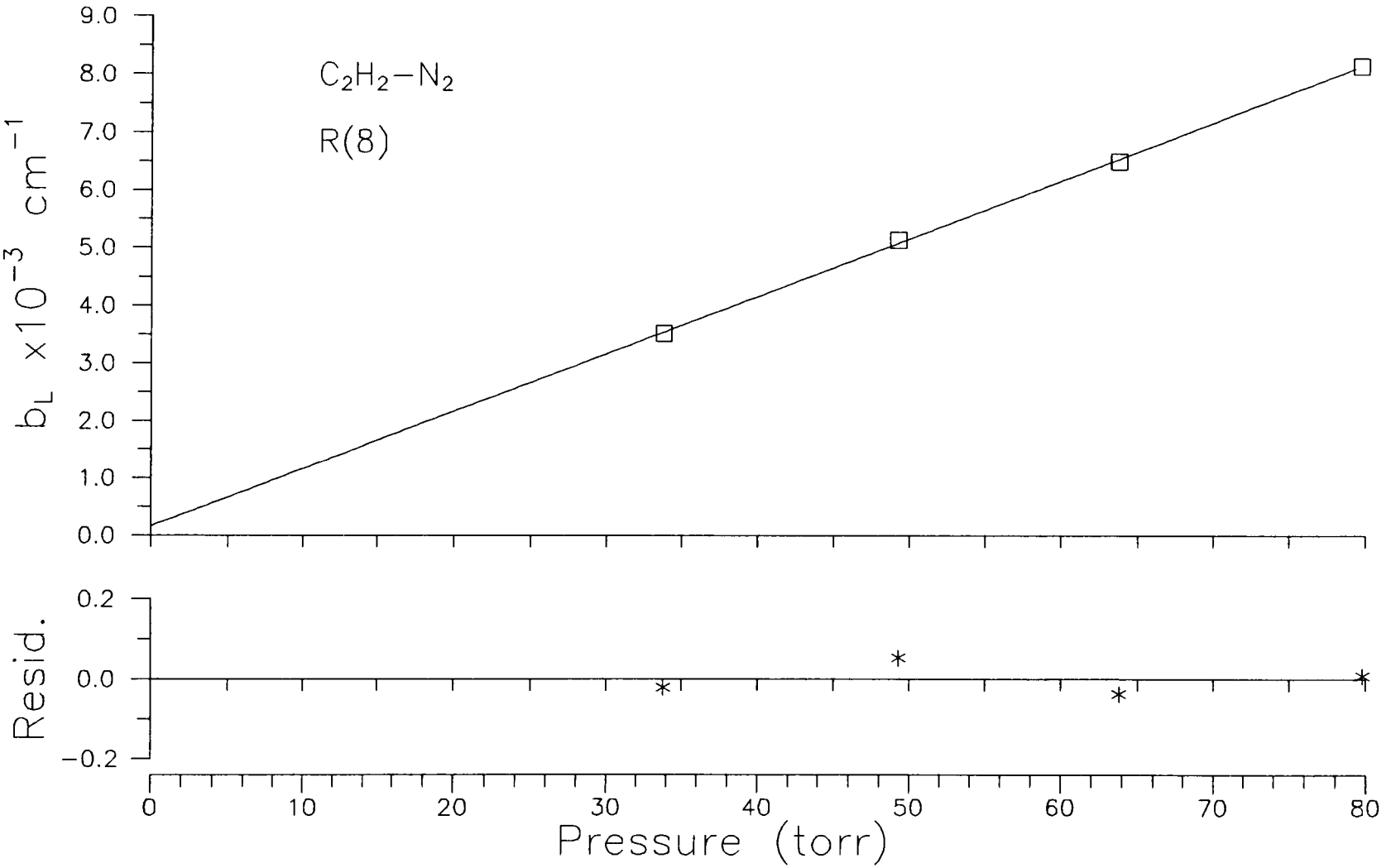

Figure 4.12: Plot of pressure versus wing corrected b_L for the R(8) line of C_2H_2 broadened by N_2. Residuals found from the linear fitting of pressure versus b_L forced through zero.

calculated for the respective lines. These comparison line intensities were calculated from a total band strength of 565 cm^{-2} atm^{-1} at 298 K for the ν_5 fundamental (23).

A FORTRAN program was written to determine the absolute line intensities. The Voigt function, evaluated at the line center, had to be calculated in order to determine the line intensity from a Voigt profile (Equation (2.19)). K(0,y) was calculated by incorporating into the line intensity program the same Voigt subroutine used in the wing correction program (52). The transmittance was determined from the wing corrected calculations and was found by subtracting the change in the transmission due to the wing corrections (Equation (2.32)) from the transmittance calculated from the original analysis of the spectral lines. This value for τ was used to calculate the line intensity S. Table 4.7 lists the intensities retrieved, the individual line intensities calculated from the total band intensity, and the residuals resulting from observed minus calculated. For lines recorded at temperatures other than 298 K, temperature corrections to the predicted line intensities were calculated using Equation (2.54).

Temperature Dependence of C_2H_4 and NH_3 Broadening Measurements

The SUNY spectral lines were analyzed using the sample/background ratio method. By using an oscilliscope and the tuning fork chopper, as described earlier, a clean mode was attained. There was little variation in the profile during the time of data acquisition for a particular set of measurements. This was determined by taking a background spectrum directly before and after the pressure broadening measurement were made. These were superimposed using a viewing program written in QuickBasic and the two were practically identical in most cases. If there had been a large change, a larger standard deviation would be found for γ_L^0 in the final analysis. Re-tuning would then be done and another set of measurements would be taken.

Data would be acquired by first taking a background profile and then an etalon trace. A gas mixture would then be introduced to the cell. If the measurements were made using the cold temperature cell, the gas was allowed to come to equilibrium with the temperature of the cell before the measurements were made. Three to four measurements would be recorded at each pressure to provide a standard deviation. This would be done for three to four different pressures for the gas at a particular temperature. At the end of the mea-

Table 4.7: Line intensities S_J (cm^{-2} atm^{-1}) calculated from the wing corrected broadening measurements for C_2H_2.

ΔJ	J	Frequency (cm^{-1})	Temp (K)	Pressure (mtorr)	S_J	S_J(ave)	S_J(calc)	Δ_{O-C}
					(cm^{-2} atm^{-1})			
0	3	729.2081	299	7.5	14.3180			
					16.4850	14.5469	15.0837	-0.5369
					13.3673	±1.3516		
					14.0171			
0	15	730.2301	298	11.1	19.1227			
					23.3810[a]			
				11.2	19.1072	19.5856	18.4722	1.1134
					20.5268	±0.8152		
0	16	730.3731	297	46.2	7.1496			
				46.6	6.9468	7.0138	5.4865	1.5273
					6.6566	±.2790		
				46.7	7.3020			
0	19	730.8553	298	14.8	10.9382			
					12.1619	11.2100	10.5030	0.7070
				15.2	10.6213	±.6671		
					11.1187			
0	24	731.8345	298	58.7	1.3008			
				59.1	1.4311	1.3051	1.2635	0.0416
				59.2	1.3666	±.1263		
				59.4	1.0966			
					1.3305			
0	26	732.2868	298	86.2	0.7185			
				87.0	0.8512	0.8002	0.7667	0.0335
					1.0034	±.1209		
				87.2	0.7185			
				88.4	0.7094			

Table 4.7: (continued).

ΔJ	J	Frequency (cm^{-1})	Temp (K)	Pressure (mtorr)	S_J	S_J(ave)	S_J(calc)	Δ_{O-C}
					(cm^{-2} atm^{-1})			
1	6	745.6135	298	88.2	6.2094			
					6.0985			
					6.0902			
					6.0831			
					6.0606	6.1623	5.0106	1.1517
					5.9816	$\pm$.1071		
					6.1769			
					6.1689			
					6.1534			
					6.3331			
					6.2941			
					6.2983			
1	6	745.6135	295	93.2	5.1190			
					5.0486			
					5.0938			
					5.2645			
					5.2988	5.2860	5.1330	0.1530
					5.2373	$\pm$.1827		
					5.4868			
					5.5124			
					5.5124			

Table 4.7: (continued).

ΔJ	J	Frequency (cm^{-1})	Temp (K)	Pressure (mtorr)	S_J	S_J(ave)	S_J(calc)	Δ_{O-C}
					(cm^{-2} atm^{-1})			
1	8	750.3105	298	72.2	5.9156			
					5.8488			
					5.6743			
					5.9983			
					5.8880			
					5.9469	6.0850	5.3192	0.7658
					6.2276	$\pm$.2347		
					6.2078			
					6.2256			
					6.3623			
					6.3857			
					6.3395			
1	8	750.3105	295	71.7	5.0841			
					5.0819			
					5.0222			
					5.4155			
					5.4101			
					5.4233	5.6338	5.4396	0.1942
					5.8320	$\pm$.4493		
					5.9485			
					5.8236			
					6.1757			
					6.1689			
					6.2198			

Value not include in average of S for Q(15).

surements the cell would be evacuated and the another background measurement would be made. If broadening measurements were desired at another temperature, the temperature controller set point would be changed and the cell allowed to come to equilibrium again, with adjustments made to the nitrogen flow rates to the cryotip and the shield as needed for that temperature (i.e. lower temperatures would need a large flow rate of nitrogen).

Ethylene broadening measurements were conducted using three different perturbing gas: hydrogen, nitrogen, and helium. Broadening measurements were carried out with each of these mixtures at four different temperatures: 295, 252, 202 and 152 K. Ammonia broadening measurements were also conducted using hydrogen and nitrogen as the perturbing gases. The ammonia broadening work was conducted at 295, 251 and 206 K. After each measurement was completed an analysis program was used to determine γ_L^0 for each line. The intensity of the ethylene line was also determined from the C_2H_4-H_2 measurements.

Analysis was carried out using a program again written in QuickBasic. The etalon trace is first imported into the analysis program and the line width frequency calibration is made. In this case the fringe spacing was taken to be 0.01634 cm^{-1}. Rather than take a large number of fringes, the amplitude on the waveform generator was adjusted to where only two or three fringes could be used for the calibration. For example, the best case would be when the etalon was superimposed on the spectral line in the analysis program, and two etalon fringes would 'bracket' the spectral line center. These two would be used to make the calibration.

As with the sample/background ratio method described above, the background profile and sample profile measurements are next imported into the analysis program. Line parameters were also included in a data file and could be called by the main program. The data file included the center of the spectral line (cm^{-1}), the temperature (K) the measurements were recorded at, the molecular weight of the molecule being observed, the mixing ratio of the gas with the perturbing gas and the path length of the absorption cell. By using these values, b_L and γ_L^0 were determined in the analysis program from Equations (2.26) and (2.49), and the intensity was determined for the ethylene line from the peak transmittance for a Voigt profile (61) with the C_2H_4-H_2 measurements. Tables 4.8-4.10

Table 4.8: Collisional broadening coefficients γ_L^0 of the $5_{0,5} \leftarrow 5_{1,5}$ line, located at 951.7393 cm^{-1}, in the ν_7 band of C_2H_4.

Broadener	γ_L^0 ($cm^{-1}atm^{-1}$)				n
	295 K	252 K	202 K	152 K	
H_2	0.1076±.0005	0.1194±.0016	0.1378±.0015	0.1668±.0019	0.66
N_2	0.0871±.0010	0.0991±.0005	0.1202±.0007	0.1495±.0008	0.82
He	0.0618±.0012	0.0672±.0008	0.0738±.0015	0.0850±.0006	0.48

Table 4.9: Intensity of the $5_{0,5} \leftarrow 5_{1,5}$ line, located at 951.7393 cm^{-1}, in the ν_7 band of C_2H_4.

S (cm^{-2} atm^{-1})			
296 K	252 K	202 K	152 K
0.9977±.0298	1.3260±.0257	1.8723±.0405	2.7146±.0342

Table 4.10: Collisional broadening coefficients γ_L^0 of the 951.7762 cm^{-1} line in the ν_2 band of NH_3.

Broadener	γ_L^0 ($cm^{-1}atm^{-1}$)			n
	295 K	251 K	206 K	
H_2	0.1023±.0005	0.1132±.0015	0.1256±.0018	0.56
N_2	0.1146±.0006	0.1302±.0024	0.1512±.0019	0.77

list the results of the broadening work conducted at SUNY.

After the collisional broadening coefficients were determined a plot of lnT versus -ln γ_L^0 was made for each line to determine the value of n in Equation (2.50). Also, for the C_2H_4-H_2 intensity calculations, a plot of 1000/T versus $\ln(S * T^{5/2})$ was made following the temperature dependence of the intensity in Equation (2.54). C_2H_4 is a non-linear molecule, and with S in units of cm^{-2} atm^{-1}, 1/T is proportional to the intensity times the temperature T to the power of 5/2. The values for n are given in Tables 4.8 and 4.10. The plots of lnT versus -ln γ_L^0, and 1000/T versus $\ln(S * T^{5/2})$ are shown in Figures 4.13-4.18.

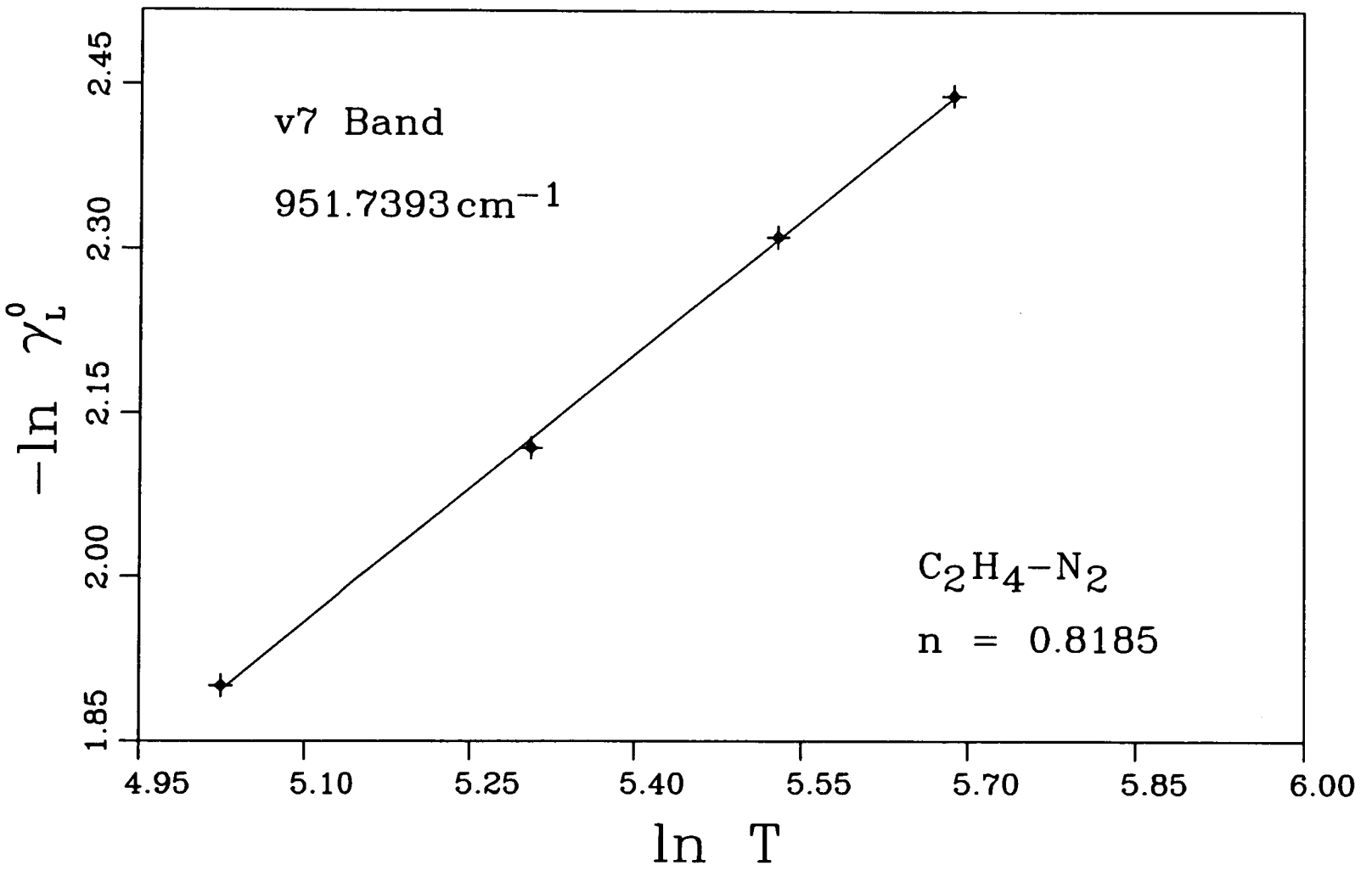

Figure 4.13: Plot of -lnγ_L^0 versus lnT for the 951.7393 cm^{-1} line of C_2H_4 broadened by N_2. The slope of the line is the exponent n defining the temperature dependence of the linewidth.

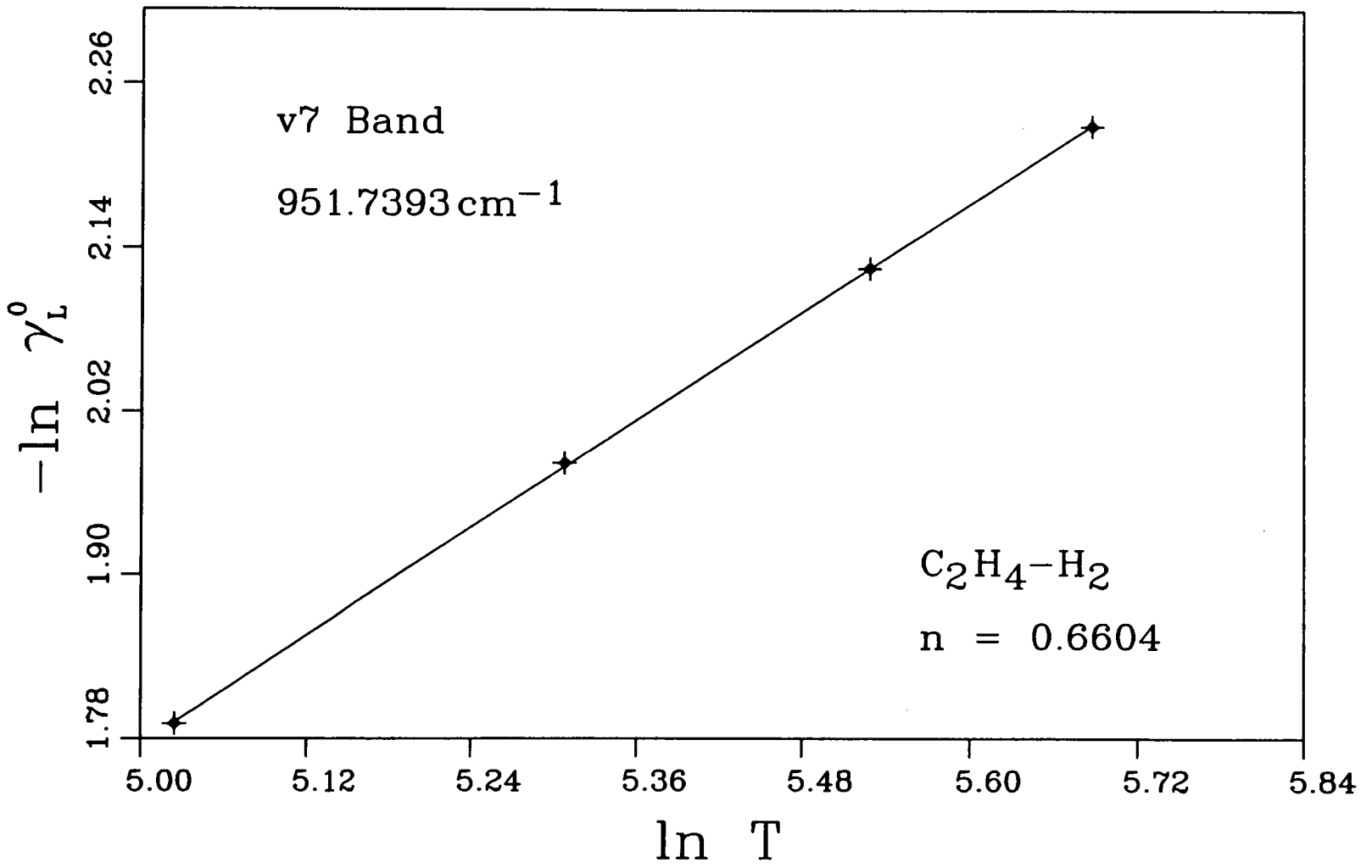

Figure 4.14: Plot of -lnγ_L^0 versus lnT for the 951.7393 cm^{-1} line of C_2H_4 broadened by H_2. The slope of the line is the exponent n defining the temperature dependence of the linewidth.

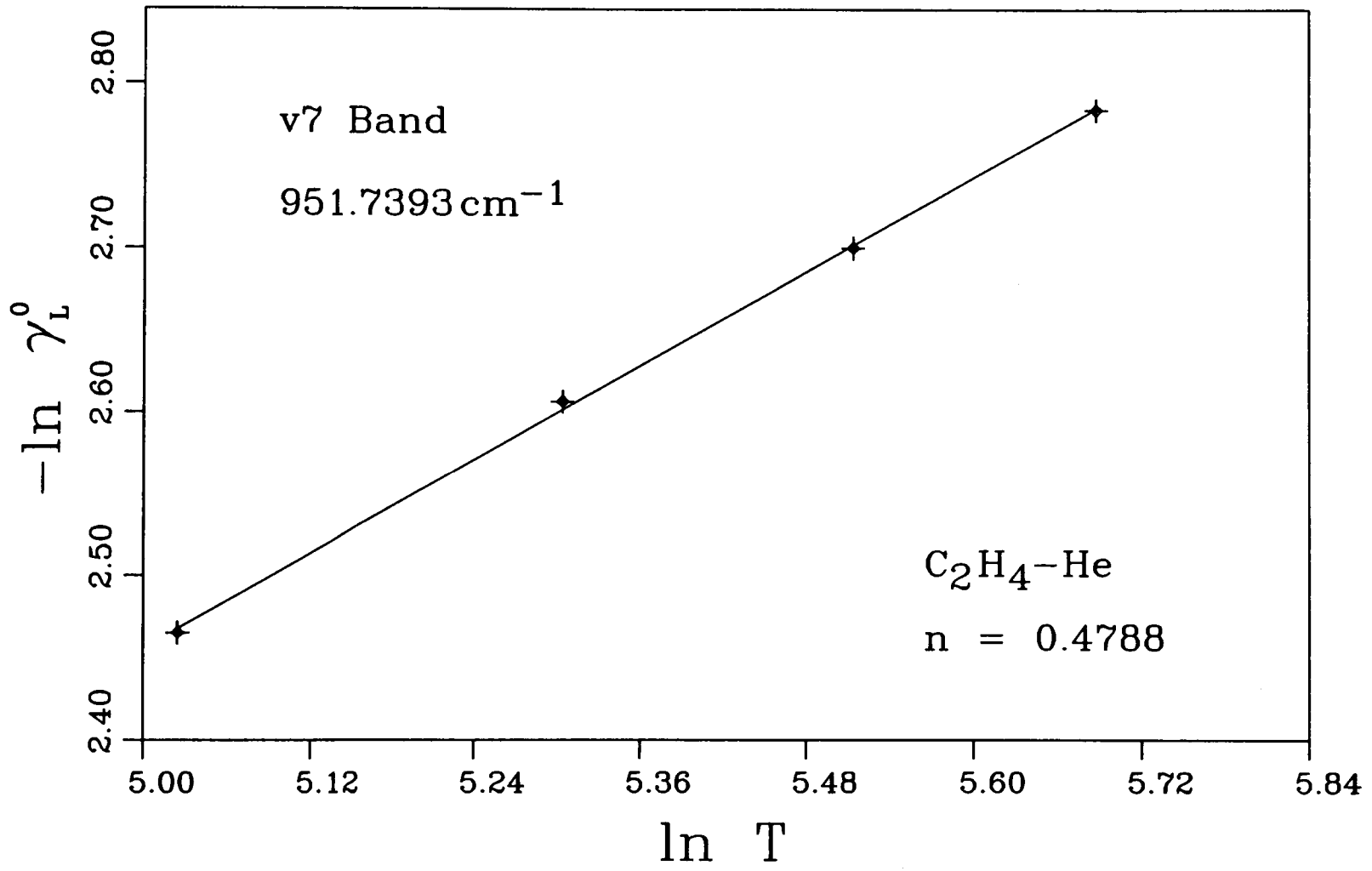

Figure 4.15: Plot of -lnγ_L^0 versus lnT for the 951.7393 cm^{-1} line of C_2H_4 broadened by He. The slope of the line is the exponent n defining the temperature dependence of the linewidth.

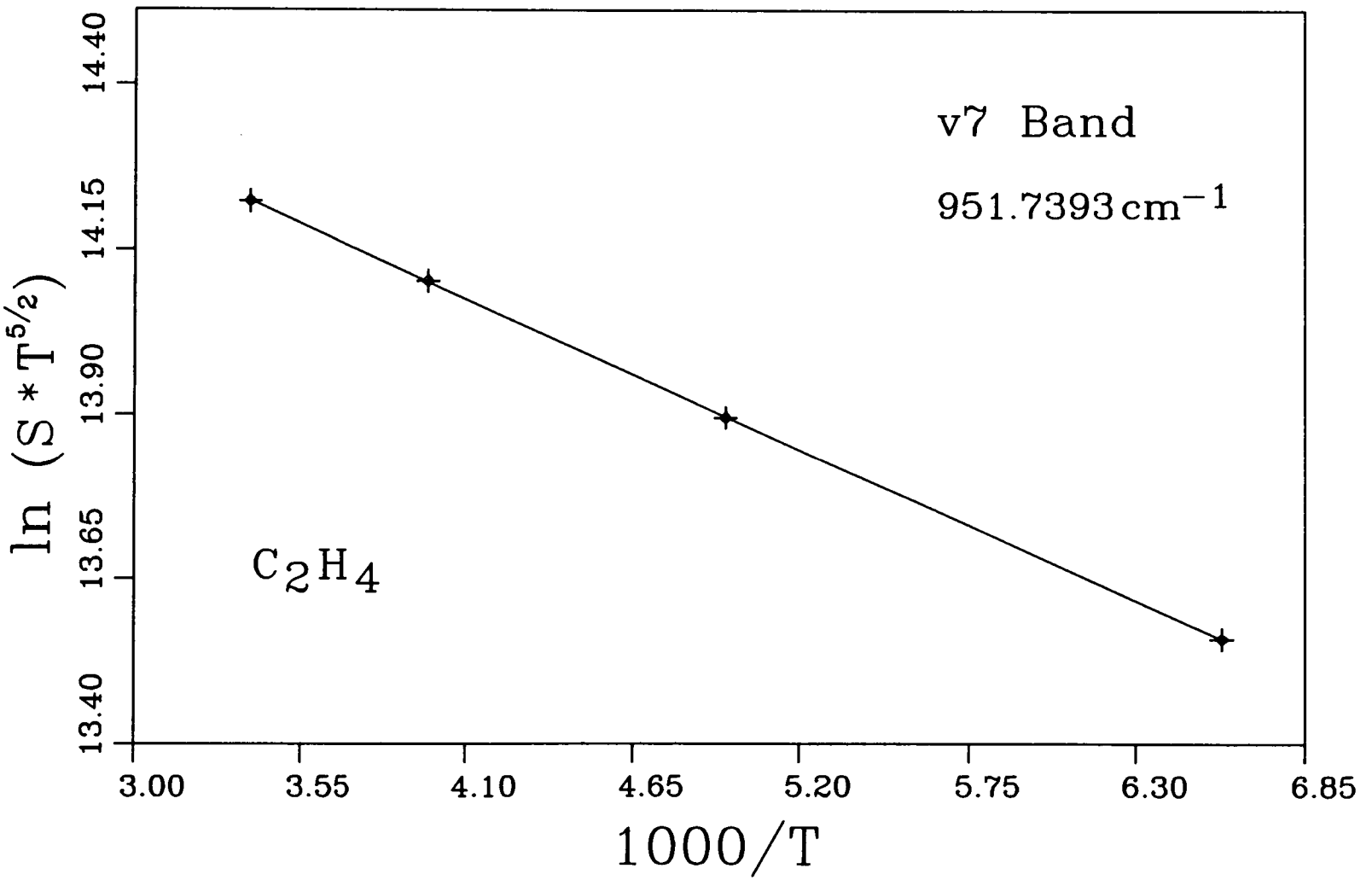

Figure 4.16: Plot of ln(S*T$^{5/2}$) versus 1000/T for the 951.7393cm^{-1} line of C_2H_4 broadened by H_2. This plot follows the temperature dependence of the intensity using Eq. (2.54).

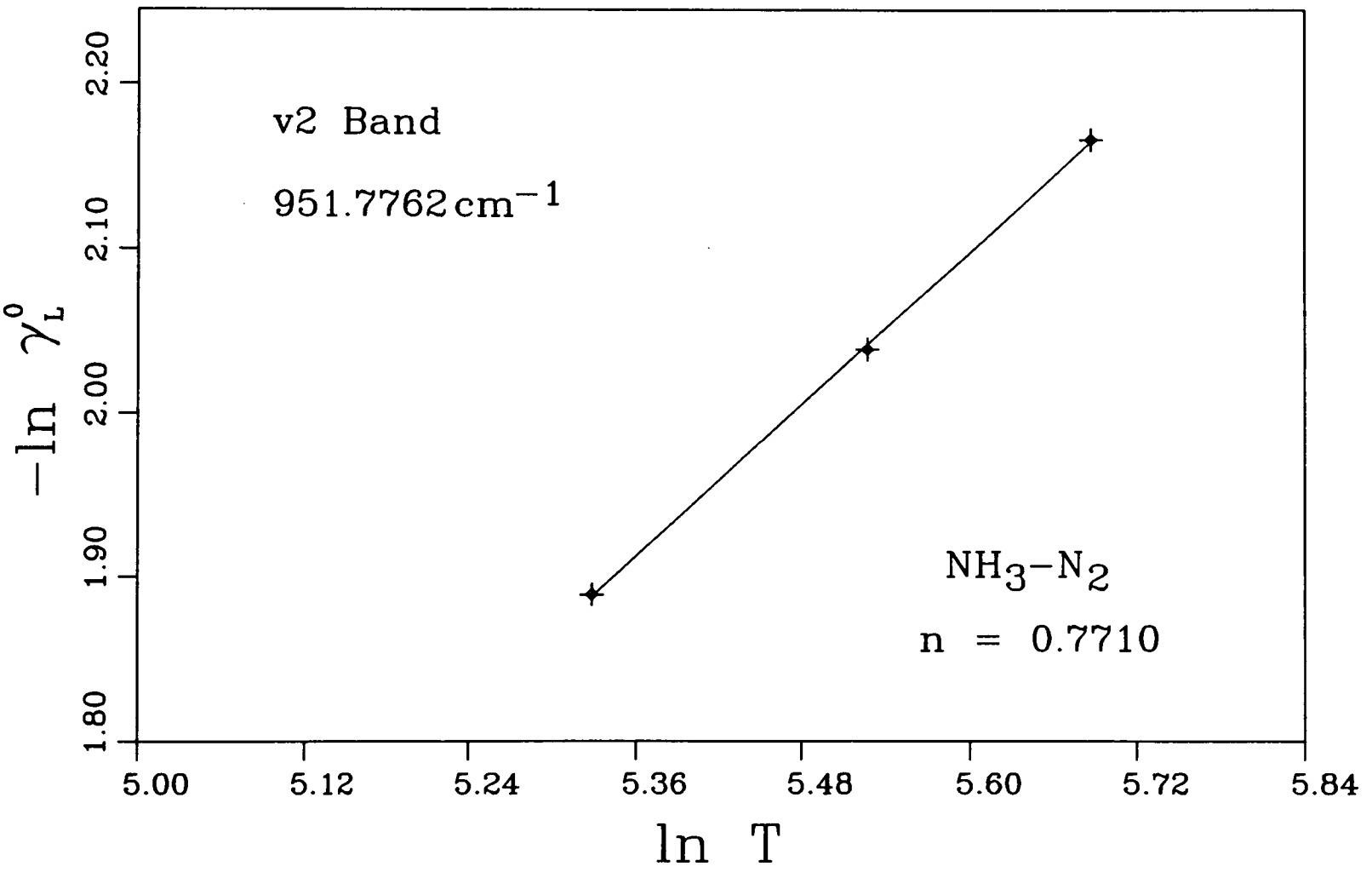

Figure 4.17: Plot of -lnγ_L^0 versus lnT for the 951.7762 cm^{-1} line of NH_3 broadened by N_2. The slope of the line is the exponent n defining the temperature dependence of the linewidth.

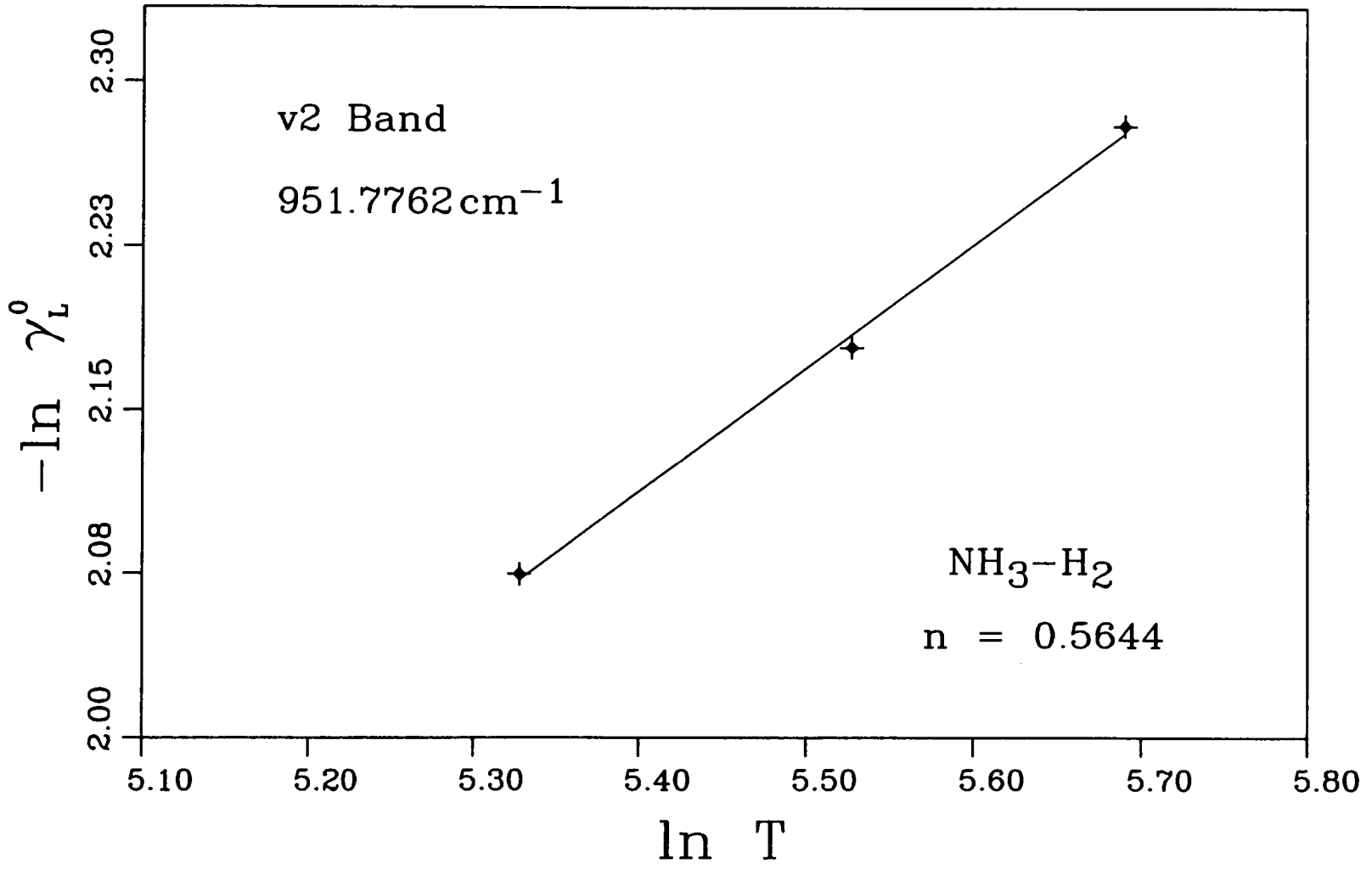

Figure 4.18: Plot of -lnγ_L^0 versus lnT for the 951.7762 cm^{-1} line of NH_3 broadened by H_2. The slope of the line is the exponent n defining the temperature dependence of the linewidth.

CHAPTER V

DISCUSSION OF RESULTS

Summary of Results and Comparison With Previous Work

Using the tunable diode laser spectrometer systems at UTK and SUNY, the collisional broadening measurements of acetylene, ethylene, and ammonia were conducted as described. The analysis was conducted and the collisional broadening coefficients were retrieved from the broadening data.

The absolute line intensity for the ethylene employed in the SUNY studies was also determined. At UTK the line intensities were determined as a gauge of the reliability of the collisional broadening. The UTK collisional broadening coefficients were determined by two independent methods to verify the retrieved results. The wing corrections provided the best fit to the linear relationship of pressure versus b_L, with a forced zero, and the γ_L^0 were determined from them. The sample/background ratio, which was used to analyze the SUNY measurements, was attempted with the UTK work but did not give as reliable results, most probably due to drift of the signal averager recordings over the length of time of the measurements. The SUNY measurements were made after the tuning provided a stable lasing mode, so that there was little variation in the averaged recordings over time. The SUNY results are given in final form in Tables 4.8-4.10 and Figs. 4.13-4.18.

Table 5.1 gives the UTK hydrogen broadening measurements with the γ_L^0 retrieved from the measurements. The γ_L^0 calculated from the pressure versus b_L fittings are also given. The residuals Δ_{O-C} tabulated are the difference between the two values for γ_L^0. Table 5.2 gives the same values for the C_2H_2-N_2 work. Table 5.3 gives the final form for the UTK broadening work, with the standard deviation for each set of measurements, and again for reference, the residuals between observed and calculated.

γ_L^0(calc) are used as a comparison with previous work that is given in Tables 5.4 and 5.5. The hydrogen broadening measurements with acetylene are compared in Table 5.4 and the nitrogen in Table 5.5. Table 5.4 lists previous measurements for the ν_5 band. The present work produced comparable results with Varanasi (62), and higher results in comparison to Blass and Chin (24). Wing corrections were not incorporated into the analysis in (24),

Table 5.1: Broadening coefficients γ_L^0 observed from the wing corrected hydrogen broadened, the γ_L^0 calculated from the linear fitting of pressure versus b_L and the resulting residuals.

ΔJ	J	Pressure (torr)	γ_L^0 (obs)	γ_L^0 (calc)	Δ_{O-C}
			($cm^{-1}atm^{-1}$)		
0	3	7.45	0.0984	0.1004	-0.0020
		14.95	0.0996	0.0985	0.0011
		24.95	0.1027	0.0978	0.0049
		32.45	0.0945	0.0976	-0.0031
0	15	16.95	0.0832	0.0855	-0.0023
		21.85	0.0846	0.0853	-0.0007
		32.85	0.0891	0.0851	0.0040
		50.90	0.0837	0.0850	-0.0013
0	16	17.45	0.0875	0.0868	0.0007
		27.35	0.0870	0.0866	0.0004
		37.35	0.0858	0.0865	-0.0007
		44.80	0.0868	0.0865	0.0003
0	19	11.30	0.0833	0.0842	-0.0009
		21.80	0.0868	0.0823	0.0045
		30.40	0.0831	0.0817	0.0014
		38.80	0.0792	0.0814	-0.0022
0	24	14.75	0.0824	0.0800	0.0024
		27.30	0.0816	0.0781	0.0035
		32.85	0.0778	0.0777	0.0001
		43.30	0.0758	0.0772	-0.0014
		56.80	0.0767	0.0769	-0.0002
0	26	14.80	0.0789	0.0777	0.0012
		19.85	0.0728	0.0787	-0.0059
		36.15	0.0792	0.0801	-0.0009

Table 5.1: (continued).

ΔJ	J	Pressure (torr)	γ_L^0 (obs) ($cm^{-1}atm^{-1}$)	γ_L^0 (calc) ($cm^{-1}atm^{-1}$)	Δ_{O-C} ($cm^{-1}atm^{-1}$)
0	26	36.15	0.0797	0.0801	-0.0004
		43.80	0.0822	0.0803	0.0019
1	6	39.80	0.0882	0.0878	0.0004
			0.0880		0.0002
			0.0877		-0.0001
		60.30	0.0878	0.0879	-0.0001
			0.0874		-0.0005
			0.0872		-0.0007
		80.30	0.0879	0.0880	-0.0001
			0.0882		0.0002
			0.0877		-0.0003
		96.30	0.0882	0.0880	0.0002
			0.0882		0.0002
			0.0882		0.0002
1	8	27.35	0.0849	0.0850	-0.0001
			0.0850		0.0000
			0.0841		-0.0009
		42.85	0.0838	0.0846	-0.0008
			0.0844		-0.0002
			0.0851		0.0005
		60.85	0.0838	0.0843	-0.0005
			0.0836		-0.0007
			0.0840		-0.0003
		77.35	0.0834	0.0842	-0.0008
			0.0842		0.0000
			0.0832		-0.0010

Table 5.2: Broadening coefficients γ_L^0 observed from the wing corrected nitrogen broadened, the γ_L^0 calculated from the linear fitting of pressure versus b_L and the resulting residuals.

ΔJ	J	Pressure	γ_L^0 (obs)	γ_L^0 (calc)	Δ_{O-C}
		(torr)	($cm^{-1}atm^{-1}$)		
1	6	41.60	0.0846	0.0842	0.0004
			0.0848		0.0006
			0.0844		0.0002
		61.60	0.0845	0.0838	0.0007
			0.0846		0.0008
			0.0841		0.0003
		78.60	0.0835	0.0837	-0.0002
			0.0831		-0.0006
			0.0830		-0.0007
1	8	33.80	0.0793	0.0789	0.0004
			0.0787		-0.0002
			0.0797		0.0008
		49.30	0.0790	0.0783	0.0007
			0.0802		0.0019
			0.0790		0.0007
		63.80	0.0779	0.0781	-0.0002
			0.0774		-0.0007
			0.0775		-0.0006
		79.80	0.0775	0.0779	-0.0004
			0.0778		-0.0001
			0.0780		0.0001

Table 5.3: Averaged wing corrected collisional broadening coefficients retrieved from the Voigt profiles γ_L^0 (obs), and γ_L^0 calculated from the linear fitting of the pressure versus Lorentz half-width plots, γ_L^0 (calc).

Broadener	ΔJ	J	Frequency	γ_L^0 (obs)	γ_L^0 (calc)	Δ_{O-C}
			(cm^{-1})	($cm^{-1}atm^{-1}$)		
H_2	0	3	729.2018	0.0988±.0034	0.0985±.0012	0.0003
	0	15	730.2301	0.0852±.0027	0.0871±.0002	-0.0019
	0	16	730.3731	0.0868±.0007	0.0866±.0001	0.0002
	0	19	730.8553	0.0831±.0031	0.0824±.0013	0.0007
	0	24	731.8345	0.0789±.0030	0.0780±.0012	0.0009
	0	26	732.2868	0.0786±.0035	0.0792±.0012	-0.0006
	1	6	745.6135	0.0879±.0003	0.0879±.0001	0.0000
	1	8	750.3105	0.0843±.0007	0.0845±.0004	-0.0002
N_2	1	6	745.6135	0.0841±.0007	0.0839±.0003	0.0002
	1	8	750.3105	0.0785±.0009	0.0783±.0004	0.0002

Table 5.4: Comparison of C_2H_2-H_2 broadening work of this investigation with previous work.

J	γ_L^0, ν_5 Band ($cm^{-1}atm^{-1}$)					
	This Work		Varanasi [a]		Blass and Chin [b]	
	Q Branch	R Branch	P Branch	R Branch	P Branch	Q Branch
3	0.0985±.0034				0.0780	0.0777
4					0.0780	0.0780
6		0.0879±.0003				0.0750
7				0.0928±.0017		0.0748
8		0.0845±.0007	0.0942±.0015			0.0729
11			0.0926±.0020			
15	0.0871±.0002				0.0684	
16	0.0866±.0001					
18				0.0851±.0016		0.0712
19	0.0824±.0013			0.0851±.0033		0.0702
21				0.0852±.0007		
24	0.0780±.0012					
26	0.0792±.0012					
	298±1 K		295 K		297 ±1.5 K	

[a]Varanasi (61), temperature correction factor to 298 K, 1.0051
[b]Blass and Chin (23), temperature correction factor to 298 K, 1.0017

Table 5.5: Comparison of C_2H_2-N_2 broadening work of this investigation with previous work.

Line	$\gamma_L^0(cm^{-1}atm^{-1})$					
	ν_5 Band				$(\nu_4+\nu_5)^0$ Band	
	This Work	Bouanich [a]	Varanasi [b]	Blass [c]	Podolske [d]	Devi [e]
P(5)						0.0877(6)
Q(5)				0.0775		
R(5)						0.0889(18)
P(6)		0.0916				
Q(6)				0.0735		
R(6)	0.0839±.0003					
P(7)		0.0917				0.0855(3)
Q(7)				0.0754		
R(7)			0.0937±.0009			0.0866(11)
R(7)			0.0877±.0003 [f]			
P(8)			0.0937±.0006			0.0853(12)
Q(8)				0.0729		
R(8)	0.0783±.0004	0.0862				0.0856(10)
P(9)						0.0863(16)
Q(9)				0.0738		
R(9)					0.0842(26)	0.0855(9)
	295 K	297±2 K	295 K	297±1.5K	296 K	296 K

[a]Bouanich et al. (25), temperature correction factor to 295 K, 0.9966
[b]Varanasi (61), temperature correction factor to 295 K, 1.0000
[c]Blass and Chin (23), temperature correction factor to 295 K, 0.9966
[d]Podolske et al. (28), temperature correction factor to 295 K, 0.9983
[e]Devi et al. (27), temperature correction factor to 295 K, 0.9983
[f]Obtained in the $(\nu_4+\nu_5)^0$ Band

and thus may be a source of difference in the two results. A temperature correction factor, calculated from a binomial expansion of Equation (2.50) with n=0.5, has been included in the footnote of Table 5.4, and may be used to correct the broadening coefficients of the previous works to the temperature of the present work.

Table 5.5 provides a listing of previously conducted nitrogen broadening work for comparison with the two nitrogen broadening measurements carried out in this work. These comparison γ_L^0 are retrieved from work conducted in the ν_5 band of acetylene as well as the $(\nu_4+\nu_5)^0$ band. A temperature correction is also included in the footnote of Table 5.5. The R(8) line of this work is low compared to the previous work, while it is rather difficult to compare the R(6) line. The line intensities retrieved from the broadening work, which are comparable to the calculated values for these lines (Table 4.7), will have to be used as an indicator of the reliability of the broadening work.

The broadening coefficients of this work were used along with the γ_L^0 of Blass and Chin (24) to qualitatively view the J dependence of γ_L^0. The γ_L^0 found from the hydrogen broadening work of each work was fit using a quadratic equation, and the plots of J(J+1) versus γ_L^0 are shown in Figure 5.1. Figure 5.2 shows the γ_L^0 of both works plotted on the same scale of γ_L^0.

Recommendations for Future Work

The most obvious need in future work is for more broadening measurements to be conducted over a wider range of J values. The comparison Tables 5.4 and 5.5 reflect this need. The number of spectral lines, coupled with the variety of perturbing gases that may be used, makes it difficult to compare with other work. Different methods of broadening measurements procedure and analysis should also be taken into account in these comparisons. R(8), however, from the present work does appear low in comparison to previous work and should be re-measured for verification.

An oscilliscope should be used to tune the TDL signal if the sample/background ratio method is to be used. Tuning with an oscilliscope would most likely provide a cleaner, more stable signal that is necessary if this method is to be used, and might provide a better signal for the TDL measurements in general.

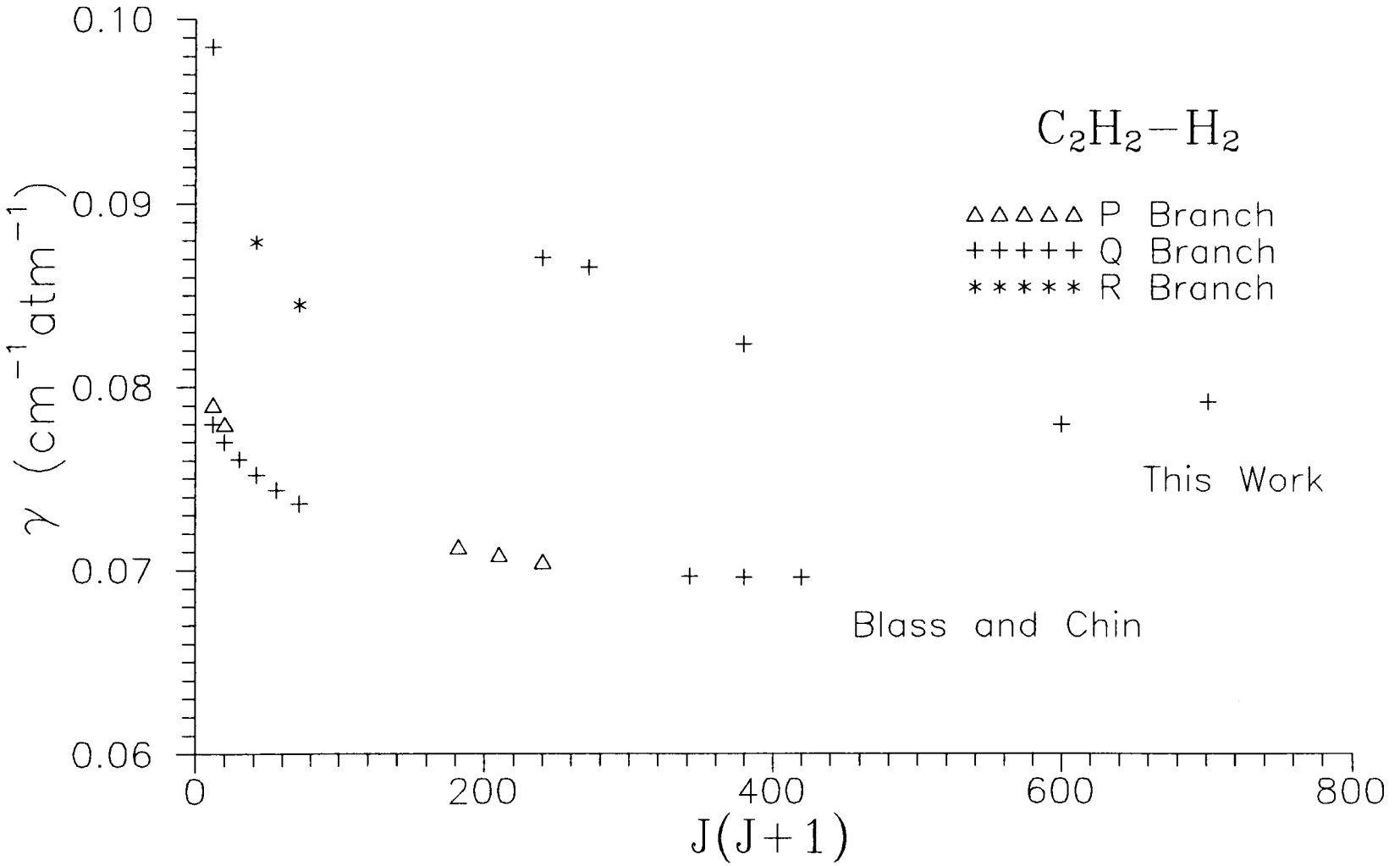

Figure 5.1: Plots of J(J+1) versus γ_L^0 for the broadening coefficients of Blass and Chin (24) and the broadening coefficients of the present work.

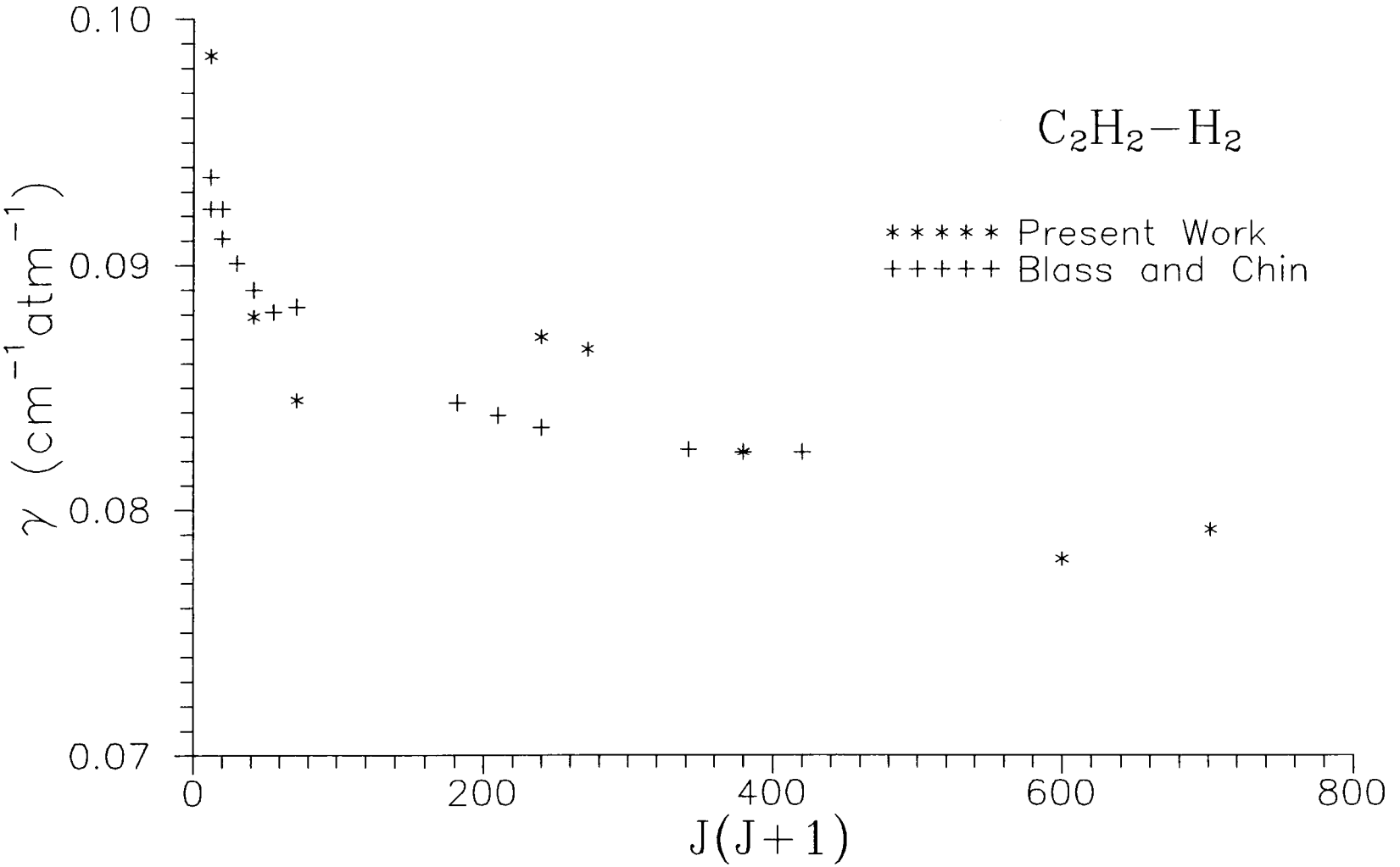

Figure 5.2: Plot of J(J+1) versus γ_L^0 for the γ_L^0 of Blass and Chin (24) and the present work. The broadening coefficients of both works are plotted on the same scale of γ_L^0.

LIST OF REFERENCES

LIST OF REFERENCES

1. D. E. JENNINGS, *J. Quant. Spectrosc. Radiat. Transfer* **40**, 221-238 (1988).
2. "The Mission to Planet Earth," handbook, NASA, 1990.
3. V. G. KUNDE, "The Cassini Mission: Infrared and Microwave Spectroscopic Measurements," NASA Reference Publication 1213, January 1989.
4. C. P. RINSLAND, A. GOLDMAN, AND G. M. STOKES, *Appl. Opt.* **24**, 2044-2046 (1985).
5. A. GOLDMAN, F. J. MURCRAY, R. D. BLATHERWICK, J. R. GILLIS, F. S. BONOMO, F. H. MURCRAY, D. G. MURCRAY, AND R. J. CICERONE, *J. Geophys. Res.* **86**, 12143-12146 (1981).
6. S. T. RIDGEWAY, *Astrophys. J. Lett.* **187**, L41-L43 (1974).
7. M. COMBES, TH. ENCRENEZ, L. VAPILLON, AND Y. ZÉAU, *Astron. and Astrophys.* **34**, 33-35 (1974).
8. R. HANEL, B. CONRATH, F. M. FLASAR, L. HERATH, V. KUNDE, P. LOWMAN, W. MAGUIRE, J. PEARL, J. PIRRAGLIA, AND R. SAMUELSON, *Science* **206**, 952-956 (1979).
9. R. HANEL, B. CONRATH, F. M. FLASAR, V. KUNDE, P. LOWMAN, W. MAGUIRE, J. PEARL, J. PIRRAGLIA, AND R. SAMUELSON, *Science* **204**, 972-976 (1979).
10. R. HANEL, B. CONRATH, F. M. FLASAR, V. KUNDE, W. MAGUIRE, J. PEARL, J. PIRRAGLIA, R. SAMUELSON, AND L. HERATH, *Science* **212**, 192-200 (1981).
11. R. COURTIN, D. GAUTIER, A. MARTEN, AND B. BÉZARD, *Astrophys. J.* **287**, 899-916 (1984).
12. C. P. RINSLAND, A. BALDACCI, AND K. RAO, *Astrophys. J.* **257**, 920 (1982).
13. M. E. SUMMERS AND D. F. STROBEL, *Astrophys. J.* **346**, 495-508 (1989).
14. P. N. ROMANI AND S. K. ATREYA, *Icarus* **74**, 424-445 (1988).
15. G. S. ORTON, D. K. AITKEN, C. SMITH, P. F. ROCHE, J. CALDWELL, AND R. SNYDER, *Icarus* **70**, 1-12 (1987).
16. W. MACY, JR., *Icarus* **41**, 153-158 (1980).
17. D. F. STROBEL, "The Photochemistry of Atmospheres," Chapter 8, J. S. LEVINE, ED., Academic Press, Orlando, FL, 1985, p. 411.
18. REF. 17, p. 428.
19. P. VARANASI, L. P. GIVER, AND F. P. J. VALERO, *J. Quant. Spectrosc. Radiat. Transfer* **30**, 497-504 (1983).
20. J. S. LEVINE, "The Photochemistry of Atmospheres," Chapter 1, J. S. LEVINE ED., Academic Press, Orlando, FL, 1985, p. 45.

21. C. W. KEENAN, D. C. KLEINFELTER, AND J. H. WOOD, "General College Chemistry," Chapter 6, Harper and Row, San Francisco, 1980, p. 175.
22. GERHARD HERZBERG, "Molecular Spectra and Molecular Structure," Volume II, "Infrared and Raman Spectra of Polyatomic Molecules," D. Van Nostrand Co., Inc., Princeton, 1945, p. 288.
23. M. WEBER, private communication.
24. W. E. BLASS AND V. W. L. CHIN, *J. Quant. Spectrosc. Radiat. Transfer* **38**, 185-188 (1987).
25. V. W. L. CHIN, Master's Thesis, University of Tennessee, 1985.
26. J.-P. BOUANICH, E. LAMBOT, G. BLANQUET, AND J. WALRAND, *J. Mol. Spectrosc.* **140**, 195-213 (1990).
27. D. LAMBOT, G. BLANQUET, AND J.-P. BOUANICH, *J. Mol. Spectrosc.* **136**, 86-92 (1989).
28. V. M. DEVI, D. C. BENNER, C. P. RINSLAND, M. A. H. SMITH, AND B. D. SIDNEY, *J. Mol. Spectrosc.* **114**, 49-53 (1985).
29. J. R. PODOLSKE, M. LOEWENSTEIN, AND P. VARANASI, *J. Mol. Spectrosc.* **107**, 241-249 (1984).
30. P. VARANASI, AND B. R. P. BANGARU, *J. Quant. Spectrosc. Radiat. Transfer* **15**, 267-273 (1975).
31. A. C. AIKIN, J. R. HERMAN, E. J. MAIER, AND C. J. MCQUILLAN, *J. Geophys. Res.* **87**, 3105-3118 (1982).
32. S. J. KIM, J. CALDWELL, A. R. RIVOLO, AND R. WAGENER, *Icarus* **64**, 233-248 (1985).
33. D. M. GOLDHABER, A. L. BETZ, AND J. J. OTTUSCH, *Astrophys. J.* **314**, 356-362 (1987).
34. A. L. BETZ, *Astrophys. J.* **244**, L103-L105 (1981).
35. REF. 21, p. 175.
36. REF. 22, p. 325.
37. CH. LAMBEAU, A. FAYT, J. L. DUNCAN, AND T. NAKAGAWA, *J. Mol. Spectrosc.* **81**, 227-247 (1980).
38. P. VARANASI AND S. CHUDAMANI, *J. Quant. Spectrosc. Radiat. Transfer* **41**, 335-343 (1989).
39. REF. 21, p. 295.
40. REF. 22, p. 173.

41. T. KOSTIUK, M. J. MUMMA, J. J. HILLMAN, D. BUHL, L. W. BROWN, J. L. FARIS, AND D. L. SPEARS, *Infrared Phy.* **17**, 431-439 (1977).
42. TH. ENCRENAZ, T. OWEN AND J. H. WOODMAN, *Astron. and Astrophys.* **37**, 49-55 (1974).
43. I. DE PATER, P. N. ROMANI, AND S. K. ATREYA, *Icarus* **82**, 288-313 (1989).
44. M. D. HOFSTADTER AND D. O. MUHLEMAN, *Icarus* **81**, 396-412 (1988).
45. L. S. ROTHMAN, R. R. GAMACH, A. GOLDMAN, L. R. BROWN, R. A. TOTH, H. M. PICKETT, R. L. POYNTER, J.-M. FLAUD, C. CAMY-PEYRET, A. BARBE, N. HUSSON, C. P. RINSLAND, AND M. A. H. SMITH, *Appl. Opt.* **26**, 4058-4097 (1985).
46. J. S. MARGOLIS AND S. SARANGI, *J. Quant. Spectrosc. Radiat. Transfer* **16**, 405-408 (1976).
47. C. E. KEFFER, C. P. CONNER, AND W. H. SMITH, *J. Quant. Spectrosc. Radiat. Transfer* **35**, 487-493 (1986).
48. CHIN, Master's Thesis, University of Tennessee, 1985, p. 2.
49. M. A. H. SMITH, C. P. RINSLAND, B. FRIDOVICH, AND K. N. RAO, "Molecular Spectroscopy: Modern Research, Volume III," Chapter 3, K. N. RAO, ED., Academic Press, New York, 1985.
50. S. S. PENNER, "Quantitative Molecular Spectroscopy and Gas Emissivities," Addison Wesley, Reading, Massachusetts, 1959.
51. D. W. POSENER, *Australian. J. Phys.* **12**, 184-196 (1959).
52. B. H. ARMSTRONG, *J. Quant. Spectrosc. Radiat. Transfer* **7**, 61-88 (1967).
53. M. WEBER, W. E. BLASS, AND J.-L. SALANAVE, *J. Quant. Spectrosc. Radiat. Transfer* **41**, 437-443. (1989).
54. E. E. WHITING, *J. Quant. Spectrosc. Radiat. Transfer* **8**, 1379-1384 (1968).
55. J. J. OLIVERO AND R. L. LONGBOTHUM, *J. Quant. Spectrosc. Radiat. Transfer* **17**, 233-236 (1977).
56. B. FRIDOVICH, *J. Mol. Spectrosc.* **105**, 53-60 (1984).
57. J. J. BELBRUNO, J. B ZUGHUL, J. GELFAND AND H. RABITZ, *J. Mol. Spectrosc.* **87**, 560-568 (1981).
58. P. VARANASI, *J. Quant. Spectrosc. Radiat. Transfer* **39**, 13-25 (1988).
59. A. GOLDMAN, M. DANG-NHU, AND J.-P. BOUANICH, *J. Quant. Spectrosc. Radiat. Transfer* **41**, 17-21 (1989).
60. G. W. HALSEY, J. J. HILLMAN, AND D. E. JENNINGS, "The 14 Micron Bands

of Acetylene– The Region of the Bending Modes," Laboratory for Extra-terrestrial Physics, Goddard Space Flight Center, NASA, 1985.

61. S. CHUDAMANI, P. VARANASI, L. P. GIVER, AND F. P. J. VALERO, *J. Quant. Spectrosc. Radiat. Transfer* **34**, 359-364 (1985).

62. P. VARANASI, private communication.

APPENDIX

APPENDIX I

FORTRAN Wing Correction Program

```
c       FORTRAN wing correction to collisional broadening
c       5/22/90 jfb
c       rev. 9/19/90 jfb
c       rev. 4/1/91
        real*8 kitot,kisum,dela,aa,ki,bbv,bbd,delbv
        real*8 bbl,blsum,ba,kitotb,kisumb,deta,kib,bt
        real*8 delv,kea,kit,bvnu,betas,blp,more,gamnu
        real*8 pr,vo,xde,bod,num
        character*8 ans*1,pcin*20,wingout*20
        real*8 b(3),c(3),a(25,5),eta(25,5),beta(25,5),P(25)
        real*8 bv(25,5),bd(25,5),bl(25),gam(25),delun(25)
        write (*,2)
2       format (' input n17 output filename')
        read (5,'(1A20)')pcin
        open (unit=3, file=pcin,status='old')
        write (*,3)
3       format (' input wing output filename')
        read (5,'(A20)')wingout
        open (unit=1, file='deriv.dat', status='old')
        open (unit=2, file=wingout, status='unknown')
        write (*,4)
4       format (' input number of data sets in file')
        read (5,'(A20)')num

        read (1,*) (b(j),c(j),j=1,3)
        more=0
        k=0.
11      k=k+1.
        more=more+1
c       read data from analysis out data file
        read (3,*) P(k),gam(k),bl(k),bv(k,4),bd(k,5),delun(k)
        write (*,*) delun(k)
14      a(k,1)=(bl(k)/bd(k,5))*sqrt(log(2.d0))
        eta(k,2)=(bv(k,4)/bd(k,5))*sqrt(log(2.d0))
        beta(k,3)=(delun(k)/bd(k,5))*sqrt(log(2.d0))
        write (*,*) a(k,1),eta(k,2),beta(k,3)
        write (2,*) a(k,1),eta(k,2),beta(k,3)
c72      write (*,500)
c500     format (' what is delbv?')
c       read (*,*) delbv
c       write (*,900)
c900     format (' what is dela?')
```

```
c           read (*,*) dela
c           write (*,910)
c910         format (' what is deta?')
c           read (*,*) deta
c           write (2,510)
c           write (*,510)
c510         format (' delbv,dela,deta')
c           write (*,*) delbv,dela,deta
c           write (2,*) delbv,dela,deta
            delbv=1e-6
            dela=1e-6
            deta=1e-6
c           calculation of dbl/dbv delta method
            blsum=0
            bt=((7.7255*(bv(k,4)+delbv))
      c  -(6.7255*sqrt((bv(k,4)+delbv)**2+(0.3195*bd(k,5)**2))))
      c  -((7.7255*(bv(k,4)-delbv))
      c  -(6.7255*sqrt((bv(k,4)-delbv)**2+(0.3195*bd(k,5)**2))))
            blsum=bt/(2*delbv)
c           calculation of dbl/dbv analytic
            ba=7.7255-(6.7255*bv(k,4)/sqrt(bv(k,4)**2+(0.3195*bd(k,5)**2)))
c           write (2,600)
            write (*,600)
600          format (' partial bl w/respect bv numeric')
c           write (2,*) blsum
            write (*,*) blsum
            write (*,700)
c           write (2,700)
700          format (' partial bl w/respect bv analytic')
c           write (2,*) ba
            write (*,*) ba
c           calculation of partial k w/respect eta
            kitot=0
            kisum=0
            do 10 j=1,3
            ki= (((a(k,1)+dela)*b(j)*(eta(k,2)**2+(a(k,1)+dela)**2
      c  +c(j)))/
      c  ((eta(k,2)**2+(a(k,1)+dela)**2+c(j))**2-(4*eta(k,2)**2
      c  *c(j))))
      c  -(((a(k,1)-dela)*b(j)*(eta(k,2)**2+(a(k,1)-dela)**2
      c  +c(j)))/
      c  ((eta(k,2)**2+(a(k,1)-dela)**2+c(j))**2-(4*eta(k,2)**2
      c  *c(j))))
            kisum=ki/(2*dela)
c           write (*,*) kisum
```

```
            kitot=kitot+kisum
10          continue
c           calculation of partial k w/respect a
            kitotb=0
            kisumb=0
            do 15 j=1,3
            kib=((a(k,1)*b(j)*((eta(k,2)+deta)**2+a(k,1)**2
     c      +c(j)))/
     c      (((eta(k,2)+deta)**2+a(k,1)**2+c(j))**2-(4*(eta(k,2)
     c      **2*c(j))))
     c      -((a(k,1)*b(j)*((eta(k,2)-deta)**2+a(k,1)**2+c(j)))/
     c      (((eta(k,2)-deta)**2+a(k,1)**2+c(j))**2-(4*(eta(k,2)
     c      -deta)**2*c(j))))
            kisumb=kib/(2*deta)
c           write (*,*) kisumb
            kitotb=kitotb+kisumb
15          continue
c           write (2,30)
            write (*,30)
30          format (' partial K w/respect a,partial K w/respect eta')
c           write (2,*) kitot,kitotb
            write (*,*) kitot,kitotb
c           write (*,31)
c           write (2,31)
c31         format (' partial K w/respect eta')
c           write (2,*) kitotb
c           write (*,*) kitotb
c           check for delta method derivs
c           write (*,71)
c71         format (' Are derivs satisfactory? y or n')
c           read (*,73) ans
c73         format (A1)
c           if (ans.eq.'n') go to 72
c           calculation of voigt halfwidth correction
            kit=0
            kea=0
            do 16 j=1,3
            kit= ((a(k,1)*b(j)*(beta(k,3)**2+a(k,1)**2+c(j)))/
     c      ((beta(k,3)**2+a(k,1)**2+c(j))**2-(4*beta(k,3)**2*
     c      c(j))))
            kea=kea+kit
16          continue
c           write (*,*) kea
            delv= ((-bd(k,5))*kea)/(2*sqrt(log(2.0))*(kitot*blsum+kitotb))
            write (*,*) delv
```

```
c            determination of new voigt halfwidth
             bvnu=bv(k,4)+delv
             write (*,*) bvnu
c            write (2,*) bvnu
            bv(k,4)=bvnu
c            determination of new broad halfwidth
             blp=(7.7255-6.7255*sqrt(1.+0.3195*(bd(k,5)/bvnu)**2))*bvnu
             write (*,*) blp
c            write (2,*) blp
             bl(k)=blp
c            determination of new broad coefficient
             gamnu=blp*760/P(k)
             write (*,*) gamnu
             write (2,*) delv,bvnu,blp,gamnu
c62          continue
            if (delv.gt.1E-6) then
c            beta(k,3)=5*beta(k,3)
c            call voigt subroutine to find wing mark position
             bod=bd(k,5)
             call marker (pr,betas,aa,blp,bod,vo,xde)
             delun(k)=xde
             goto 14
            else
            endif
c            write (*,12)
c12          format (' Another calculation?')
c            read (*,74) more
c74          format (a1)
            if (more.le.num) go to 11
            stop
            end

            subroutine marker (pro,bet,aa,bbl,bbd,voi,xdel)
            xdel=0.d0
            voi=0.d0
            bet=0.d0
            do 11 xdel=5.d0,25.d0,1.d-5
            bet=(xdel/bbd)*sqrt(log(2.d0))
             aa=(bbl/bbd)*sqrt(log(2.d0))
             voi=voigt(bet,aa)
c            write(*,*) xdel,bet,voi
             if (voi.lt.1.0d-8) go to 10
             pro=(1/bbd)*sqrt(log(2.0)/3.1415927)*voi
11           continue
10           write (*,*) xdel,bet,voi
```

```
      write (2,*) xdel,bet,voi
      return
      end
c     calculation of parameters for voigt profile comparison
c     xsi,a are x,y to give to sub to find K(x,y)
c     voigt profile calculation subprogram
c     b.h. armstrong,jqsrt,vol7,p61,1967
c     rev. a. atakan, m. weber
c     rev 9/25/90 jfb
c     If K(x,y) (VOIGT FUNCTION) is desired use the key-
c     board input below and not the 1st do loop. will
c     accept x,y from          keyboard and give K(x,y) which is
c     VOI and K(x,y)/K(0,y) which is TOT. VOIGT
c     PROFILE given by PRO.

      REAL*8 FUNCTION VOIGT(xsi,a)
      IMPLICIT REAL*8 (A-H,O-Z)
      DIMENSION W(10),T(10),C(34)
      DATA W / 4.62243670D-01, 2.86675505D-01, 1.09017206D-01,
     * 2.48105209D-02, 3.24377334D-03, 2.28338636D-04,
     * 7.80255648D-06, 1.08606937D-07, 4.39934099D-10,
     * 2.22939365D-13 /
      DATA T / 0.245340708D+00, 0.737473729D+00, 1.234076220D+00,
     * 1.738537710D+00, 2.254974000D+00, 2.788806060D+00,
     * 3.347854570D+00, 3.944764040D+00, 4.603682450D+00,
     * 5.387480890D+00 /
      DATA C / 0.1999999999972224D+00, -0.1840000000029998D+00,
     * 0.1558399999965025D+00, -0.1216640000043988D+00,
     * 0.0877081599940391D+00, -0.0585141248086907D+00,
     * 0.0362157301623914D+00, -0.0208497654398036D+00,
     * 0.0111960116346270D+00, -0.5623189616710900D-02,
     * 0.2648763417226500D-02, -0.1173267075770400D-02,
     * 0.4899519978088000D-03, -0.1933630801528000D-03,
     * 0.7228774467880000D-04, -0.2565551249790000D-04,
     * 0.8662073684100000D-05, -0.2787637971900000D-05,
     * 0.8566873627000000D-06, -0.2518433784000000D-06,
     * 0.7093602210000000D-07, -0.1917322570000000D-07,
     * 0.4980125600000000D-08, -0.1244773400000000D-08,
     * 0.2997777000000000D-09, -0.6964500000000000D-10,
     * 0.1562620000000000D-10, -0.3389700000000000D-11,
     * 0.7116000000000000D-12, -0.1447000000000000D-12,
     * 0.2850000000000000D-13, -0.5500000000000000D-14,
     * 0.1000000000000000D-14, -0.2000000000000000D-15 /
      QWQW=88.0D0
      A2=A**2
```

```
      IF (((A.LT.1.D0).AND.(XSI.LT.4.D0)).OR.(A.LT.1.8D0/(XSI+1.D0)))
     GO TO 40
      IF ((A.LT.2.5D0).AND.(XSI.LT.4.D0)) GO TO 20
      G=0.D0
      DO 10 I=1,10
10     G=G+(1./((XSI-T(I))**2+A2)+1./((XSI+T(I))**2+A2))*W(I)
      VOIGT=0.318309886D0*A*G
      RETURN
20     G=0.D0
      DO 30 I=1,10
      R=T(I)-XSI
      S=T(I)+XSI
c     V=(4.D0*T(I)**2-2.D0)*W(I)
c     H=R*DATAN(R/A)+S*DATAN(S/A)-.5D0*A*(DLOG(A2+R**2)
c     +DLOG(A2+S**2))
c30     G=G+V*H
30     G=G+(4.D0*T(I)**2-2.D0)*(R*DATAN(R/A)+S*DATAN(S/A)-
     c .5D0*A*(DLOG(A2+R**2)+DLOG(A2+S**2)))*W(I)
      VOIGT=0.318309886D0*G
      RETURN
40     WQWQ=XSI**2-A2
      U1=0.0D0
      IF (WQWQ.LT.QWQW) U1=DEXP(-WQWQ)*DCOS(2.D0*XSI*A)
      IF (XSI.GT.5.D0) GO TO 60
      BN1=0.D0
      BN2=0.D0
      X1=XSI/5.D0
      COEF=4.D0*X1**2-2.D0
      DO 50 I=1,34
      II=35-I
      BN=COEF*BN1-BN2+C(II)
      BN2=BN1
50     BN1=BN
      F=X1*(BN-BN2)
      .=1.D0-2.D0*XSI*F
      DN2=F
      GO TO 70
60     QQQ=1.D0/XSI**2
C     DN1=((1055.7421D0*QQQ+162.4218D0)*QQQ+29.53125D0)*QQQ
C     DN1=-((((DN1+6.5625D0)*QQQ+1.875D0)*QQQ+.75D0)*QQQ
C     +.5D0)*QQQ
     DN1=-(.5D0/XSI**2+.75D0/XSI**4+1.875D0/XSI**6+6.5625D0/XSI**8
     C +29.53125D0/XSI**10+1162.4218D0/XSI**12+1055.7421D0/XSI**14)
      DN2=(1.D0-DN1)/(2.D0*XSI)
70     FUNCT=A*DN1
```

```
      IF (A.LE.1.D-8) GO TO 100
      Q=1.D0
      AN=A
      DO 90 I=2,50
      DN=-2.D0*(XSI*DN1+DN2)/I
      DN2=DN1
      DN1=DN
      IF (MOD(I,2).EQ.0) GO TO 90
80     Q=-Q
      AN=AN*A2
      G=DN*AN
      FUNCT=FUNCT+Q*G
      IF (DABS(G/FUNCT).LE.1.D-8) GO TO 100
90     CONTINUE
100    VOIGT=U1-1.12837917D0*FUNCT
      RETURN
      END
```

VITA

John Franklin Brannon, Jr. was born in Blount County, Tennessee on October 26, 1965. He attended public school at Greenback, Tennessee until his graduation from high school in 1983. The following fall he entered the University of Tennessee and completed his B.S. degree in Physics in June 1987, graduating Phi Beta Kappa.

He began graduate school and a teaching assistantship with the Physics and Astronomy Department at the University of Tennessee in the fall of 1987. After receiving a summer assistantship in 1990 at the State University of New York at Stony Brook, he returned to the University of Tennessee to complete his Master's degree, graduating in August 1991.

The author is a member of Phi Beta Kappa, Sigma Pi Sigma and the Coblentz Society. Mr. Brannon will continue his graduate work at the State University of New York at Stony Brook.